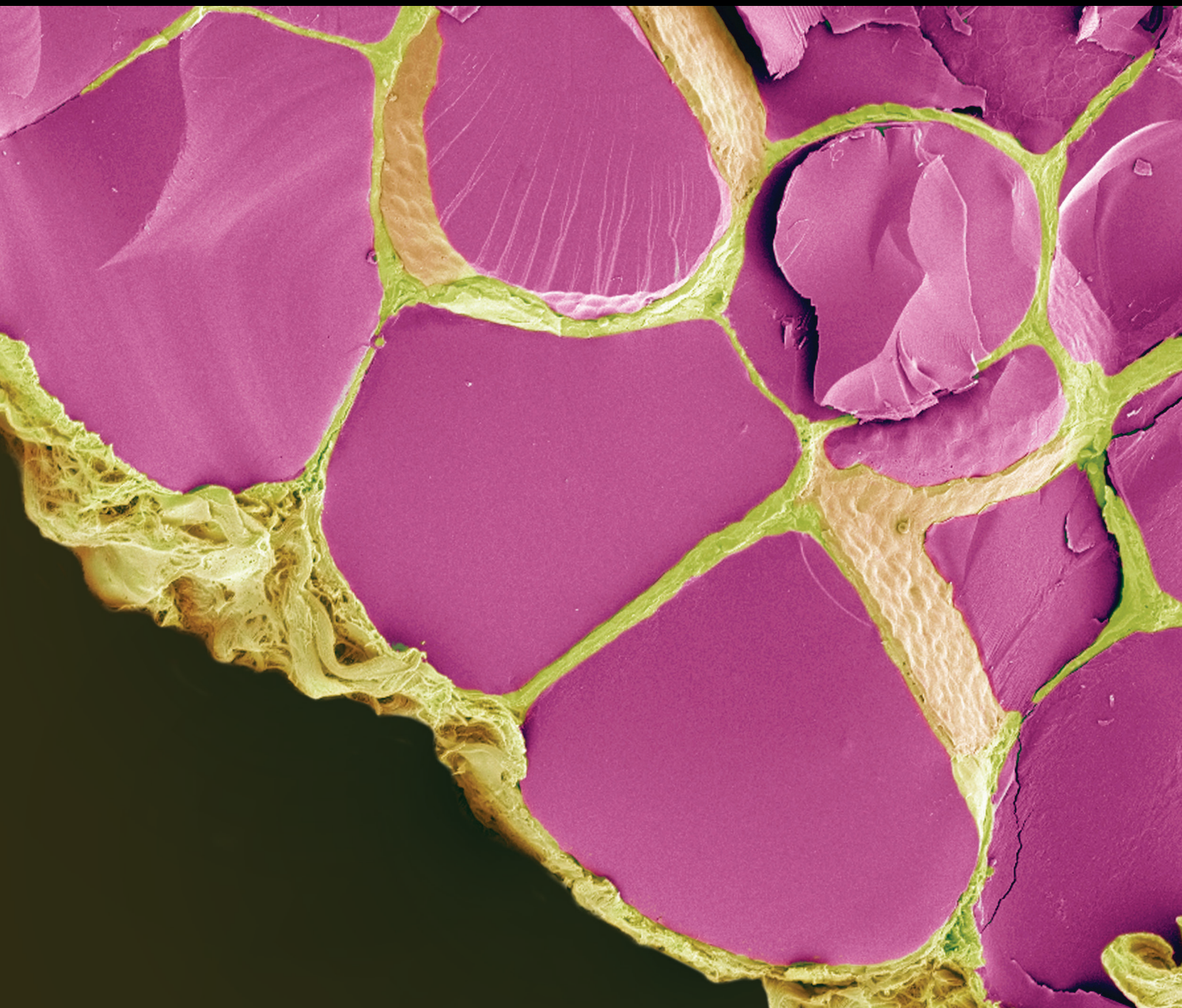


International Journal of Endocrinology

Animal Models of Diabetes and Related Metabolic Diseases

Lead Guest Editor: Tomohiko Sasase

Guest Editors: Fatchiyah Fatchiyah, Katsuhiro Miyajima, and Masayo Koide





Animal Models of Diabetes and Related Metabolic Diseases

International Journal of Endocrinology

Animal Models of Diabetes and Related Metabolic Diseases

Lead Guest Editor: Tomohiko Sasase

Guest Editors: Fatchiyah Fatchiyah, Katsuhiko Miyajima,
and Masayo Koide



Copyright © 2019 Hindawi. All rights reserved.

This is a special issue published in “International Journal of Endocrinology.” All articles are open access articles distributed under the Creative Commons Attribution License, which permits unrestricted use, distribution, and reproduction in any medium, provided the original work is properly cited.

Editorial Board

D. Acuña-Castroviejo, Spain
Anil K. Agarwal, USA
Ch.-H. Anderwald, Austria
John Ayuk, UK
Arturo Bevilacqua, Italy
Marek Bolanowski, Poland
Amelie Bonnefond, France
Giorgio Borretta, Italy
Marco Bugliani, Italy
Aldo E. Calogero, Italy
Donatella Capalbo, Italy
Carlo Cappelli, Italy
Claudio Casella, Italy
Shern L. Chew, UK
GianLuca Colussi, Italy
Sabrina Corbetta, Italy
Giuseppe Damante, Italy
Patrizia D'Amelio, Italy
Giuseppe D'Annunzio, Italy
Dario de Biase, Italy
Reinhard Depping, Germany
Maria L. Dufau, USA
Dariush Elahi, USA
Katherine Esposito, Italy
Thomas J. Fahey, USA
Henrik Falhammar, Sweden
Marco Faustini-Fustini, Italy
Alberto Ferlin, Italy
Davide Francomano, Italy
Vito A. Giagulli, Italy

Christian Goebel, Austria
Riccarda Granata, Italy
Pawel Grzmil, Poland
Mahin Hashemipour, Iran
Anna Hejmej, Poland
Per Hellström, Sweden
Andreas Höflich, Germany
Michael Horowitz, Australia
Maurizio Iacobone, Italy
Dario Iafusco, Italy
Giorgio Iervasi, Italy
Daniela Jezova, Slovakia
Janaka Karalliedde, UK
Tatsuya Kin, Canada
Małgorzata Kotula-Balak, Poland
Nils Krone, UK
Antonio S. Laganà, Italy
Andrea G. Lania, Italy
Claudio Letizia, Italy
Michaela Luconi, Italy
Mario Maggi, Italy
Flavia Magri, Italy
Ludwik K. Malendowicz, Poland
Paolo Marzullo, Italy
Rosaria Meccariello, Italy
Maria C. Meriggiola, Italy
Antonio Molina-Carballo, Spain
Matteo Monami, Italy
Silvia Monticone, Italy
Robert D. Murray, UK






Andrea Palermo, Italy
Pierlorenzo Pallante, Italy
Sergio D. Paredes, Spain
Faustino R. Perez-Lopez, Spain
Francesco Perticone, Italy
Luigi Petramala, Italy
Raffaele Pezzani, Italy
Stefan Pilz, Austria
Basilio Pintaudi, Italy
Dario Pitocco, Italy
Flavia Prodam, Italy
Giuseppe Reimondo, Italy
Lodovico Rosato, Italy
Mario Rotondi, Italy
Diego Russo, Italy
Ichiro Sakata, Japan
Javier Salvador, Spain
Daniele Santini, Italy
Alexander Schreiber, USA
Muhammad Shahab, Pakistan
Kazuhiro Shiizaki, Japan
Jean-Claude Souberbielle, UK
Ajai K. Srivastav, India
Andrea Tura, Italy
Franco Veglio, Italy
Jack Wall, Australia
Vincent Woo, Canada
Aimin Xu, Hong Kong
Paul M. Yen, USA
H. L. Claahsen-van der Grinten, Netherlands

Contents




Animal Models of Diabetes and Related Metabolic Diseases

Tomohiko Sasase , Fatchiyah Fatchiyah , Katsuhiro Miyajima, and Masayo Koide
Editorial (2 pages), Article ID 6147321, Volume 2019 (2019)




Aerobic Training Associated with Arginine Supplementation Reduces Collagen-Induced Platelet Hyperaggregability in Rats under High Risk to Develop Metabolic Syndrome

Nadia A. V. Motta , Milla M. Fumian, Renata F. Medeiros, Gabriel F. Lima ,
Christianne B. V. Scaramello , Karen J. Oliveira, Antonio C. L. Nóbrega , and Fernanda C. F. Brito 
Research Article (8 pages), Article ID 8919435, Volume 2019 (2019)

Vanadyl Sulfate Effects on Systemic Profiles of Metabolic Syndrome in Old Rats with Fructose-Induced Obesity

Diego Ortega-Pacheco , María Marcela Jiménez-Pérez, Jeanet Serafín-López,
Juan Gabriel Juárez-Rojas , Arturo Ruiz-García, and Ursino Pacheco-García 
Research Article (12 pages), Article ID 5257216, Volume 2018 (2019)



Verification That Mouse Chromosome 14 Is Responsible for Susceptibility to Streptozotocin in NSY Mice

Naru Babaya , Hironori Ueda , Shinsuke Noso, Yoshihisa Hiromine, Michiko Itoi-Babaya,
Misato Kobayashi, Tomomi Fujisawa, and Hiroshi Ikegami 
Research Article (7 pages), Article ID 7654979, Volume 2018 (2019)

Spontaneously Diabetic Torii (SDT) Fatty Rat, a Novel Animal Model of Type 2 Diabetes Mellitus, Shows Blunted Circadian Rhythms and Melatonin Secretion

Katsuya Sakimura , Tatsuya Maekawa , Shin-ichi Kume, and Takeshi Ohta
Research Article (7 pages), Article ID 9065690, Volume 2018 (2019)

Long-Term Dietary Nitrate Supplementation Does Not Prevent Development of the Metabolic Syndrome in Mice Fed a High-Fat Diet

V. B. Matthews , R. Hollingshead, H. Koch, K. D. Croft, and N. C. Ward 
Research Article (8 pages), Article ID 7969750, Volume 2018 (2019)

Focusing on Sodium Glucose Cotransporter-2 and the Sympathetic Nervous System: Potential Impact in Diabetic Retinopathy

Lakshini Y. Herat, Vance B. Matthews , P. Elizabeth Rakoczy, Revathy Carnagarin, and Markus Schlaich
Review Article (8 pages), Article ID 9254126, Volume 2018 (2019)

Editorial

Animal Models of Diabetes and Related Metabolic Diseases

Tomohiko Sasase ¹, **Fatchiyah Fatchiyah** ², **Katsuhiro Miyajima**³ and **Masayo Koide**⁴

¹Biological/Pharmacological Research Laboratories, Central Pharmaceutical Research Institute, Japan Tobacco Inc., Osaka, Japan

²Department of Biology, Faculty of Mathematics and Natural Sciences, Research Center of Smart Molecule of Natural Genetics Resources, Brawijaya University, Malang, East Java, Indonesia

³Department of Nutritional Science and Food Safety, Faculty of Applied Bioscience, Tokyo University of Agriculture, Tokyo, Japan

⁴Department of Pharmacology, University of Vermont College of Medicine, Burlington, VT, USA

Correspondence should be addressed to Tomohiko Sasase; tomohiko.sasase@jt.com

Received 10 December 2018; Accepted 10 December 2018; Published 6 January 2019

Copyright © 2019 Tomohiko Sasase et al. This is an open access article distributed under the Creative Commons Attribution License, which permits unrestricted use, distribution, and reproduction in any medium, provided the original work is properly cited.

Metabolic syndrome including diabetes and its complications (e.g., obesity, dyslipidemia, and hypertension) are common diseases and frequently occur in combination. The animal models of metabolic diseases are essential tools to reveal the pathophysiology and provide novel insights to develop new therapies and drugs. To this day, many animal models such as hereditary models, chemical- or diet-induced models, and gene-engineered models have been developed and studied to elucidate molecular mechanisms and functional alterations associated with metabolic diseases. In this special issue, we aimed to provide information on recent developments on experimental animal models in this field and up-to-date information on the pathophysiology, therapeutic drugs/strategies, and diagnosis of metabolic diseases. Here, we bring together 6 excellent articles related to diabetes and related metabolic diseases from all over the world.

The review article “Focusing on Sodium Glucose Cotransporter-2 and the Sympathetic Nervous System: Potential Impact in Diabetic Retinopathy” by L. Y. Herat et al. comprehensively covers the etiology of diabetic retinopathy (DR) and highlights novel targets, SGLT2 and the sympathetic nervous system, for the management of this pathology. DR is a serious microvascular complication observed in many diabetic patients that can ultimately lead to vision loss. Prevention of DR and other diabetes-related microvascular complications is a major treatment goal. Today, SGLT2 inhibitors provide a new therapeutic option

to control blood glucose levels and prevent the subsequent development of diabetic complications in retinal microvasculature. This in-time review summarizes current evidence on the use of SGLT2 inhibitors and identifies gaps that need to be addressed.

In the article entitled “Spontaneously Diabetic Torii (SDT) Fatty Rat, a Novel Animal Model of Type 2 Diabetes Mellitus, Shows Blunted Circadian Rhythms and Melatonin Secretion,” K. Sakimura et al. demonstrate the deficits in the circadian rhythms and dysregulation of melatonin secretion in SDT fatty rat, a new animal model of type 2 diabetic obesity. Since hyperglycemia, hyperlipidemia, and insulin resistance are all observed in these SDT fatty rats from a young age, this exciting new animal model will undoubtedly be useful for future studies investigating the relationship between deficits in the circadian rhythm and metabolic dysfunction in obese type 2 diabetics.

Nitric oxide (NO) is a potent vasodilator released from vascular endothelial cells and plays a crucial role in vascular homeostasis. In many cardiovascular diseases and type 2 diabetes, NO bioavailability is reduced primarily due to endothelial dysfunction. It is also known that metabolic syndrome including obesity and glucose tolerance is associated with impairment of NO signaling. Dietary supplementation of nitrate is an alternate source of NO when the endothelium-dependent, endogenous NO synthesis system is compromised. V. B. Matthews et al. examined whether the dietary supplementation of nitrate prevents the development

of the metabolic syndrome in mice fed a high-fat diet, in their paper “Long-Term Dietary Nitrate Supplementation Does Not Prevent Development of the Metabolic Syndrome in Mice Fed a High-Fat Diet.” The authors also discuss the importance of short-chain fatty acids in the context of metabolic syndrome.

Abnormal platelet function such as platelet hyperreactivity and hyperaggregability is commonly observed in metabolic syndrome. It has been reported that arginine supplementation and aerobic exercise training enhance vascular NO activity, resulting in the inhibition of platelet hyperaggregability. However, the mechanisms underlying these beneficial effects remain unclear. In the article entitled “Aerobic Training Associated to Arginine Supplementation Reduces Platelet Hyperaggregability Collagen-Induced in Rats under High Risk to Develop Metabolic Syndrome,” Motta et al. examined the impact of aerobic training and/or arginine supplementation on platelet hyperaggregability, inflammatory mediators (i.e., IL-6 and IL-8), serum lipid profile, and serum lipid peroxidation in fructose-administered rats. The authors demonstrate that the combination of aerobic training and arginine supplementation provides benefit by prevention of collagen-induced platelet hyperaggregability and reduction of inflammatory markers that are not observed animal groups receiving either only aerobic training or only arginine supplementation. These findings suggest that the combination of currently available therapeutic options has greater benefit than monotherapy to delay the onset of cardiovascular diseases in patients with metabolic syndrome.

Vanadium derivatives have hypoglycemic effects in animal models and humans. Due to their role on insulin signaling and enzymatic processes regulation, these compounds are clinically used to patients with poorly controlled type 2 diabetes. “Vanadyl Sulfate Effects on Systemic Profiles of Metabolic Syndrome in Old Rats with Fructose-Induced Obesity” written by Ortega-Pacheco et al. describes the anti-obese, hypoglycemic, and hypolipidemic effects of vanadyl sulfate on fructose-induced metabolic syndrome in aged rats. In addition to an antiobesity effect in aged obese rats, vanadyl sulfate improved insulin sensitivity and oral glucose tolerance tests in rats with fructose-induced chronic obesity. Vanadyl sulfate may be a valuable therapeutic agent in preventing insulin resistance, the development and progression of obesity, and metabolic syndrome complications in aged patients with obesity or type 2 diabetes.

N. Babaya et al. demonstrate that NSY-Chr14 is a streptozotocin- (STZ-) susceptible chromosome and that the STZ-susceptible region is located in the distal segment of NSY-Chr14 in their paper “Verification That Mouse Chromosome 14 Is Responsible for Susceptibility to Streptozotocin in NSY Mice.” Construction of new congenic strains will lead to fine mapping and identification of causal variants of the genes responsible for STZ susceptibility in the NSY mouse.

We hope these articles bring further light in the research field of diabetes and related metabolic diseases and contribute to the development of new therapeutic strategies and drugs in the future.






Conflicts of Interest

Tomohiko Sasase is an employee of Japan Tobacco Inc. Fatchiyah Fatchiyah has no potential COI to disclose. Katsuhiko Miyajima has no potential COI to disclose. Masayo Koide has no potential COI to disclose.

*Tomohiko Sasase
Fatchiyah Fatchiyah
Katsuhiko Miyajima
Masayo Koide*

Research Article

Aerobic Training Associated with Arginine Supplementation Reduces Collagen-Induced Platelet Hyperaggregability in Rats under High Risk to Develop Metabolic Syndrome

Nadia A. V. Motta ¹, Milla M. Fumian,¹ Renata F. Medeiros,² Gabriel F. Lima ¹,
Christianne B. V. Scaramello ^{1,2}, Karen J. Oliveira,² Antonio C. L. Nóbrega ²,
and Fernanda C. F. Brito ^{1,2}

¹Laboratory of Experimental Pharmacology (LAFE), Department of Physiology and Pharmacology, Biomedical Institute, Fluminense Federal University (UFF), Room 204-A, 24420-210 Niterói, RJ, Brazil

²Department of Physiology and Pharmacology, Fluminense Federal University (UFF), 24420-210 Niterói, Rio de Janeiro, Brazil

Correspondence should be addressed to Fernanda C. F. Brito; nandacarla16@yahoo.com.br

Received 5 July 2018; Revised 24 September 2018; Accepted 11 November 2018; Published 6 January 2019

Guest Editor: Masayo Koide

Copyright © 2019 Nadia A. V. Motta et al. This is an open access article distributed under the Creative Commons Attribution License, which permits unrestricted use, distribution, and reproduction in any medium, provided the original work is properly cited.

Background. Increased platelet response is seen in individuals with metabolic syndrome. Previous reports have shown that arginine supplementation and aerobic exercise training enhance vascular nitric oxide (NO) activity and inhibit platelet hyperaggregability; however, the effects of their association remain unknown. **Aim.** To investigate whether arginine supplementation and aerobic exercise association may exert beneficial effects, reducing platelet hyperaggregability in rats under high risk to develop metabolic syndrome. **Methods.** Wistar rats were divided into two groups: control (C) and fructose (F – water with 10% of fructose). After two weeks, the F group was subdivided into four groups: F, the same as before; fructose + arginine (FA – 880 mg/kg/day of L-arginine by gavage); fructose + training (FT); and fructose + arginine + training (FTA). Treatment lasted for eight weeks. **Results.** The fructose administration was able to increase the collagen-induced platelet aggregation ($27.4 \pm 2.7\%$) when compared to the C group ($8.0 \pm 3.4\%$). Although the arginine supplementation ($32.2 \pm 6.3\%$) or aerobic training ($23.8 \pm 6.5\%$) did not promote any change in platelet collagen-induced hyperaggregability, the association of arginine supplementation and aerobic exercise promoted an inhibition of the platelet hyperaggregability induced by fructose administration ($13.9 \pm 4.4\%$) ($P < 0.05$). These effects were not observed when ADP was employed as an agonist. In addition, arginine supplementation associated with aerobic exercise promoted a decrease in interleukin-6 (IL-6) and interleukin-8 (IL-8) serum levels when compared to the fructose group, demonstrating an anti-inflammatory effect. **Conclusions.** Our data indicate an important role of arginine supplementation associated with aerobic exercise, reducing platelet hyperaggregability and inflammatory biomarker levels in rats under high risk to develop metabolic syndrome.

1. Introduction

Platelets are small, anucleated cell fragments that are activated in response to a wide variety of stimuli, triggering a complex series of intracellular pathways leading to a hemostatic thrombus formation at vascular injury sites. Reported abnormalities in platelet functions, such as platelet hyperactivity and hyperaggregability to several agonists, contribute to the pathogenesis and complications of thrombotic events

associated with hypertension [1]. Metabolic syndrome (MS) represents a collection of cardiovascular risk factors: hypertension, hyperglycemia, dyslipidemia, and abdominal obesity. More than 312 million adults worldwide have been diagnosed with MS, and it is estimated that this number will rise to 1 billion by 2025 [2]. MS is linked to chronic inflammation. Normal physiological coagulation is altered when the inflammatory mediators modify the endothelium in the damaged area which becomes proinflammatory and

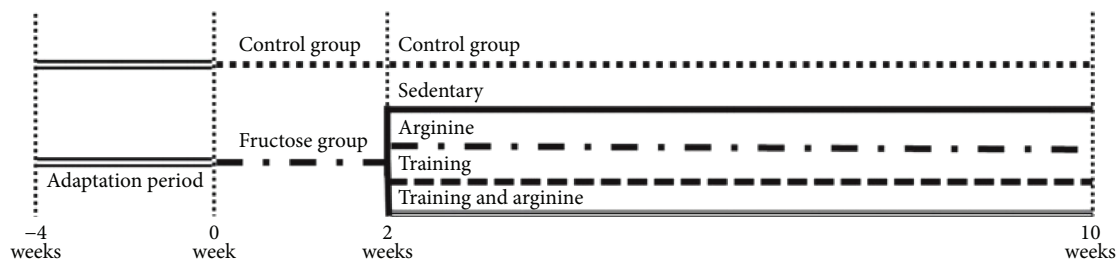


FIGURE 1: Experimental protocol.

prothrombotic [3]. Increased platelet response is seen in individuals with MS, supported by the main features of MS: insulin resistance, hyperglycemia, dyslipidemia, oxidative stress, products of adipose tissue (adipokines), and inflammation [4]. In hypercholesterolemic rabbits and humans, arginine administration enhances vascular nitric oxide activity and inhibits platelet reactivity [5, 6]. L-Arginine is also known to directly inhibit platelet reactivity, probably through its metabolism to nitric oxide (NO) by platelet-derived nitric oxide synthase (NOS) [6]. It is well known that an exercise conditioning program results in a downregulated hemostatic potential by reducing platelet activation, diminishing procoagulant platelet levels and increasing fibrinolysis activity, therefore contributing to a reduced risk of thrombotic events [7, 8]. High fructose consumption has been correlated to the onset of cardiometabolic alterations in world population. Chronic fructose ingestion has been used as a model of cardiovascular disease, characterized by increased serum insulin and triglyceride levels as well as vascular disorder development [9]. Some mechanisms associated with arginine supplementation and aerobic training effects on different cardiovascular disease models have been described, but their effects at platelet aggregation remain unclear. Thus, our hypothesis is that arginine supplementation and aerobic exercise may exert beneficial effects on MS development through reducing platelet hyperaggregability.

2. Material and Methods

2.1. Experimental Design. The handling and experimental protocols were approved by the Ethics Committee for Care and Use of Laboratory Animals at Fluminense Federal University (protocol 466/2013) and complied with the ethical guidelines of the Brazilian Society of Laboratory Animal Science. Before beginning the experimental protocol, all animals were submitted to an adaptation period for 4 weeks and then we started the protocol. Experiments were performed on 3-month-old male Wistar rats ($n = 7/\text{group}$; $329.9 \pm 8.9 \text{ g}$). The experimental model has been previously described by our group [9]. Animals were maintained under controlled temperature conditions ($24 \pm 1^\circ \text{C}$) on a 12-hour light cycle (lights on at 7 a.m.).

Animals were randomly allocated, initially, into two groups: a control group (C) that received water and commercial chow for two weeks and a fructose group (F) that received an overload of 10% of D-fructose in drinking water and commercial chow for two weeks. After two weeks, seven

TABLE 1: Nutritional information of Nuvilab Cr-1 commercial chow.

Nutritional information	1 kg of chow
Calories	3.360 kcal
Carbohydrates	530.0 g
Proteins	220.0 g
Lipids	40.0 g

Ingredients

Ground whole corn, soybean meal, wheat bran, calcium carbonate, dicalcium phosphate, sodium chloride, vitamins A, D3, E, K2, B1, B6, B12, niacin, calcium pantothenate, folic acid, biotin, chloride choline, iron sulfate, manganese monoxide, zinc oxide, calcium sulfate, sodium selenite, cobalt sulfate, lysine, methionine, and butylated hydroxytoluene.

Nutritional information and ingredient composition were obtained from chow label.

animals from each group were euthanized, and the remaining animals from the control group ($n = 7$) were kept in the same previously described conditions for an additional eight weeks. Rats from the fructose group were subdivided into four further groups, and all of them continued receiving D-fructose in drinking water for an additional eight weeks. The fructose arginine (FA) group received 880 mg/kg/day of arginine by orogastric gavage. The fructose training (FT) group was submitted to aerobic exercise training, and the fructose training arginine (FTA) group was subjected to a combination of aerobic training with arginine supplementation (Figure 1).

2.2. Dietary Assessment. All experimental groups were maintained under the same commercial chow (Nuvilab Cr-1®, NuVital, Paraná, Brazil) *ad libitum*, according to Table 1. Caloric intake was assessed twice weekly, and it was calculated by considering that 1.0 g of chow corresponds to 3.36 kcal and 1.0 g of fructose corresponds to 4.0 kcal.

Fructose groups received 10% diluted D-fructose (Sigma-Aldrich, St. Louis, MO, USA) in water *ad libitum* [10]. The L-arginine-supplemented groups received 880 mg/kg/day (Sigma-Aldrich, St. Louis, MO, USA) for the last 8 weeks; this dose was calculated according to the formula for dose translation based on body surface area [11], considering 10 g for an adult person [12]. In this context, it is important to notice that this amino acid is naturally found in human nutrition in edible mushrooms [13] and in meals as beef, pork, and poultry [14].

TABLE 2: Evaluation of body weight, lipids, and MDA serum levels.

Parameters evaluated	Experimental groups				
	C	F	FA	FT	FTA
Initial body weight (g)	334.5 ± 3.2	334.3 ± 3.1	311.7 ± 15.1	332.9 ± 11.3	336.0 ± 11.7
Δ weight (g)	83.2 ± 3.5	85.1 ± 4.2	85.5 ± 3.7	86.3 ± 4.4	81.3 ± 3.1
Total cholesterol (mg/dl)	30.5 ± 5.7	51.0 ± 4.7	32.3 ± 6.6	57.2 ± 5.8	44.4 ± 14.6
LDL (mg/dl)	22.1 ± 4.0	26.2 ± 9.4	19.7 ± 3.5	28.4 ± 12.0	27.0 ± 9.8
HDL (mg/dl)	11.2 ± 0.5	13.2 ± 1.1	14.4 ± 1.7	21.9 ± 2.9 ^{*#}	17.8 ± 1.5
MDA (nmol/dl)	11.2 ± 0.7	14.8 ± 1.5	14.3 ± 1.1	9.6 ± 0.9 ^{*#}	17.3 ± 2.0

Data are presented as means ± SEM. Δ weight (g) = (final body weight – initial body weight). Statistical analysis (one-way ANOVA and post hoc Bonferroni multiple-comparison test): * $P < 0.05$ v. C group; # $P < 0.05$ v. F group.

2.3. Aerobic Exercise Protocol. Before beginning the experimental protocol, all animals were submitted to an adaptation period on a treadmill (Inbrasport®, Brasília, Brazil) for 4 weeks (5 minutes/day; 0.3 km/h–1.0 km/h, increased weekly). All animals underwent a maximal exercise test (MET) on a treadmill with an 11% inclination and an initial speed of 1.0 km/h, with an increment of velocity of 0.1 km/h every two minutes. The MET protocol was performed before the beginning of the experiment, two weeks thereafter, and at the end of the experiment to determine maximum running speed [9].

The groups assigned to aerobic training initiated a moderate-intensity exercise training regimen (50–75% maximal running speed), with a 0 to 7% inclination on a treadmill 4 days per week during the last 8 weeks of the experiment protocol [9]. All animals allocated to sedentary groups, in order to maintain their adaptation to the treadmill, were submitted to five minutes in the treadmill with low intensity (0.3 km/h), once a week.

At the end of the experimental period, all the animals were euthanized by cervical dislocation under anesthesia (thiopental sodium, 80 mg/kg) (Sigma-Aldrich, St. Louis, MO, USA). The blood samples were collected from each animal.

2.4. Biochemical Analysis. Serum lipid profile (levels of total cholesterol (TC), triglycerides (TG), low-density lipoprotein cholesterol (LDL), and high-density lipoprotein cholesterol (HDL)) was determined by using standard assay kits (Labtest, Minas Gerais, Brazil). The units were expressed in mg/dl.

2.5. Determination of Lipid Peroxidation in Serum Samples. The mean concentration of malondialdehyde (MDA), a measure of lipid peroxidation, was assayed in the form of thiobarbituric acid-reacting substances (TBARS) [15].

2.6. Platelet Aggregation Studies. The rat blood was removed by cardiac puncture and was collected into tubes containing a 3.8% trisodium citrate (9:1 v/v) solution. The rat platelet-rich plasma was prepared by centrifugation at $250 \times g$ for 10 min at room temperature. The platelet-poor plasma was prepared by centrifugation of the pellet at $1500 \times g$ for 10 min at room temperature.

Platelet aggregation was monitored by the turbidimetric method described by Born and Cross [16], using a platelet lumi-aggregometer (Model 560CA; Chrono-log Corporation, Havertown, PA, USA).

The platelet-rich plasma (400 μ l) was incubated at 37°C for 1 min with continuous stirring at 1200 rpm. The aggregation of the platelet-rich plasma was induced using platelet agonists as adenosine diphosphate (ADP) at (0.5 and 1 μ M) and collagen at (0.5 and 1 μ g/ml) (Sigma-Aldrich). Platelet aggregation was expressed as percentage of aggregation in response to ADP or collagen.

2.7. Interleukin-6 (IL-6) and Interleukin-8 (IL-8) Measurements. The serum levels of IL-6 and IL-8 were assessed using the commercially available Quantikine Rat IL-6 and IL-8 Immunoassay. The levels of IL-6 and IL-8 in the serum were assessed by measuring the absorbance at 450 nm using an ELISA reader (Tp Reader, Thermo Plate®) and extrapolating from a standard curve.

2.8. Statistical Analysis. The five experimental groups were compared using one-way ANOVA followed by a post hoc Bonferroni multiple-comparison test, when appropriate. All variables are expressed as means ± SEM. For all analyses, a value of $P < 0.05$ was considered to be statistically significant. All analyses were performed using the GraphPad Prism 5.0 software (GraphPad, San Diego, CA, USA).

3. Results

As described in Table 2, no significant difference in body weights of the five experimental groups was observed through the experimental period. Evaluating the serum levels of total cholesterol and LDL, we could not notice any statistical difference among the groups. However, an increase in serum HDL levels associated with the training ($13.2 \pm 1.1 \times 21.9 \pm 2.9$ mg/dl) when compared to the Fructose group was observed, as well as a decrease in MDA concentrations in the serum of the training group ($14.8 \pm 1.5 \times 9.6 \pm 0.9$ nmol/dl) (Table 2).

Evaluating the fructose administration effects in collagen-induced platelet aggregation (0.5 μ g/ml), we could evidence an enhancement of platelet aggregation ($27.4 \pm 2.7\%$) when compared to the C group ($8.0 \pm 3.4\%$). Arginine supplementation ($32.2 \pm 6.3\%$) or aerobic training

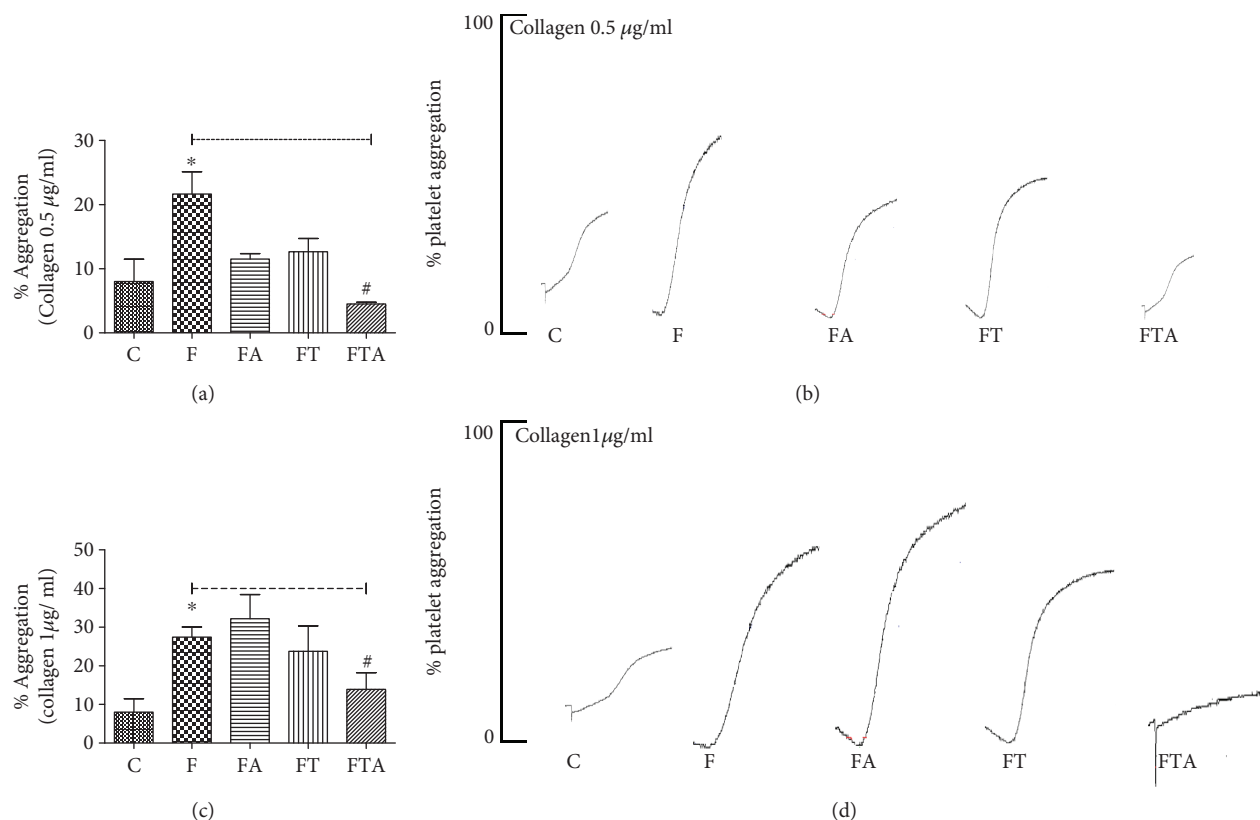


FIGURE 2: Platelet aggregation induced by collagen 0.5 $\mu\text{g/ml}$ (a, b) and collagen 1 $\mu\text{g/ml}$ (c, d) after 8 weeks of fructose overload. C group: control group; F group: fructose group; FA group: fructose + arginine group; FT group: fructose + training group; FTA group: fructose + training + arginine group. Data are presented as means \pm SEM. Statistical analysis (one-way ANOVA and post hoc Bonferroni multiple-comparison test): * $P < 0.05$ v. the C group and # $P < 0.05$ v. the F group.

($23.8 \pm 6.5\%$) was not able to promote any change at the platelet hyperaggregability. On the other hand, arginine supplementation associated with aerobic exercise promoted an inhibition in the platelet hyperaggregability induced by fructose administration (Figures 2(a) and 2(b)). Similar results were observed at 1 $\mu\text{g/ml}$ collagen concentration (Figures 2(c) and 2(d)).

We have also evaluated the effects of fructose administration in platelet aggregation ADP-mediated (0.5 μM and 1 μM). When ADP was employed as an agonist, we could not notice any effect at the different employed conditions (Figure 3).

In our study, we have observed that fructose administration promoted a significant increase in IL-6 (15.87 ± 0.35 pg/dl) and IL-8 (592.40 ± 12.69 pg/dl) levels when compared to the control group (IL-6: 12.96 ± 1.60 ; IL-8: 500.20 ± 15.91 pg/dl). Concerning IL-6 serum levels, we have observed that arginine supplementation (10.89 ± 0.87 pg/dl) and aerobic exercise (IL-6: 11.16 ± 1.15 pg/dl) alone as well as associated (9.56 ± 0.61 pg/dl) reduced these interleukin levels. When we evaluated IL-8 levels, only arginine supplementation associated with aerobic exercise was able to reduce IL-8 levels (472.10 ± 19.41 pg/dl). There was no difference between arginine supplementation and aerobic exercise isolated when compared to the fructose group ($P > 0.05$, Figure 4).

4. Discussion

The present study was designed to investigate the antiplatelet effects associated with arginine supplementation, aerobic exercise, and these two concomitant interventions in rats at high risk of developing metabolic syndrome.

In our study, we have observed an increase in serum HDL levels and a decrease in MDA concentrations in the serum of the training group. These results corroborate the work of Farah et al. [17], which demonstrated that moderate aerobic exercise training prevented unfavorable changes in oxidative stress profile in rats submitted to a fructose overload and also the Ranjbar et al. [18] study, which described that L-arginine appears to have additive effects on cardiac function but has no effect on oxidative stress indices.

Evaluating the fructose administration effects at collagen-induced platelet aggregation, we could evidence an enhancement of platelet aggregation when compared to the C group. The arginine supplementation or aerobic training was not able to promote any change at the platelet hyperaggregability. On the other hand, arginine supplementation associated with aerobic exercise promoted an inhibition of the platelet hyperaggregability induced by fructose administration. We have also evaluated the effects of fructose administration at ADP-induced platelet aggregation. When ADP

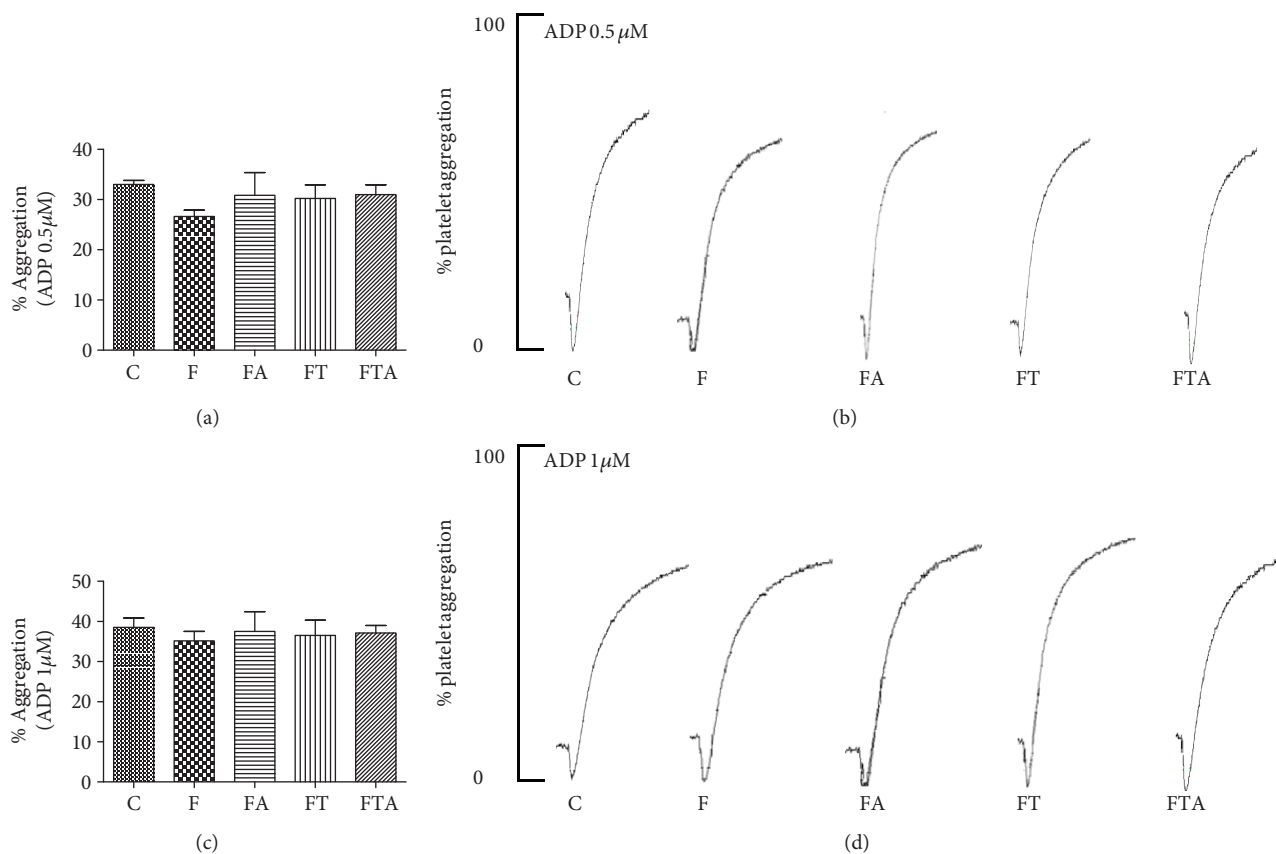


FIGURE 3: Platelet aggregation induced by ADP 0.5 μM (a, b) and ADP 1 μM (c, d) after 8 weeks of fructose overload. C group: control group; F group: fructose group; FA group: fructose + arginine group; FT group: fructose + training group; FTA group: fructose + training + arginine group. Data are presented as means \pm SEM. Statistical analysis (one-way ANOVA and post hoc Bonferroni multiple comparison test): * $P < 0.05$ v. the C group and # $P < 0.05$ v. the F group.

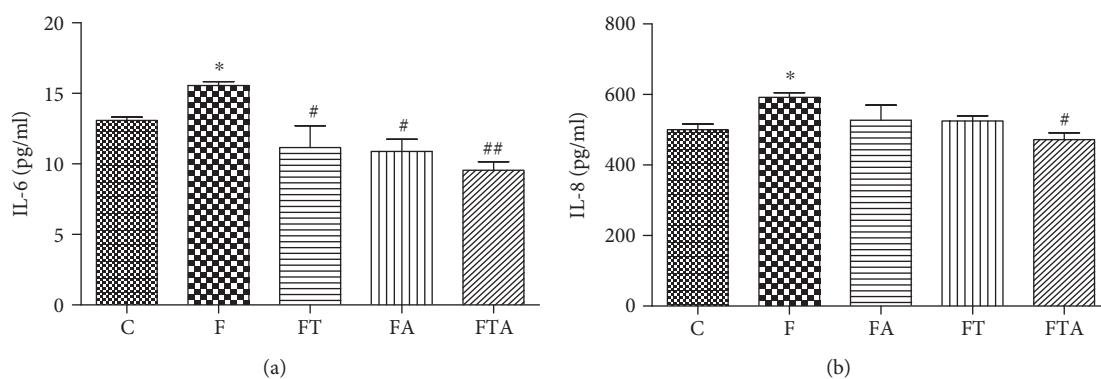


FIGURE 4: Effects of fructose intake, arginine supplementation, and aerobic exercise on IL-6, and IL-8 production in serum. C group: control group; F group: fructose group; FA group: fructose + arginine group; FT group: fructose + training group; FTA group: fructose + training + arginine group. Data are presented as means \pm SEM. Statistical analysis (one-way ANOVA and post hoc Bonferroni multiple comparison test): * $P < 0.05$ v. the C group # $P < 0.05$ and ## $P < 0.01$ v. the F group.

was employed as an agonist, we could not notice any effect at the different experimental groups.

Our data suggest that high fructose consumption results in an enhanced platelet response to collagen. This effect is reverted through the association of arginine supplementation with aerobic exercise. Interestingly, we could not observe this hyperaggregability effect when ADP is employed as

an agonist, and the different treatments isolated were not able to have any antiplatelet effect. These results point out the antiplatelet effects when arginine supplementation is associated with aerobic exercise. Our research group [19] showed a vasodilator activity associated with an improvement of endothelial function and an increased NO bioavailability, observed in the group that received

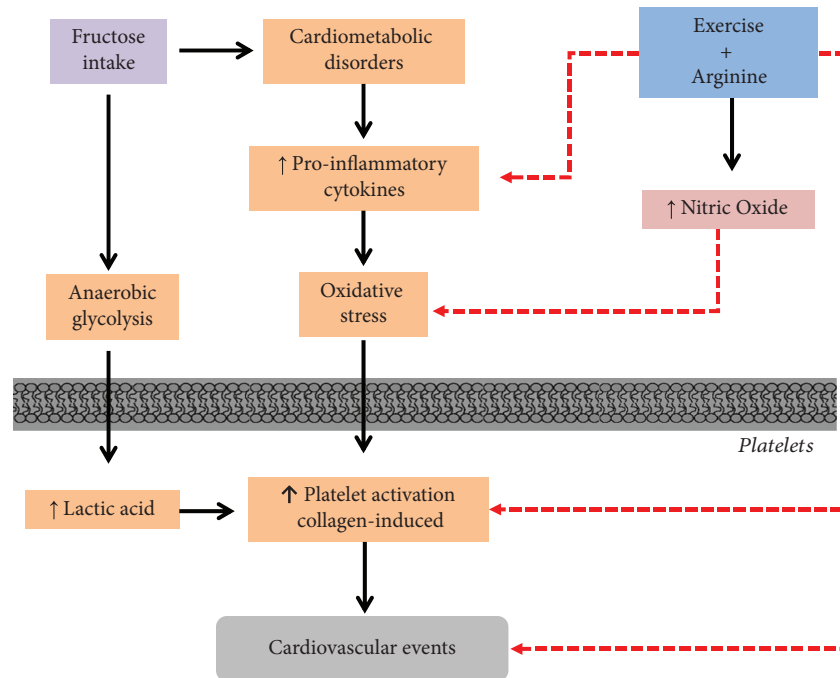


FIGURE 5: The hypothesis of inhibitory effect of exercise and arginine association in platelet activation of rats under high risk to develop metabolic syndrome. The high fructose intake triggers several cardiometabolic disorders, reflecting in an increase in lactic acid, proinflammatory cytokines, and oxidative stress. These events contribute to collagen-induced platelet activation. In addition, the increase in lactic acid produced by anaerobic glycolysis in platelets might be a mediator in platelet hyperaggregability. On the other hand, aerobic training associated with arginine supplementation decreases platelet hyperaggregability collagen-induced probably related to enhancement of NO production, inhibition of proinflammatory cytokines and oxidative stress, and finally inhibition of platelet aggregation.

arginine supplementation, as well as in the aerobic exercise group treated with fructose. On the other hand, no additive effect in vascular relaxation in the interventions associated was observed [19].

Several studies have shown that IL-6 and IL-8 are important mediators of inflammation and contribute to the development of cardiovascular diseases. Independently of body mass index, sedentary lifestyle is a risk factor [20] and a strong predictor [21] for chronic disease and premature mortality. These proinflammatory cytokines exert a key player in the pathogenesis of cardiometabolic diseases [22] and thrombogenesis [23]. Additionally, activated platelets induce endothelial secretion of IL-8 in vitro. These data provide an important relationship between inflammation and cardiovascular events. In our experimental model, we observed that fructose intake was able to increase serum inflammatory mediators such as IL-6 and IL-8, corroborating to previous reports that demonstrated an increase in these cytokine levels in several pathological conditions [24–26]. In our experimental conditions, we observed that arginine supplementation, aerobic exercise, and the two associated interventions were able to reduce serum IL-6 levels. Concerning IL-8, only arginine supplementation associated with aerobic exercise reduced these proinflammatory marker levels, which was similar to our results observed in the platelet aggregation study. These observations are in line with previous work which reinforces that exercise plays an advantageous role in thrombogenesis by reducing inflammatory processes and potentiating fibrinolytic features [27], besides highlighting

L-arginine's role in inflammatory cytokine inhibition through modulation of nuclear factor kappa B (NF- κ B) [28].

Collagen is a component of the subendothelium which becomes exposed to flowing blood in the context of vascular injury. Collagen binds directly to two platelet surface receptors: integrin $\alpha_2\beta_1$ and glycoprotein (GP) VI. Collagen also binds to the von Willebrand factor under shear, which binds to the GPIb-IX-V complex on platelets, resulting in vascular tethering and initiates signal transduction [29]. Collagen evokes a stable aggregation in rat platelets, and the main signaling pathways involved are ADP secretion and thromboxane A₂ (TXA₂) production [30]. Kobzar et al. [31] demonstrated that short-term exposure of platelets to monosaccharides as glucose, fructose, and galactose impairs inhibition of platelet aggregation by cyclooxygenase inhibitors like aspirin. These authors aimed to explain the reason why aspirin treatment is not effective in reducing cardiovascular events in diabetic patients. They suggested that lactic acid produced by anaerobic glycolysis in platelets might be a mediator of the effect of monosaccharides on aspirin inhibition in platelets, probably through an enhancement of arachidonic acid production.

There is evidence that spontaneous platelet aggregation was significantly higher in MS patients compared with healthy volunteers. The curves of the mean aggregate sizes and light transmission characteristics suggested that the rates of collagen-induced aggregation of isolated platelets in MS patients significantly exceeded the corresponding values in the group of healthy volunteers [32].

Patients with MS have high risk of microcirculation complications and microangiopathies. Inflammation influences coagulation by increasing the production of coagulation proteins, reducing the activity of the anticoagulant pathway and by preventing fibrinolysis. Together, these alterations could lead to the formation of pathological thrombi resulting in heart or brain infarcts. The presence of MS could affect the coagulation system in some way before atherosclerosis development [33].

ADP is considered a weak agonist which promotes platelet aggregation through activation of purinergic receptors [34]. Collagen represents a strong platelet agonist, activating different signal pathways. Our results demonstrated collagen-induced platelet hyperaggregability in rats under high risk of developing metabolic syndrome. These contribute to better understanding of the role of platelet alterations in MS development.

Interestingly, the association of aerobic exercise and arginine supplementation abolished this effect, but none of the isolated conditions presented any antiplatelet effect. These data support the idea that aerobic training associated with arginine supplementation decreases collagen-induced platelet hyperaggregability in an experimental model, with a continued exposure to a causal factor of metabolic alterations, therefore preventing cardiovascular disease development. The antiplatelet effect observed is probably related to the association of an enhancement of NO production and a reduction in oxidative stress and inflammatory cytokines, resulting in a reduction in platelet TXA₂ production and platelet activation and aggregation (Figure 5). Similar results were observed by our group in vascular beds [9, 19].

5. Conclusion

High fructose intake leads to cardiometabolic alterations that precede cardiovascular disease. High fructose administration enhanced platelet aggregation and arginine supplementation associated with aerobic exercise can reduce platelet hyperaggregability in rats under high risk to develop metabolic syndrome.

Since a large number of individuals that are affected by MS suffer cardiovascular events, finding new therapeutic targets by elucidating new factors that contribute to these incidents is crucial to the treatment and prevention of cardiovascular events.

Data Availability

The platelet aggregation data used to support the findings of this study are partially included within the article, but all the platelet aggregation registers and spectrophotometric registers used to support the findings of this study are available from the corresponding author upon request.

Conflicts of Interest

The authors of this manuscript have certified that they comply with the Principles of Ethical Publishing in the International Journal of Endocrinology.

Acknowledgments

This study was financed in part by the Coordenação de Aperfeiçoamento de Pessoal de Nível Superior - Brasil (CAPES) - Finance Code 001; FAPERJ (BR, #E-26/110.420/2014; E-26/110743/2012); and Universidade Federal Fluminense/ FOPESQ 2013, 2014 (BR).

References

- [1] D. Varga-Szabo, I. Pleines, and B. Nieswandt, "Cell adhesion mechanisms in platelets," *Arteriosclerosis, Thrombosis, and Vascular Biology*, vol. 28, no. 3, pp. 403–412, 2008.
- [2] S. M. Grundy, "Does the metabolic syndrome exist?," *Diabetes Care*, vol. 29, no. 7, pp. 1689–1692, 2006.
- [3] M.-J. van Rooy, W. Duim, R. Ehlers, A. V. Buys, and E. Pretorius, "Platelet hyperactivity and fibrin clot structure in transient ischemic attack individuals in the presence of metabolic syndrome: a microscopy and thromboelastography® study," *Cardiovascular Diabetology*, vol. 14, no. 1, p. 86, 2015.
- [4] R. B. Arteaga, J. A. Chirinos, A. O. Soriano et al., "Endothelial microparticles and platelet and leukocyte activation in patients with the metabolic syndrome," *The American Journal of Cardiology*, vol. 98, no. 1, pp. 70–74, 2006.
- [5] X. J. Girerd, A. T. Hirsch, J. P. Cooke, V. J. Dzau, and M. A. Creager, "L-Arginine augments endothelium-dependent vasodilation in cholesterol-fed rabbits," *Circulation Research*, vol. 67, no. 6, pp. 1301–1308, 1990.
- [6] A. Wolf, C. Zalpour, G. Theilmeyer et al., "Dietary L-arginine supplementation normalizes platelet aggregation in hypercholesterolemic humans," *Journal of the American College of Cardiology*, vol. 29, no. 3, pp. 479–485, 1997.
- [7] J. J. Posthuma, P. E. J. van der Meijden, H. ten Cate, and H. M. H. Spronk, "Short- and long-term exercise induced alterations in haemostasis: a review of the literature," *Blood Reviews*, vol. 29, no. 3, pp. 171–178, 2015.
- [8] J. P. Bantle, J. E. Swanson, W. Thomas, and D. C. Laine, "Metabolic effects of dietary fructose in diabetic subjects," *Diabetes Care*, vol. 15, no. 11, pp. 1468–1476, 1992.
- [9] R. F. Medeiros, T. G. Gaique, T. Bento-Bernardes et al., "Aerobic training prevents oxidative profile and improves nitric oxide and vascular reactivity in rats with cardiometabolic alteration," *Journal of Applied Physiology*, vol. 121, no. 1, pp. 289–298, 2016.
- [10] A. Ahangarpour, M. Mohammadian, and M. Dianat, "Antidiabetic effect of hydroalcoholic *Urtica dioica* leaf extract in male rats with fructose-induced insulin resistance," *Iranian Journal of Medical Sciences*, vol. 37, no. 3, pp. 181–186, 2012.
- [11] S. Reagan-Shaw, M. Nihal, and N. Ahmad, "Dose translation from animal to human studies revisited," *The FASEB Journal*, vol. 22, no. 3, pp. 659–661, 2008.
- [12] A. Siani, E. Pagano, R. Iacone, L. Iacoviello, F. Scopacasa, and P. Strazzullo, "Blood pressure and metabolic changes during dietary L-arginine supplementation in humans," *American Journal of Hypertension*, vol. 13, no. 5, pp. 547–551, 2000.
- [13] L. Sun, Q. Liu, C. Bao, and J. Fan, "Comparison of free total amino acid compositions and their functional classifications in 13 wild edible mushrooms," *Molecules*, vol. 22, no. 3, p. 350, 2017.

- [14] A. Varnam and J. M. Sutherland, *Meat and Meat Products: Technology, Chemistry and Microbiology, Vol 3*, Springer, 1995.
- [15] H. Ohkawa, N. Ohishi, and K. Yagi, "Assay for lipid peroxides in animal tissues by thiobarbituric acid reaction," *Analytical Biochemistry*, vol. 95, no. 2, pp. 351–358, 1979.
- [16] G. V. R. Born and M. J. Cross, "The aggregation of blood platelets," *The Journal of Physiology*, vol. 168, no. 1, pp. 178–195, 1963.
- [17] D. Farah, J. Nunes, M. Sartori et al., "Exercise training prevents cardiovascular derangements induced by fructose overload in developing rats," *PLoS One*, vol. 11, article e0167291, no. 12, 2016.
- [18] K. Ranjbar, F. Nazem, and A. Nazari, "Effect of exercise training and L-arginine on oxidative stress and left ventricular function in the post-ischemic failing rat heart," *Cardiovascular Toxicology*, vol. 16, no. 2, pp. 122–129, 2016.
- [19] R. F. Medeiros, T. G. Gaique, T. Bento-Bernardes et al., "Arginine and aerobic training prevent endothelial and metabolic alterations in rats at high risk for the development of the metabolic syndrome," *British Journal of Nutrition*, vol. 118, no. 1, pp. 1–10, 2017.
- [20] B. K. Pedersen, "Body mass index-independent effect of fitness and physical activity for all-cause mortality," *Scandinavian Journal of Medicine & Science in Sports*, vol. 17, no. 3, pp. 196–204, 2007.
- [21] J. Myers, A. Kaykha, S. George et al., "Fitness versus physical activity patterns in predicting mortality in men," *American Journal of Medicine*, vol. 117, no. 12, pp. 912–918, 2004.
- [22] P. Libby, Y. Okamoto, V. Z. Rocha, and E. Folco, "Inflammation in atherosclerosis: transition from theory to practice," *Circulation Journal*, vol. 74, no. 2, pp. 213–220, 2010.
- [23] R. J. Shebuski and K. S. Kilgore, "Role of inflammatory mediators in thrombogenesis," *Journal of Pharmacology and Experimental Therapeutics*, vol. 300, no. 3, pp. 729–735, 2002.
- [24] D. Reihmane and F. Dela, "Interleukin-6: possible biological roles during exercise," *European Journal of Sport Science*, vol. 14, no. 3, pp. 242–250, 2014.
- [25] G. Kaplanski, R. Porat, K. Aiura, J. K. Erban, J. A. Gelfand, and C. A. Dinarello, "Activated platelets induce endothelial secretion of interleukin-8 in vitro via an interleukin-1-mediated event," *Blood*, vol. 81, no. 10, pp. 2492–2495, 1993.
- [26] R. Supriya, B. T. Tam, A. P. Yu et al., "Adipokines demonstrate the interacting influence of central obesity with other cardio-metabolic risk factors of metabolic syndrome in Hong Kong Chinese adults," *PLoS One*, vol. 13, no. 8, article e0201585, 2018.
- [27] Y. W. Chen, S. Apostolakis, and G. Y. H. Lip, "Exercise-induced changes in inflammatory processes: implications for thrombogenesis in cardiovascular disease," *Annals of Medicine*, vol. 46, no. 7, pp. 439–455, 2014.
- [28] K. Hnia, J. Gayraud, G. Hugon et al., "L-Arginine decreases inflammation and modulates the nuclear factor- κ B/matrix metalloproteinase cascade in Mdx muscle fibers," *The American Journal of Pathology*, vol. 172, no. 6, pp. 1509–1519, 2008.
- [29] J. Chen and J. A. López, "Interactions of platelets with subendothelium and endothelium," *Microcirculation*, vol. 12, no. 3, pp. 235–246, 2005.
- [30] S. Roger, M. Pawlowski, A. Habib, M. Jandrot-Perrus, J. P. Rosa, and M. Bryckaert, "Costimulation of the Gi-coupled ADP receptor and the Gq-coupled TXA₂ receptor is required for ERK2 activation in collagen-induced platelet aggregation," *FEBS Letters*, vol. 556, no. 1-3, pp. 227–235, 2004.
- [31] G. Kobzar, V. Mardla, and N. Samel, "Short-term exposure of platelets to glucose impairs inhibition of platelet aggregation by cyclooxygenase inhibitors," *Platelets*, vol. 22, no. 5, pp. 338–344, 2011.
- [32] T. E. Suslova, A. V. Sitozhevskii, O. N. Ogurkova et al., "Platelet hemostasis in patients with metabolic syndrome and type 2 diabetes mellitus: cGMP- and NO-dependent mechanisms in the insulin mediated platelet aggregation," *Frontiers in Physiology*, vol. 5, p. 501, 2015.
- [33] M. Idzko, D. Ferrari, and H. K. Eltzschig, "Nucleotide signaling during inflammation," *Nature*, vol. 509, no. 7500, pp. 310–317, 2014.
- [34] I. Mattiasson, S. Lethagen, and A. Hillarp, "Increased sensitivity to ADP-aggregation in aspirin treated patients with recurrent ischemic stroke?," *International Angiology*, vol. 22, no. 3, pp. 239–242, 2003.

Research Article

Vanadyl Sulfate Effects on Systemic Profiles of Metabolic Syndrome in Old Rats with Fructose-Induced Obesity

Diego Ortega-Pacheco ¹, María Marcela Jiménez-Pérez,² Jeanet Serafín-López,³ Juan Gabriel Juárez-Rojas ⁴, Arturo Ruiz-García,² and Ursino Pacheco-García ²

¹Universidad de la Sierra Sur, Miahuatlán city, State of Oaxaca, Mexico

²Renal Pathophysiology Laboratory, Department of Nephrology, Instituto Nacional de Cardiología “Ignacio Chávez”, Mexico City, Mexico

³Department of Immunology, Escuela Nacional de Ciencias Biológicas (ENCB), Instituto Politécnico Nacional (IPN), Mexico City, Mexico

⁴Department of Endocrinology, Instituto Nacional de Cardiología “Ignacio Chávez”, Mexico City, Mexico

Correspondence should be addressed to Ursino Pacheco-García; upacheco@yahoo.com.mx

Received 6 July 2018; Revised 23 September 2018; Accepted 15 October 2018; Published 25 December 2018

Guest Editor: Fatchiyah Fatchiyah

Copyright © 2018 Diego Ortega-Pacheco et al. This is an open access article distributed under the Creative Commons Attribution License, which permits unrestricted use, distribution, and reproduction in any medium, provided the original work is properly cited.

Background. Currently, energy obtained from hypercaloric diets has been part of the obesity and type 2 diabetes mellitus (T2DM) epidemics from childhood to old age. Treatment alternatives have been sought from plants, minerals, and trace elements with metabolic effects. Vanadyl sulfate (VS) has been investigated as a hypoglycemic compound in animal and human studies showing effective insulin-mimetic properties. This characteristic encompasses several molecules that have beneficial pleiotropic effects. *The aim* was to determine the antiobesity, hypoglycemic, and hypolipidemic effects of VS on fructose-induced metabolic syndrome in aged rats. *Material and Methods.* Five groups of male Wistar rats were made, each with six rats: two groups with normal diet (ND) and three with high-fructose diet (HFD). The first ND group was treated with saline solution (SS), the second with VS; treatment for HFD groups was in the first group with SS, second with VS, and third with metformin. Weight, body mass index (BMI), blood glucose, and lipidic profile were measured; water, food, fructose and energy consumption were also determined. All parameters were compared among groups. *Results and Discussion.* Although obese rats treated with VS presented anorexia, oligodipsia, and a marked weight loss in the first two weeks. They recovered food and water intake in the third week with a slow recovery of some weight weeks later. VS normalized blood glucose level and decreased triglyceride and insulin levels in obese rats. These results suggest that vanadyl sulfate shows antiobesity, hypoglycemic, and hypolipidemic properties in old obese rats and could be useful as an alternative, additional, and potent preventive treatment for obesity and T2DM control in elderly obese and poorly controlled diabetic patients. *Conclusion.* VS could play an important role in the treatment of metabolic syndrome, contributing to a decrease in obesity and T2DM, through different ways, such as euglycemia, satiety, weight loss, and lipid profile optimization, among others. However, more research is needed to confirm this suggestion.

1. Introduction

The prevalence of diabetes mellitus type 2 (T2DM) increased from 1980 to 2014 approximately 4 times and follows this pattern according to the projections of the World Health Organization [1, 2]. It is a serious public health problem with a high health burden taking top positions in the public agenda of both developing countries, such as Mexico, and

developed countries [3, 4]. Indeed, the increase is due to aspects such as sedentary lifestyle, high consumption of high-energy diets resulting in obesity, insulin resistance, hyperglycemia, dyslipidemia, hypertension, and systemic inflammation. This brings with it several serious known complications [5]. A risk phase to develop T2DM and cardiovascular and hepatic diseases is the metabolic syndrome (MetS), which is defined as the combination of insulin

resistance with three or more of the metabolic abnormalities mentioned above [6].

MetS engages several vital organs and tissues that maintain optimal health when functioning properly. As is known during old age, this function decreases, so when developing morbid processes, the organism degenerates faster, leading to a deplorable quality of life [7]. They especially develop an acute inflammatory profile that promotes greater metabolic abnormalities and cardiovascular complications [8–11]. Frequently, these patients do not respond adequately to conventional pharmacotherapy and their adherence to a diet and exercise programs is nil, so that alternative treatment based on new synthetic drugs, secondary metabolites, or minerals is necessary [12, 13].

Vanadium derivatives such as vanadyl sulfate (VS), sodium orthovanadate, and vanadium complexes with several ligands have shown hypoglycemic effects in animal models and humans [14–16]. In addition, due to their role on insulin signaling and enzymatic process regulation, these compounds are used to treat diabetes, obesity [17], hypertension [18], endothelial dysfunction [19], cancer [20], and mainly the effects in patients with poorly controlled T2DM [21, 22]. VS reduces fasting plasma glucose, glycated hemoglobin (HbA1c), low-density-lipoprotein cholesterol, triglycerides, and body mass index (BMI). These improvements have been shown to be maintained for 2 weeks after the end of administration [23, 24]; compared to orthovanadate, VS shows insulinic properties at very low doses, reducing the presence of adverse effects [16, 25].

In spite of these beneficial effects, vanadium compounds have not been approved for human therapeutic use, because they showed some undesirable collateral effects such as gastrointestinal alteration [14]. However, in older patients with morbid obesity and MetS or patients with poorly controlled T2DM, beneficial effects could be more important than those undesirable effects [18, 22]. Several studies showed that dietary fructose has a direct impact on hepatic lipid metabolism by bypassing the enzyme phosphofructokinase, the regulatory step imposed on glucose. This allows unregulated flow of fructose-derived carbons into lipogenesis, decreasing lipolysis and increasing plasma fasting and postprandial very low-density-lipoprotein triacylglycerols, whole-body lipid oxidation, and lipid droplets, among others [26–29]. In rats, high-fructose diets induce obesity and can be used as metabolic syndrome in an animal model [30–32]. The aim of the present study was to determine the antiobese, hypoglycemic, and hypolipidemic effects of VS on fructose-induced MetS in aged rats.

2. Experimental Development

2.1. Animals and Diets. All experimental procedures were approved by the Bioethics and Research Committees of the *Instituto Nacional de Cardiología Ignacio Chávez* and were performed in accordance with the Mexican Federal Regulation for Animal Experimentation and Care (NOM-062-ZOO-2001). Male Wistar rats were obtained from the institutional animal facilities.

Male young Wistar rats (6–8 weeks of age) weighing 180–220 g were maintained in their housing conditions under controlled humidity (55%) at $21 \pm 1^\circ\text{C}$ temperature with a 12 h : 12 h light : dark cycle.

Control diet was from Harlan Laboratories (2018S Teklad Global 18% protein rodent diet), containing 4.07 kcal/g (18.6% proteins, 44.2% carbohydrates, and 6.2% fat). Rats were initially divided into two groups and treated for 6 months under the following conditions: the normal diet (ND) group with regular chow and drinking water (negative control) and the high-fructose diet (HFD) group was kept with normal chow and 15% fructose (4 kcal/g) in the drinking water.

2.2. Administration of Vanadyl Sulfate. On the 28th week, rats of the ND group with similar weights were distributed in two subgroups, and the HFD group was subdivided in three subgroups. These subgroups were followed for the next 4 weeks to confirm no changes in body weight and water and food intake. After that, on the 32nd week, one ND subgroup was treated with isotonic saline solution (100 ml/kg/day) (ND + SS), and the other ND group was treated with vanadyl sulfate (Sigma-Aldrich, USA), 2.72 mg/kg/day (0.015 mmol), which contains 0.750 mg of elemental vanadium, dissolved in SS (ND + VS). On the other hand, one HFD group received saline solution (HFD + SS), the other received metformin (MET) (Sigma-Aldrich, USA) (100 mg/kg/day) (HFD + MET), and the other vanadyl sulfate (2.72 mg/kg/day) (HFD + VS). Metformin and vanadyl sulfate were administered intragastrically.

VS dosage was determined based on previous studies of vanadium [15, 33, 34]. All groups were maintained under the initial diet conditions, and drug treatments were administered daily for 8 weeks. Metformin dosage was determined based on previous studies of metformin treatment [31, 35–37].

2.3. Clinical Measurements and Samplings. Body weight (BW) was measured weekly, body length (nasal length; mm) monthly, and food and water consumption was measured daily which allows the kilocalorie consumption estimation. Serum samples were obtained at 32 and 40 weeks (before and after drug treatments). An oral glucose tolerance test (OGTT) was performed at week 40, and finally, at the end of the test (week 8 after treatment), animals were anesthetized with pentobarbital; blood samples were obtained by cardiac puncture for biochemical analysis, and liver and retroperitoneal white adipose tissue (WAT) were obtained too. Serum and organs were immediately placed in liquid N_2 and conserved at -70°C until use for analysis.

Body mass index (BMI) was calculated from the formula $\text{BMI} = \text{body weight (g)} / \text{length}^2 \text{ (cm}^2\text{)}$ [32].

Adiposity index was expressed as a percentage of the ratio of WAT (retroperitoneal adipose tissue) weight (g), divided by the total BW (g) at the time of death, multiplied by 100.

2.4. Oral Glucose Tolerance Test (OGTT). At the end of experimentation (week 40), OGTT was performed in 12 h fasted rats. Glucose was administered intraperitoneally at a final dose of 2 g/kg body weight (dissolved in purified saline solution), and glucose plasma levels were measured at 0, 15,

30, 45, 60, 90, 120, 150, and 180 min using an Accutrend Sensor glucometer (Roche).

2.5. Biochemical Parameters. Glucose, triglycerides, and total and high-density-lipoprotein cholesterol concentrations were determined in plasma with colorimetric-enzymatic methods (Roche Diagnostics GmbH, Mannheim, Germany) using a Hitachi 902 autoanalyzer (Hitachi Ltd, Tokyo, Japan) using blood samples drawn from the tail vein on weeks 32 and 40 in 12 h fasted animals [38]. Accuracy and precision of lipid measurements are under periodic surveillance by the Centers for Disease Control and Prevention Services (Atlanta, GA, USA). Interassay coefficients of variation were less than 6% for all these assays.

2.6. Insulin Quantification. Serum insulin was quantified using a commercial rat ELISA strip purchased from Crystal Chem (USA), as described in the manufacturer's protocol to attain the corresponding profile.

2.7. Statistical Analysis. Data were analyzed through SPSS 22 and described as mean \pm SEM. Statistical significance was calculated by one-way analysis of variance (ANOVA) (Dunnett's *post hoc* test) to examine the statistical significance among experimental groups vs. control. The null hypothesis was rejected when $P < 0.05$ [39].

3. Results

3.1. HFD-Induced Body Weight Gain and Food Intake Disorder. Over the 28 weeks of evolution, rats fed HFD increases body weight and body mass index as compared to the ND group ($P < 0.05$). These latter rats maintained their weights over the 4 weeks before the VS treatment. Food intake decreased in rats with HFD compared with ND rats, but their water intake was higher (see Supplementary Materials (available here)). This decreased food consumption and increased water consumption were observed from the third or fourth week after initiating HFD, as reported for this model [31, 40].

Since the beginning of the administration of fructose in drinking water, the rats with a high-fructose diet show an increased consumption of fructose solution and gradually a decrease in the consumption of normal food, and they showed more gain of weight compared with ND rats. Initially, total caloric intake is higher in rats that consume fructose, but after week 20 of the HFD, their total caloric consumption begins to decrease (data not shown); it is then lower than that of the normal diet rats (Supplementary Materials). However, these rats do not decrease their body weight and as it is seen at the end, their fat/body weight ratio is higher compared to normal diet rats (Figure 1(c)); this could be due to the fact that due to its chronic obesity status, the rats have less caloric expenditure compared with normal diet rats.

3.2. VS Induced Body Weight Decrease in Both Aged Normal and Obese Rats. During the first week of treatment, the obese rats with VS showed a decrease in weight compared to the other experimental groups ($P < 0.05$). In Figure 1(a), it can

be seen how the groups treated with VS decrease their weight and the behavior of the weight is similar between the groups under treatment with VS ($P > 0.05$). This difference is maintained until the last week of treatment in the study. However, as the treatment time prolonged, the weight evolution of the VS-treated groups seemed to approach that of the ND + SS group. This aspect is of interest since an optimization of weight is inferred through the use of VS.

The BMI was calculated in each experimental group, before, during, and after the treatment (Figure 1(b)). In fact, at the end of the treatment, it was decreased in the HFD + VS group ($P < 0.0001$); however, in rats of the ND + VS group, there was no significant difference ($P > 0.05$). With respect to the adipose tissue/body weight ratio, the rats under the diet with fructose and treated with VS showed a decreased ratio ($P = 0.05$), which indicates a decrease in fat tissue with respect to body weight.

3.3. VS Induced Decreased Food and Fructose-Water Intake in Old Obese Rats. From the first day of treatment, HFD + VS rats showed decreased food and fructose-water consumption ($P < 0.0001$) (Figures 2(a) and 2(c)) and decreased total calorie consumption, as compared to all other groups (Figure 3). Anorexia and oligodipsia were less remarkable in ND rats receiving VS, although the differences are significant ($P < 0.0001$). ND rats normalized their water intake in the second week after VS administration ($P = 0.409$), and their food intake remained decreased for the 8 weeks of VS treatment. In the third week, the differences between the two VS-treated groups were not significant (Figures 2(b) and 2(c)).

Obese rats treated with VS slowly increased food consumption at the third week of treatment, although not reaching the level before treatment. In the fourth week of treatment, their food consumption was higher than that of the HFD + SS and HFD + MET groups. Nevertheless, these differences were not statistically significant ($P = 0.966$ and $P = 0.440$; respectively). This feeding pattern continued until the eighth week. In the same group, fructose-water consumption decreased in the first week of treatment ($P < 0.0001$), but it increased slowly at the sixth week of treatment, although not reaching the level before treatment ($P < 0.0001$). In the sixth week post-treatment, their water consumption was lesser than that of ND + SS and ND + VS groups, revealing less water intake as compared to the other HFD groups too ($P < 0.0001$) (Figure 2(c)). These results show a possible VS effect on the food consumption regulation in rats.

3.4. VS Induced Decreased Calorie Intake in Aged Obese Rats. In general, food intake is decreased in rats with HFD compared to ND rats, while they drank more water than did ND rats. Although drinking water contained fructose at 15%, their total caloric intake was lower in HFD rats than in ND rats because they did not eat much food. At the beginning of treatments, caloric consumption was reduced in rats under VS treatment, as the latter induced anorexia and oligodipsia immediately from the first week ($P < 0.05$); from the third week on, obese rats and obese rats treated with VS

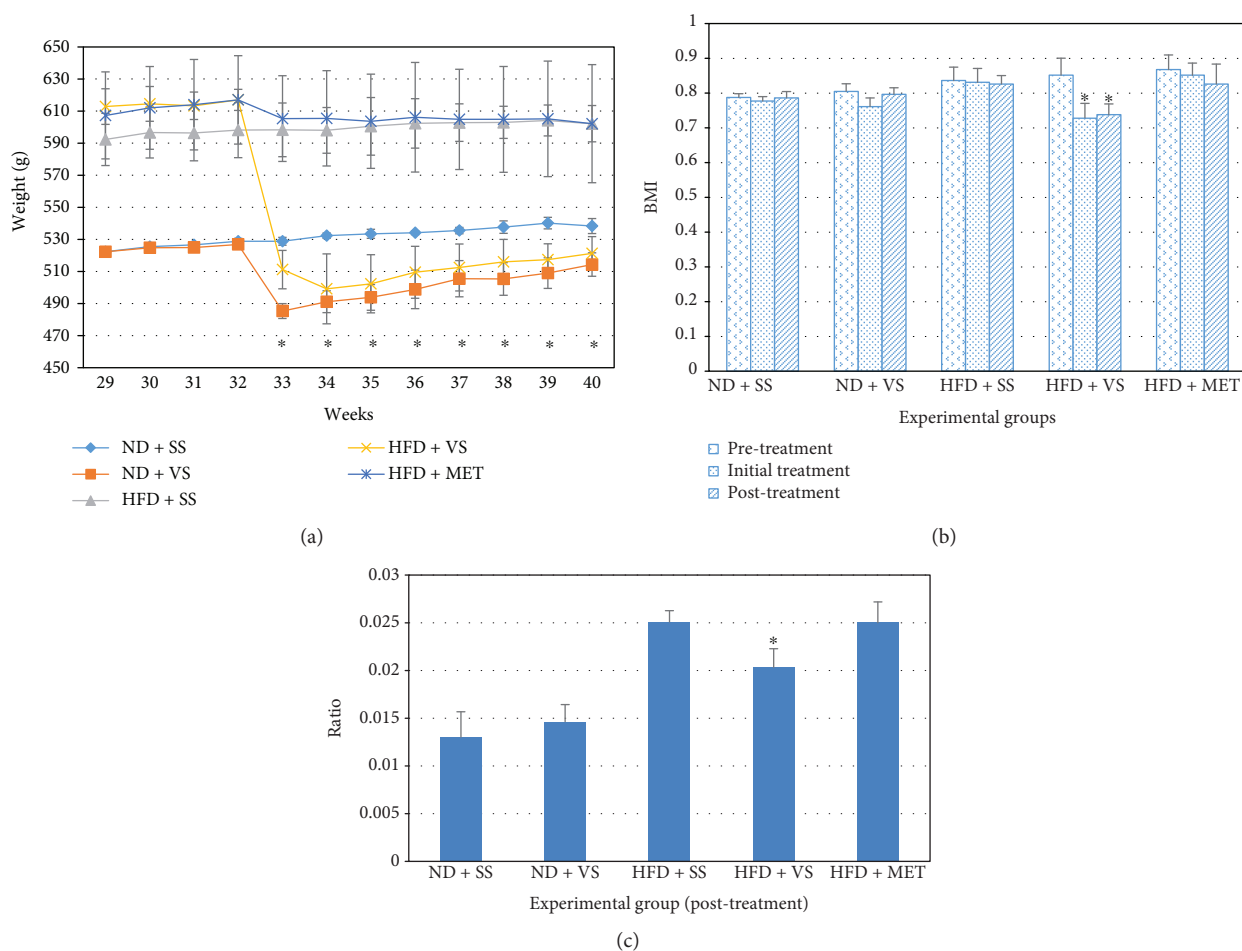


FIGURE 1: Vanadyl sulfate (VS) effect on body mass of old obese male Wistar rats. Obesity was induced in rats with high-fructose diet (HFD) during 28 weeks, using a set of normal diet (ND) rats as comparative groups; stability in weight was observed during the next 4 weeks. After that, insulin sensitizer treatment (metformin (MET) or VS) was applied from week 32 to week 40, using saline solution (SS) as a control. (a) Body mass evolution after treatment with ND or HFD, and insulin sensitizers (starting week 32). * $P < 0.05$ comparing the HFD + VS group versus HFD plus MET or SS. (b) Body mass index (BMI) in animals after 28 weeks on ND or HFD (pretreatment bars), animals with a week of insulin sensitizer treatment (initial treatment bars), and animals with 8 weeks of insulin sensitizer treatment (posttreatment bars). * $P < 0.05$ comparing pretreatment versus initial treatment or posttreatment. (c) Abdominal fat tissue/body weight ratio in old obese male Wistar rats after 8 weeks with insulin sensitizer treatment. * $P < 0.05$ comparing the HFD + VS group versus HFD plus MET or SS. Data are mean \pm SEM ($n = 6$).

recovered their total calorie intake, mainly from food intake. At the sixth week of treatment, these groups recovered the original levels of calories from fructose. ND rats treated with VS remained with less total calorie intake during the 8 weeks of treatment as compared to the nontreated ND rats (Figures 3(a)–3(c)).

3.5. VS Induced Decreased Blood Glucose, Insulin Level, and Insulin Resistance in Both Aged Normal and Obese Rats. Rats fed with HFD showed moderate increase of blood glucose, compared to the respective control group ($P < 0.0001$), resulting in a compensatory hyperinsulinemia and insulin resistance. Nevertheless, treatment with VS maintained for 8 weeks induced an important blood glucose level decrease in the ND + VS ($P = 0.002$) and HFD + VS ($P < 0.0001$) groups. VS decreased the levels of insulin in the HFD + VS compared to HFD + SS group ($P = 0.0001$). Values showed that VS exerted an important effect on improving the

hyperglycemia and insulin resistance in aged obese rats with a chronic high-fructose diet without negatively affecting these levels in the ND group (Figure 4(a)).

When comparing the HFD + MET group to the HFD + VS group, the latter group showed a greater decrease in blood glucose ($P < 0.0001$) and HOMA-IR index ($P = 0.004$). Blood insulin in the HFD + VS group was lower than in the HFD + MET group, but not significantly ($P = 0.39$). This suggests that VS could have a potent hypoglycemic effect than metformin, at least at the dosages used in these experiments (Figures 4(b) and 4(c)).

3.6. VS Effect on Blood Triglycerides and Total, HDL, and LDL Cholesterol in Both Old Normal and Obese Rats. Rats fed with HFD showed a large increase in triglycerides and cholesterol ($P < 0.05$) compared to the respective control group. Treatment with VS maintained for 8 weeks induced a large decrease in triglyceride levels in obese rats compared

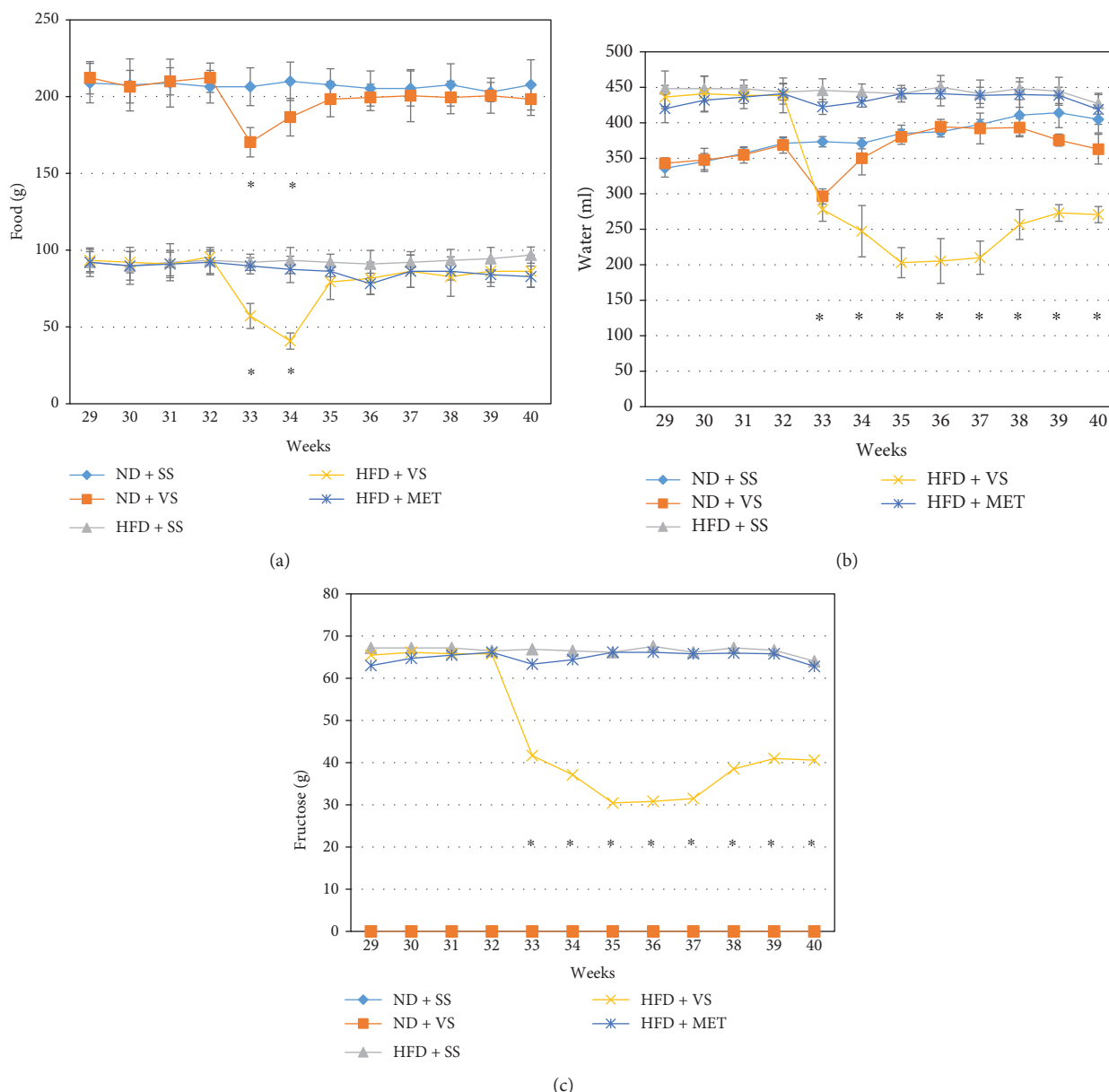


FIGURE 2: Vanadyl sulfate (VS) effect on food, liquid, and fructose consumption in old obese male Wistar rats. Obesity was induced in rats with high-fructose diet (HFD) during 28 weeks, using a set of normal diet (ND) rats as comparative groups; stability in food and liquid consumption was observed during 4 weeks. After that, insulin sensitizer treatment (metformin (MET) or VS) was applied from week 32 to week 40, using saline solution (SS) as a control. (a) Weekly food intake after treatment with insulin sensitizers (starting week 32) in both lean (ND) and obese (HFD) rats. * $P < 0.05$ comparing VS treatment versus MET and/or SS treatment in lean or obese animals. (b) Weekly water drink consumption after treatment with insulin sensitizers. * $P < 0.05$ comparing HFD + VS treatment versus HFD + MET or SS treatment. (c) Weekly fructose consumption after treatment with insulin sensitizers. * $P < 0.05$ comparing HFD + VS treatment versus HFD + MET or SS treatment. Data are mean \pm SEM ($n = 6$).

to control groups ($P < 0.0001$). Triglyceride reduction in ND + VS was not significant ($P = 0.48$). Although VS and metformin increased the levels of HDL cholesterol in this experiment, differences among groups were not significant ($P = 0.272$). Neither did LDL and total cholesterol show significant differences ($P > 0.05$). Metformin induced a slight decrease in these parameters in obese rats. In the ND group, VS did not significantly affect blood triglyceride and cholesterol levels (Figures 5(a)–5(d)).

3.7. VS Administration Effect on the Oral Glucose Tolerance Test. In this experiment, the OGTT curve was more extended than commonly reported for rats from younger animals or in short-term induced metabolic syndrome (Figure 6). Treatment with VS during 8 weeks improved OGTT in both ND and HFD groups, compared to the control group, and the improvement was better than that induced by metformin in HFD rats. Groups of obese rats represent the highest curves until the 45th minute where the curves begin to fall. Each

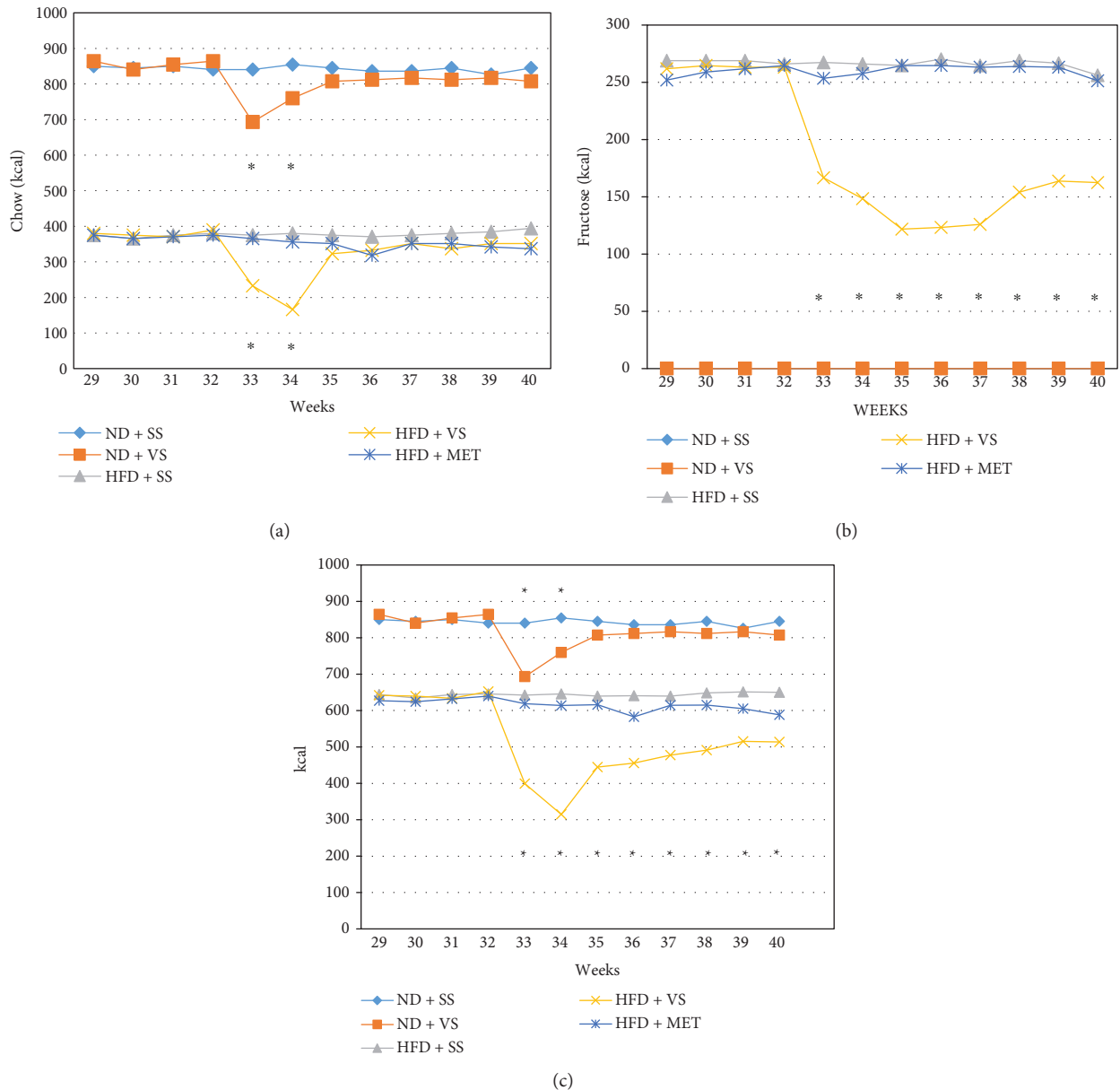


FIGURE 3: Vanadyl sulfate (VS) effect on calorie intake in old obese male Wistar rats. After obesity induced with high-fructose diet (HFD) during 28 weeks, stability in food and liquid consumption was observed during 4 weeks; then, insulin sensitizer treatment (metformin (MET) or VS) was applied from week 32 to week 40, using saline solution (SS) as a control. Kilocalories were estimated considering the amounts of food and fructose consumption registered per week. (a) Weekly food kilocalorie intake in all experimental groups. $*P < 0.05$ comparing VS treatment versus MET and/or SS treatment in both lean and obese animals. (b) Weekly fructose kilocalorie intake after treatment with insulin sensitizers. $*P < 0.05$ comparing HFD + VS treatment versus HFD + MET or SS treatment. (c) Weekly total kilocalorie intake in all experimental groups. $*P < 0.05$ comparing VS treatment versus MET and/or SS treatment in both lean and obese animals. Data are mean values ($n = 6$).

treatment with VS is compared with its controls. The HFD+VS group represented the highest curve. At the end (180 minutes), the value of 108.6 mg/dl was reached, which is a lower value than the control group for obese rats ($P < 0.05$). Although it represents a borderline value of glycemia, it has a more potent therapeutic effect than metformin, as has been shown in several studies. The ND+VS group represented the curve that was most suitable and was lower than the rats with a normal diet ($P = 0.05$).

4. Discussion

Most studies on metabolic syndrome in animal models are made for short periods in young individuals. Humans develop T2DM and other metabolic syndrome complications after many years of bad lifestyles, such as high caloric diets and sedentary life. On the other hand, adults or aged people are the ones to present the worst MetS-derived complications and for whom the treatment is more difficult. For these

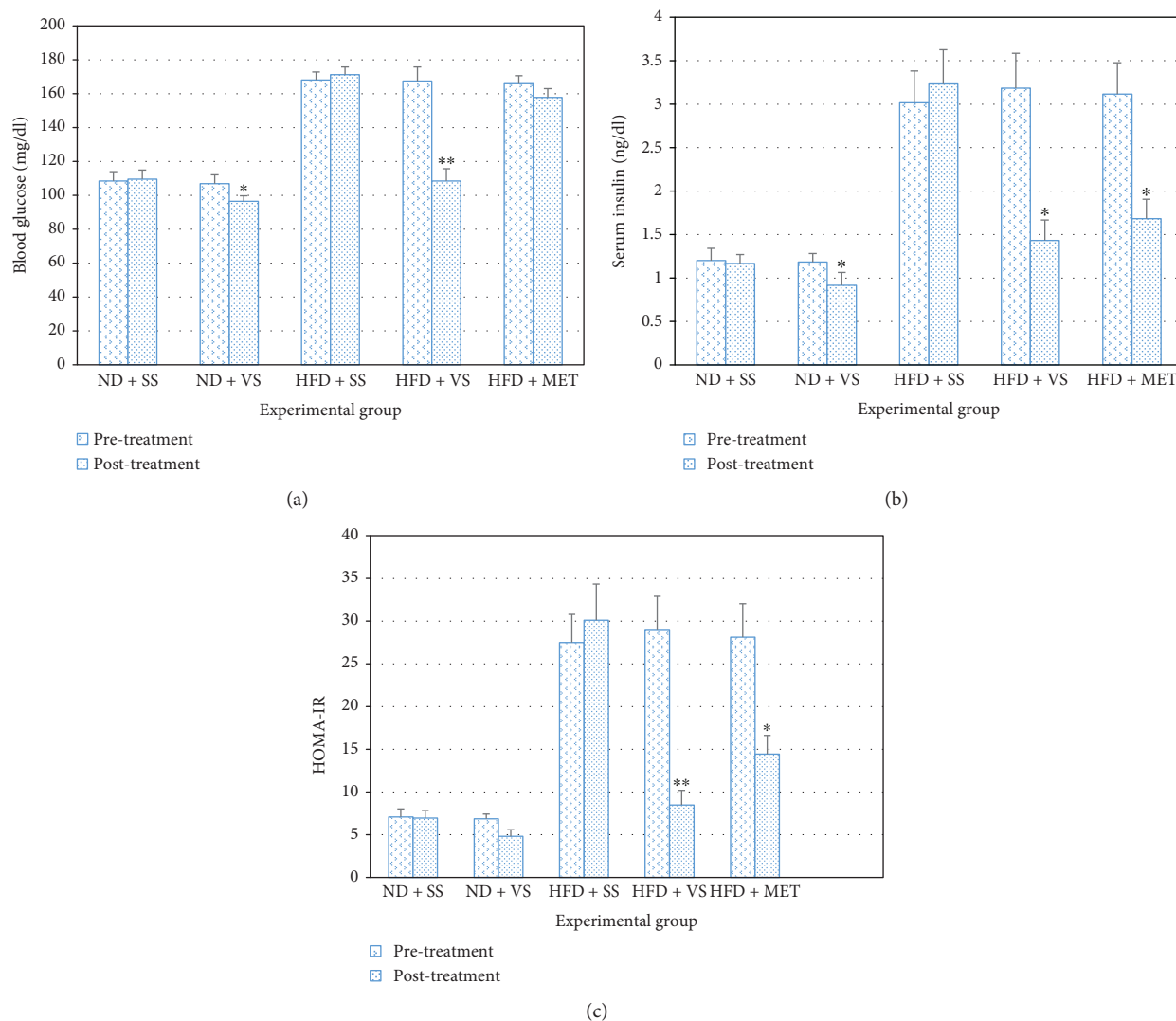


FIGURE 4: Effect of VS on serum glucose and insulin levels in old obese male Wistar rats. After obesity induced with high-fructose diet (HFD) during 28 weeks, insulin sensitizers treatment (metformin (MET) or VS) was applied from week 32 to week 40, using saline solution (SS) as a control. (a) Postprandial blood glucose levels in rats after 32 weeks on ND or HFD (pretreatment bars) and after 8 weeks of insulin sensitizer treatment (posttreatment bars). * $P < 0.05$ comparing ND + VS pre-treatment versus ND + VS post-treatment. ** $P < 0.05$ comparing HFD + VS post-treatment versus HFD plus SS or MET post-treatment. (b) Postprandial blood insulin levels in rats after 32 weeks on ND or HFD (pretreatment bars) and after 8 weeks of insulin sensitizer treatment (post-treatment bars). * $P < 0.05$ comparing pre-treatment versus post-treatment. (c) Homeostatic model assessment for insulin resistance (HOMA-IR) in rats after 32 weeks on ND or HFD (pretreatment bars) and after 8 weeks of insulin sensitizer treatment (posttreatment bars). * $P < 0.05$ HFD + MET pre-treatment versus HFD + SS post-treatment. ** $P < 0.05$ HFD + VS post-treatment versus HFD + VS pre-treatment HFD + SS or HFD + MET post-treatment. Data are mean \pm SEM ($n = 6$).

reasons, we approached the study of vanadyl sulfate treatment on a long-term metabolic syndrome, using a similar animal model.

Our interest was to study the possible beneficial effects of vanadyl sulfate on the treatment of metabolic syndrome complications in adult human patients, who develop obesity, morbid obesity, and T2DM. Vanadyl sulfate effects on biochemical, anthropometrical, and food intake parameters were measured in rats that developed obesity through a diet high in fructose and compared to normal diet rats.

Fructose is present in sweeteners, like sucrose and high-fructose corn syrup (HFCS), in most industrialized food

products; high sugar consumption has severe consequences for health, such as diabetes, hypertension, obesity development, uric acid accumulation, and a proinflammatory effect [26, 41]. In fact, several physiological mechanisms are related to a high-fructose diet such as insulin signaling and peripheral and central satiety [29].

High-fructose diet (HFD) is a model used in laboratory animals to induce body weight increase, obesity, and metabolic syndrome; rats fed HFD show increased body weight and body mass index. Food intake is decreased in rats given HFD compared with ND rats, but the intake of fructose-water is increased, resulting in increased total

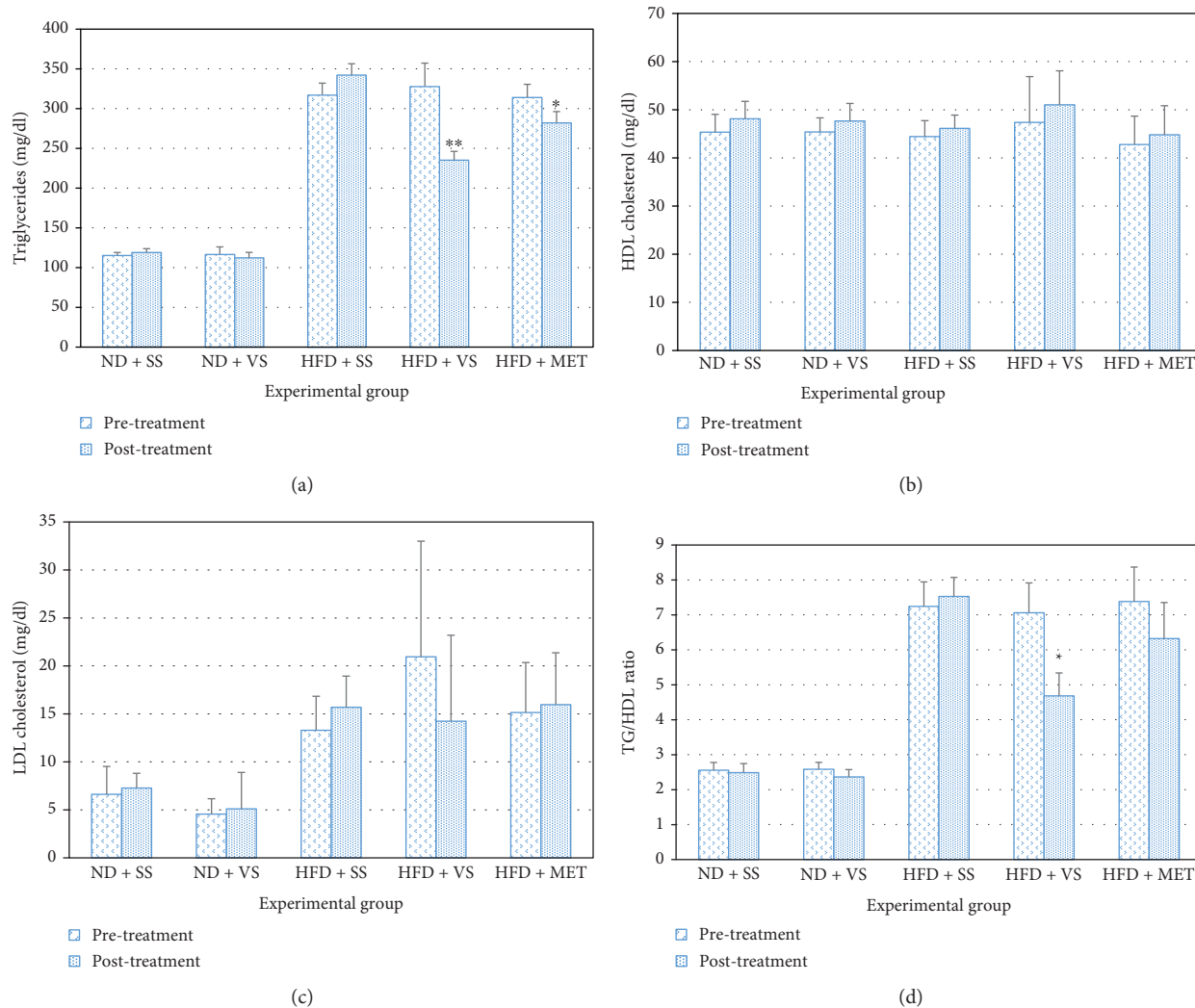


FIGURE 5: Effect of VS on lipid plasma levels in old obese male Wistar rats. After obesity induced with high-fructose diet (HFD) during 28 weeks, insulin sensitizer treatment (metformin (MET) or VS) was applied from week 32 to week 40, using saline solution (SS) as a control. (a) Triglyceride fasting plasma levels in rats after 32 weeks on ND or HFD (pretreatment bars) and after 8 weeks of insulin sensitizer treatment (posttreatment bars). * $P < 0.05$ HFD + SS post-treatment. ** $P < 0.05$ comparing HFD + VS post-treatment versus HFD + SS or HFD + MET post-treatment. (b, c) HDL and LDL cholesterol plasma levels in rats after 32 weeks on ND or HFD (pretreatment bars) and after 8 weeks of insulin sensitizer treatment (posttreatment bars) (nonsignificant differences were found). (d) Triglyceride/HDL ratio in rats after 32 weeks on ND or HFD (pretreatment bars) and after 8 weeks of insulin sensitizer treatment (posttreatment bars). * $P < 0.05$ comparing HFD + VS post-treatment versus HFD + SS or HFD + MET post-treatment. Data are mean \pm SEM ($n = 6$).

calorie consumption. This decreased food and increased water consumption was observed from the third or fourth week of HFD in our experiment similarly to other reports for this model in short-term experiments. However, in our long-term obesity trial, old rats with HFD showed a diminished total calorie consumption without loss of body weight. This decrement is shown after the 20th week of HFD (Supplementary Materials).

Vanadium is an omnipresent and essential micronutrient in the human diet through different inorganic compounds, such as VS, sodium metavanadate, sodium orthovanadate, and vanadium pentoxide [14, 42]. Although vanadium is toxic at high doses, its absorption, which is mediated by the duodenum, is poor [14, 23]. VS has pleiotropic organic

effects like regenerative, antihypertensive, immune modulator, antitumor, and hypoglycemic [14, 20, 22, 23, 43].

In this study, VS was orally administered, dissolved in saline solution, because some authors have reported that rats drink less water when vanadium compounds are administered in drinking water, arguing that this is due to an unpleasant flavor. Our results show that VS had an anorexic effect, diminishing body weight, BMI, food, water, and fructose intake in obese and nonobese rats.

VS was applied at a dose of 2.72 mg/kg/day; this dose was calculated to provide 0.750 mg/kg/day of the vanadium element. Oral administration allows us to control the amount of VS administered, because when it is administered in drinking water, rats decrease the consumption of water in a

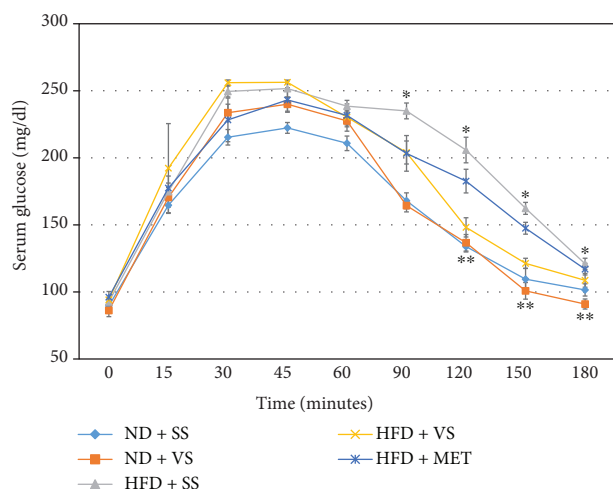


FIGURE 6: Effect of VS on oral glucose tolerance test in old obese male Wistar rats. Obesity was induced in rats with high-fructose diet (HFD) during 28 weeks, using a set of normal diet (ND) rats as comparative groups; stability in weight was observed during the next 4 weeks. After that, insulin sensitizer treatment (metformin (MET) or VS) was applied from week 32 to week 40, using saline solution (SS) as a control. * $P < 0.05$ comparing HFD + SS versus ND + SS. ** $P < 0.05$ comparing HFD + VS versus HFD + SS or HFD + MET. Data are mean \pm SEM ($n = 6$).

variable manner, which has been attributed to the bad taste. However, in this experiment we observed that both the animals that receive water alone (unflavored) and those that receive sweetened water with fructose decrease their water consumption after the administration of VS.

On the other hand, when we apply this same dose of VS intraperitoneally or subcutaneously, VS shows the same effects, but the rats show constant anorexia and oligodipsia with chronic cachexia and die in the second or third week of administration, even if the treatment is withdrawn (data not shown). In contrast, rats that received oral VS at this dose show a cachexic state at the beginning, but they recover from this aspect; some rats have mild diarrhea and all show greenish-colored stool throughout the treatment, indicating that part of the VS is not absorbed and is eliminated by fecal route. The recovery from its bad general state could be attributed to the fact that rats diminish their capacity to uptake VS from the gastrointestinal tissue. They improve their capacity of elimination of the VS by fecal way and/or that they adapt to eliminate or transform VS mainly in the liver. These adaptation mechanisms cannot develop them when VS is administered subcutaneously or intraperitoneally.

During treatment, BMI values were similar in both groups until the last week. In this time, the BMI of the HFD and ND with VS groups stayed within error of the values of the normal group without treatment. BMI and weight reduction started together with food, water, and fructose intake decrement. Nevertheless, food intake increased in the third treatment week until it was equal to the respective control group. Although food intake is normalized in a few weeks, BMI, water, and fructose are not. Water intake in obese rats was maintained among all groups until the last

week, but in ND-treated rats, consumption was recovered. This effect has been seen in other studies [18]. Despite these results, fructose consumption remained diminished in obese rats treated with VS for the first week until the eighth week. These characteristics suggest that VS could be a fructose intake regulator or a sweet beverage regulator independently from the food intake. If this aspect is applicable to humans, it could be used to improve current consumption of beverages with high fructose without affecting the food consumption, thereby improving the anthropometric profile as a preventive measure and contributing to public health.

Fructose decreases central and peripheral satiety through inhibition of neuropeptide YY (PYY), ghrelin, and proopiomelanocortin (POMC) mRNA or by an increase in circulating leptin levels [29, 44]. Additionally, leptin resistance is observed in animal models with high lipids in their diet and it is related to inflammation that decrease TNF- α and its toxicity [45]. Nevertheless, hormones like insulin, glucocorticoids, and estrogens are positive leptin regulators [44]; therefore, the insulin-mimetic effect of VS can modify these pathways or molecules, by incrementing satiety for fructose independently from food intake.

Several studies have shown the insulin-mimetic effects of VS, and its hypoglycemic effect is the most investigated currently [18, 21, 23, 46]. In fact, our results are similar, old obese rats treated with VS-diminished glucose and insulin blood levels compared to respective control groups. In fat rats with VS, glucose decrease was more efficient than metformin treatment ($P > 0.0001$), whereas the insulin level decrement was similar in both treatments ($P = 0.399$). ND rats with VS treatment showed a significant blood glucose decrement ($P = 0.002$). Goldfine et al. [21] exhibited the VS effect in T2DM patients; they concluded that VS acts on human skeletal muscle in the early insulin signaling steps. These steps are on basal insulin receptor, substrate tyrosine phosphorylation, and PI-3-kinase activation [21]. In fact, this molecular cascade has action on other enzymes, such as PI3K-PK β /Akt-mTOR, NF- $\kappa\beta$, and MEK1/2-ERK activation. These messengers are related to GLUT transporter insertion into the plasma membrane, which results in increased glucose transport into the cells and subsequently decreased blood glucose and insulin [21, 23, 47, 48]. Gluconeogenesis and hepatic glucose output are decreased in treatment with vanadium; consequently, this compound could diminish the loss of muscle protein that occurs in T2DM patients [16].

Studies in mice treated with vanadium compounds revealed an antiobesity effect, adiponectin segregation, increment of insulin product, and adipogenic effect [42]. These mechanisms are related to adiponectin, leptin, and insulin hormones and their effects on satiety and body weight [29, 30, 44, 49]. Insulin production increases adiponectin synthesis through adipocytes, improving satiety, which probably influenced the BMI of obese rats in this study, as shown by Maachi et al. [50].

On the other hand, a study in the mouse preadipocyte fibroblast cell line 3T3-L1 showed an adipocyte differentiation inhibitory effect of vanadium dissolved in water through PPAR γ and C/EBP α gene downregulation [17]. PPAR γ , as a peroxisome proliferator, is a nuclear receptor implicated in

fat accumulation in adipocytes, weight increment, and leptin negative regulation. It is thiazolidinedione's therapeutic target with secondary effects [44, 51, 52].

It has been evidenced that VS treatment of T2DM patients reduces serum cholesterol, triglycerides, and glucose [21, 25, 46]. In our study, total cholesterol and triglycerides decreased in treated aged rats but differences in other parameters, such as HDL and LDL, were not significant ($P > 0.05$). It should not be discarded that this lack of significance could be due to the fact that results of the present study show a high standard deviation in obese rats treated with vanadyl sulfate (HFD + VS group). Moreover, it has been previously reported that HDL decreases in T2DM patients treated with VS [21]. Although results of the present study show a slightly increased in HDL ($P =$ nonsignificant), triglyceride/HDL and fat tissue/body weight ratios were the lowest in VS-treated obese aged rats ($P = 0.003$), suggesting a fat tissue loss and HDL increment. In fact, in our analysis an elevated triglyceride/HDL ratio was correlated with insulin resistance observed in HFD aged rats. These effects can be explained because VS can stimulate other nuclear receptors, like PPAR γ , involved in fatty acid mitochondrial oxidation, energy consumption, thermogenesis, HDL increment, and triglyceride decrease as reported by Bermúdez et al. [51].

Obesity is a chronic inflammatory state with different factors involved in its development and many consequences, like T2DM. According to our results, VS can act like a potent preventive dietary compound that improves insulin resistance, hyperglycemia, OGTT, high cholesterol, and high triglyceride levels. Although this study was made in an animal model, currently beneficial properties of VS have been demonstrated in humans by decreasing the same parameters as in this investigation without affecting hepatic enzymes [21]. People consume diets with a high-fructose or -sucrose content; these sugars are elevated in industrialized sweetened beverages and foods with unclear health regulation [53]. Consequently, the entire population is immersed in an obesogenic environment that has several consequences, one of them the metabolic syndrome [41, 54]. Thus, the parameters evaluated show a possible alternative treatment and a preventive dietary compound. It is necessary to investigate the role of VS on fructose as well as on water and food decreased consumption.

5. Conclusions

According to our results, VS has an antiobesity effect in aged obese rats. VS induces decreased fructose consumption and oligodipsia, decreasing the total calorie intake inducing the immediate loss of weight in these aged obese rats. VS induces decreases in levels of blood glucose, triglycerides, cholesterol, and triglyceride/HDL ratio and improves insulin sensitivity and oral glucose tolerance test results at 8 weeks of treatment in rats with fructose-induced chronic obesity.

VS can be a valuable therapeutic agent in preventing insulin resistance, as well as the development and progression of obesity and metabolic syndrome complications in aged patients with obesity or T2DM. However, research on undesirable side effects in long-term trials is necessary. With

this experiment, we obtained serum and organ samples that permit us to study beneficial or undesirable effects on other metabolic parameters such as inflammatory state, oxidative stress, and organ damage, results that will allow us to evaluate the convenience of vanadyl sulfate administration in human patients.

Data Availability

The data used to support the findings of this study are available from the corresponding author upon request. Information about the evolution of old rats from week 0 to 25 is available in supplementary data.

Conflicts of Interest

The authors declare that they have no competing interests.

Acknowledgments

This work was supported by a grant from the *Instituto Nacional de Cardiología Ignacio Chávez* through the program "Fondos del Gasto Directo Autorizado a la Subdirección de Investigación Básica".

Supplementary Materials

This file contains the data obtained during 25 weeks of evolution of the metabolic syndrome in Wistar rats used to be treated with vanadyl sulfate (VS). From the first week, the rats with normal diet (ND) received normal food and pure water as a drink, and the rats with high-fructose diet (HFD) received normal food and water with fructose at 15% as drinking water. All rats had ad libitum access to food and drinking water. At week zero, all the young rats (200-240 g) received pure water as a drink. Body weight, food consumption, drinking water consumption, fructose consumption, and calculation of total kilocalories and from each source are indicated weekly. As indicated in the article, vanadyl sulfate effects on systemic profiles of metabolic syndrome in old rats with fructose-induced obesity these rats were reclassified according to their weight at week 28 and treated with VS from week 32 onwards. (*Supplementary Materials*)

References

- [1] H. King, R. E. Aubert, and W. H. Herman, "Global Burden of Diabetes, 1995-2025: prevalence, numerical estimates, and projections," *Diabetes Care*, vol. 21, no. 9, pp. 1414-1431, 1998.
- [2] J. E. Shaw, R. A. Sicree, and P. Z. Zimmet, "Global estimates of the prevalence of diabetes for 2010 and 2030," *Diabetes Research and Clinical Practice*, vol. 87, no. 1, pp. 4-14, 2010.
- [3] A. Arredondo and E. De Icaza, "Costos de la Diabetes en America Latina: Evidencias del Caso Mexicano," *Value in Health*, vol. 14, no. 5, pp. s85-s88, 2011.
- [4] A. A. Agudelo-Suárez, M. T. Ruiz-Cantero, L. I. González-Zapata, J. C. Restrepo-Medrano, and G. M. Ortiz-Barreda, "The parliamentary political agenda: a tool for policy analysis

- of diabetes priorities in Spain,” *Gaceta Sanitaria*, vol. 26, no. 6, pp. 554–559, 2012.
- [5] R. Gabriel, M. Alonso, A. Segura et al., “Prevalence, geographic distribution and geographic variability of major cardiovascular risk factors in Spain. Pooled analysis of data from population-based epidemiological studies: the ERICE study,” *Revista Española de Cardiología*, vol. 61, no. 10, pp. 1030–1040, 2008.
- [6] A. Rodríguez, M. Sánchez, and L. Martínez, “Síndrome metabólico,” *Revista Cubana de Endocrinología*, vol. 13, no. 3, pp. 238–252, 2002.
- [7] J. I. Barzilay, L. Abraham, S. R. Heckbert et al., “The relation of markers of inflammation to the development of glucose disorders in the elderly: the cardiovascular health study,” *Diabetes*, vol. 50, no. 10, pp. 2384–2389, 2001.
- [8] S. Mottillo, K. B. Filion, J. Genest et al., “The metabolic syndrome and cardiovascular risk a systematic review and meta-analysis,” *Journal of the American College of Cardiology*, vol. 56, no. 14, pp. 1113–1132, 2010.
- [9] G. Marchesini, M. Brizi, G. Bianchi et al., “Nonalcoholic fatty liver disease a feature of the metabolic syndrome,” *Diabetes*, vol. 50, no. 8, pp. 1844–1850, 2001.
- [10] G. E. Sonnenberg, G. R. Krakower, and A. H. Kissebah, “A novel pathway to the manifestations of metabolic syndrome,” *Obesity Research*, vol. 12, no. 2, pp. 180–186, 2004.
- [11] Federation International Diabetes, *IDF Diabetes Atlas*, Brussels, Belgium, 2017 <http://www.diabetesatlas.org>.
- [12] K. G. M. M. Alberti, P. Zimmet, and J. Shaw, “Metabolic syndrome—a new world-wide definition. A consensus statement from the International Diabetes Federation,” *Diabetic Medicine*, vol. 23, no. 5, pp. 469–480, 2006.
- [13] E. A. Medina, K. L. Erickson, K. L. Stanhope, and P. J. Havel, “Evidence that tumor necrosis factor- α -induced hyperinsulinemia prevents decreases of circulating leptin during fasting in rats,” *Metabolism*, vol. 51, no. 9, pp. 1104–1110, 2002.
- [14] B. Mukherjee, B. Patra, S. Mahapatra, P. Banerjee, A. Tiwari, and M. Chatterjee, “Vanadium—an element of atypical biological significance,” *Toxicology Letters*, vol. 150, no. 2, pp. 135–143, 2004.
- [15] I. Goldwaser, D. Gefel, E. Gershonov, M. Fridkin, and Y. Shechter, “Insulin-like effects of vanadium: basic and clinical implications,” *Journal of Inorganic Biochemistry*, vol. 80, no. 1–2, pp. 21–25, 2000.
- [16] L. Marzban and J. H. McNeill, “Insulin-like actions of vanadium: potential as a therapeutic agent,” *Journal of Trace Elements in Medicine and Biology*, vol. 16, no. 4, pp. 253–267, 2003.
- [17] S.-J. Park, C. K. Youn, J. W. Hyun, and H. J. You, “The anti-obesity effect of natural vanadium-containing Jeju ground water,” *Biological Trace Element Research*, vol. 151, no. 2, pp. 294–300, 2013.
- [18] S. Bhanot, A. Michoulas, and J. H. McNeill, “Antihypertensive effects of vanadium compounds in hyperinsulinemic, hypertensive rats,” *Molecular and Cellular Biochemistry*, vol. 153, no. 1–2, pp. 205–209, 1995.
- [19] D. I. Shah and M. Singh, “Inhibition of protein tyrosin phosphatase improves vascular endothelial dysfunction,” *Vascular Pharmacology*, vol. 44, no. 3, pp. 177–182, 2006.
- [20] A. Bishayee, A. Waghay, M. A. Patel, and M. Chatterjee, “Vanadium in the detection, prevention and treatment of cancer: the *in vivo* evidence,” *Cancer Letters*, vol. 294, no. 1, pp. 1–12, 2010.
- [21] A. B. Goldfine, M. E. Patti, L. Zuberi et al., “Metabolic effects of vanadyl sulfate in humans with non—insulin-dependent diabetes mellitus: in vivo and in vitro studies,” *Metabolism*, vol. 49, no. 3, pp. 400–410, 2000.
- [22] S. Missaoui, K. Ben Rhouma, M. T. Yacoubi, M. Sakly, and O. Tebourbi, “Vanadyl sulfate treatment stimulates proliferation and regeneration of beta cells in pancreatic islets,” *Journal Diabetes Research*, vol. 2014, article 540242, 7 pages, 2014.
- [23] J. Korbecki, I. Baranowska-Bosiacka, I. Gutowska, and D. Chlubek, “Biochemical and medical importance of vanadium compounds,” *Acta Biochimica Polonica*, vol. 59, no. 2, pp. 195–200, 2012.
- [24] J. L. Ingram, A. Antao-Menezes, E. A. Turpin et al., “Genomic analysis of human lung fibroblasts exposed to vanadium pentoxide to identify candidate genes for occupational bronchitis,” *Respiratory Research*, vol. 8, no. 1, 2007.
- [25] K. Cusi, S. Cukeir, and R. A. DeFronzo, “Metabolic effects of treatment with vanadyl sulfate in NIDDM,” *Diabetes*, vol. 46, no. 34, 1997.
- [26] E. Tapia, M. Cristóbal, F. E. García-Arroyo et al., “Synergistic effect of uricase blockade plus physiological amounts of fructose-glucose on glomerular hypertension and oxidative stress in rats,” *American Journal of Physiology - Renal Physiology*, vol. 304, no. 6, pp. F727–F736, 2013.
- [27] A. C. Rutledge and K. Adeli, “Fructose and the metabolic syndrome: pathophysiology and molecular mechanisms,” *Nutrition Reviews*, vol. 65, no. 6, pp. 13–S23, 2007.
- [28] M. E. Bocarsly, E. S. Powell, N. M. Avena, and B. G. Hoebel, “High-fructose corn syrup causes characteristics of obesity in rats: increased body weight, body fat and triglyceride levels,” *Pharmacology Biochemistry and Behavior*, vol. 97, no. 1, pp. 101–106, 2010.
- [29] A. Lindqvist, A. Baelemans, and C. Erlanson-Albertsson, “Effects of sucrose, glucose and fructose on peripheral and central appetite signals,” *Regulatory Peptides*, vol. 150, no. 1–3, pp. 26–32, 2008.
- [30] A. Alzamendi, A. Giovambattista, A. Raschia et al., “Fructose-rich diet-induced abdominal adipose tissue endocrine dysfunction in normal male rats,” *Endocrine*, vol. 35, no. 2, pp. 227–232, 2009.
- [31] R. F. de Moura, C. Ribeiro, J. A. de Oliveira, E. Stevanato, and M. A. R. de Mello, “Metabolic syndrome signs in Wistar rats submitted to different high-fructose ingestion protocols,” *British Journal of Nutrition*, vol. 101, no. 8, pp. 1178–1184, 2009.
- [32] B. Altunkaynak and E. Özbek, “Overweight and structural alterations of the liver in female rats fed a high-fat diet: a stereological and histological study,” *The Turkish Journal of Gastroenterology*, vol. 20, no. 2, pp. 93–103, 2009.
- [33] J. M. Llobet and J. L. Domingo, “Acute toxicity of vanadium compounds in rats and mice,” *Toxicology Letters*, vol. 23, no. 2, pp. 227–231, 1984.
- [34] J. Rodríguez-Mercado and M. Altamirano-Lozano, “Vanadio: contaminación, metabolismo y genotoxicidad,” *Revista Internacional de Contaminación Ambiental*, vol. 22, no. 4, pp. 173–189, 2006.
- [35] J. Chidambaram and A. Carani Venkatraman, “*Cissus quadrangularis* stem alleviates insulin resistance, oxidative injury and fatty liver disease in rats fed high fat plus fructose diet,” *Food and Chemical Toxicology*, vol. 48, no. 8–9, pp. 2021–2029, 2010.

- [36] P. K. Bagul, H. Middela, S. Matapally et al., "Attenuation of insulin resistance, metabolic syndrome and hepatic oxidative stress by resveratrol in fructose-fed rats," *Pharmacological Research*, vol. 66, no. 3, pp. 260–268, 2012.
- [37] P. V. G. Katakam, M. R. Ujhelyi, M. Hoenig, and A. W. Miller, "Metformin improves vascular function in insulin-resistant rats," *Hypertension*, vol. 35, no. 1, pp. 108–112, 2000.
- [38] H. Sigiuchi, Y. Uji, H. Okabe et al., "Direct measurement of high-density lipoprotein cholesterol in serum with polyethylene glycol-modified enzymes and sulfated α -cyclodextrin," *Clinical Chemistry*, vol. 40, pp. 717–723, 1995.
- [39] S. M. Alwahsh, M. Xu, H. A. Seyhan et al., "Diet high in fructose leads to an overexpression of lipocalin-2 in rat fatty liver," *World Journal of Gastroenterology*, vol. 20, no. 7, pp. 1807–1821, 2014.
- [40] N. Mamikutty, Z. C. Thent, S. R. Sapri, N. N. Sahruddin, M. R. Mohd Yusof, and F. Haji Suhaimi, "The establishment of metabolic syndrome model by induction of fructose drinking water in male Wistar rats," *BioMed Research International*, vol. 2014, Article ID 263897, 8 pages, 2014.
- [41] D. P. Figlewicz, G. Ioannou, J. Bennett Jay, S. Kittleson, C. Savard, and C. L. Roth, "Effect of moderate intake of sweeteners on metabolic health in the rat," *Physiology & Behavior*, vol. 98, no. 5, pp. 618–624, 2009.
- [42] D. A. Contreras-Cadena, C. Gómez-Pech, M. Rangel-García, A. Ruiz-Hernández, P. Martínez-Bulit, and N. Barba-Behrens, "La importancia del vanadio en los seres vivos," *Educación Química*, vol. 25, no. E1, pp. 245–253, 2014.
- [43] L. Pirmoradi, A. Noorafshan, A. Safaee, and G. A. Dehghani, "Quantitative assessment of proliferative effects of Oral vanadium on pancreatic islet volumes and beta cell numbers of diabetic rats," *Iranian Biomedical Journal*, vol. 20, no. 1, pp. 18–25, 2016.
- [44] J. Almanza-Pérez, G. Blancas-Flores, R. García-Macedo, F. Alarcón-Aguilar, and M. Cruz, "Leptina y su relación con la obesidad y la diabetes mellitus tipo 2," *Gaceta Médica de México*, vol. 144, no. 6, pp. 535–542, 2008.
- [45] M. Halle and P. B. Persson, "Role of leptin and leptin receptor in inflammation," *American Journal of Physiology-Regulatory, Integrative and Comparative Physiology*, vol. 284, no. 3, pp. R760–R762, 2003.
- [46] H. Ahmadi-Eslamloo, G. A. Dehghani, and S. M. S. Moosavi, "Long-term treatment of diabetic rats with vanadyl sulfate or insulin attenuate acute focal cerebral ischemia/reperfusion injury via their antiglycemic effect," *Metabolic Brain Disease*, vol. 33, no. 1, pp. 225–235, 2018.
- [47] Q. Zhao, D. Chen, P. Liu, T. Wei, F. Zhang, and W. Ding, "Oxidovanadium (IV) sulfate-induced glucose uptake in HepG2 cells through IR/Akt pathway and hydroxyl radicals," *Journal of Inorganic Biochemistry*, vol. 149, pp. 39–44, 2015.
- [48] C. E. Pinzón, M. L. Serrano, and M. C. Sanabria, "Papel de la vía fosfatidilinositol 3 kinasa (PI3K/Akt) en humanos," *Revista Ciencias de la Salud*, vol. 7, no. 2, pp. 47–66, 2009.
- [49] S. S. Martin, A. Qasim, and M. P. Reilly, "Leptin resistance: a possible interface of inflammation and metabolism in obesity-related cardiovascular disease," *Journal of the American College of Cardiology*, vol. 52, no. 15, pp. 1201–1210, 2008.
- [50] M. Maachi, L. Piéroni, E. Bruckert et al., "Systemic low-grade inflammation is related to both circulating and adipose tissue TNF α , leptin and IL-6 levels in obese women," *International Journal of Obesity and Related Metabolic Disorders*, vol. 28, no. 8, pp. 993–997, 2004.
- [51] V. Bermúdez, F. Finol, N. Parra et al., "PPAR-gamma agonists and their role in type 2 diabetes mellitus management," *American Journal of Therapeutics*, vol. 17, no. 3, pp. 274–283, 2010.
- [52] A. Sandoval, F. Manzur, D. Gómez, and C. Gómez, "Receptores nucleares y metabolismo de lípidos: implicaciones cardiovasculares," *Revista Colombiana de Cardiología*, vol. 16, pp. 29–34, 2009.
- [53] A. Calvillo, F. Espinosa, M. Macari, S. Platas, and D. Rojas, "Contra la obesidad y la diabetes: una estrategia secuestrada," 2015, http://elpoderdelconsumidor.org/wp-content/uploads/2015/04/Contra-la-Obesidad-y-Diabetes_Una-Estrategia-Secuestrada.pdf.
- [54] S. S. Elliott, N. L. Keim, J. S. Stern, K. Teff, and P. J. Havel, "Fructose, weight gain, and the insulin resistance syndrome," *The American Journal of Clinical Nutrition*, vol. 76, no. 5, pp. 911–922, 2002.

Research Article

Verification That Mouse Chromosome 14 Is Responsible for Susceptibility to Streptozotocin in NSY Mice

Naru Babaya ¹, Hironori Ueda ², Shinsuke Noso,¹ Yoshihisa Hiromine,¹ Michiko Itoi-Babaya,³ Misato Kobayashi,⁴ Tomomi Fujisawa,⁵ and Hiroshi Ikegami ¹

¹Department of Endocrinology, Metabolism and Diabetes, Kindai University Faculty of Medicine, Osaka, Japan

²Department of Molecular Endocrinology, Osaka University Graduate School of Medicine, Osaka, Japan

³Health Care Center, Rinku General Medical Center, Osaka, Japan

⁴Department of Applied Molecular Bioscience, Graduate School of Bioagricultural Sciences, Nagoya University, Aichi, Japan

⁵Sakai City Medical Center, Osaka, Japan

Correspondence should be addressed to Hiroshi Ikegami; ikegami@med.kindai.ac.jp

Received 2 July 2018; Accepted 27 September 2018; Published 21 November 2018

Guest Editor: Fatchiyah Fatchiyah

Copyright © 2018 Naru Babaya et al. This is an open access article distributed under the Creative Commons Attribution License, which permits unrestricted use, distribution, and reproduction in any medium, provided the original work is properly cited.

Introduction. Streptozotocin- (STZ-) induced diabetes is under polygenic control, and the genetic loci for STZ susceptibility are mapped to chromosome (Chr) 11 in Nagoya-Shibata-Yasuda (NSY) mice. In addition to Chr11, other genes on different chromosomes may contribute to STZ susceptibility in NSY mice. The aim of this study was to determine whether NSY-Chr14 contributes to STZ susceptibility and contains the STZ-susceptible region. **Materials and Methods.** A consomic C3H-14^{NSY} strain (R0: homozygous for NSY-derived whole Chr14 on the control C3H background), two congenic strains (R1: the region retained proximal and middle segments of NSY-Chr14 and R2: the region retained a proximal segment of NSY-Chr14), and parental NSY and C3H mice were intraperitoneally injected with a single injection of STZ at a dose of 175 mg/kg body weight at 12 weeks of age. Blood glucose levels and body weights were measured at days 0, 1, 2, 4, 5, 7, 8, and 14 after STZ injection. At day 14 after STZ injection, pancreata were dissected and fixed. **Results.** After STZ injection, blood glucose levels were significantly higher in R0 mice than in C3H mice. However, blood glucose levels in R0 mice were not as severely affected as those in NSY mice. In R1 and R2 mice, blood glucose levels were similar to those in C3H mice and were significantly lower than those in R0 mice. Body weights were decreased in NSY and R0 mice; however, this change was not observed in R1, R2, and C3H mice. Although islet tissues in all strains exhibited degeneration and cellular infiltration, histological changes in NSY and R0 mice were more severe than those in R1, R2, and C3H mice. **Conclusions.** These data demonstrated that NSY-Chr14 was a STZ-susceptible chromosome and that STZ susceptibility was mapped to the distal segment of NSY-Chr14.

1. Introduction

Streptozotocin (STZ) has been widely used to induce diabetes through pancreatic islet destruction in experimental animals [1–3]. STZ, a small molecule that resembles glucose, is taken up to bind glucose transporter-2 [1, 3]. In islet β -cells, STZ decomposes and damages DNA, which leads to cell death [1, 3]. Among inbred mouse strains, varying susceptibility to STZ-induced diabetes has been reported. Nonobese diabetic (NOD) mice, an inbred strain of type 1 diabetes [4], are extremely susceptible to β -cell destruction by STZ [5].

Although susceptibility to type 1 diabetes is primarily determined by the immunological factor, several studies have indicated that the intrinsic vulnerability of β -cells is also involved in susceptibility to type 1 diabetes, which suggests shared mechanisms between STZ-induced diabetes and type 1 diabetes [5–8].

Nagoya-Shibata-Yasuda (NSY) mice [9], an inbred strain of type 2 diabetes with moderate obesity and fatty liver, were established by selective breeding for glucose intolerance from an outbred colony, Jcl:ICR mice, from which NOD mice were also derived [10]. Both NSY and NOD mice are extremely

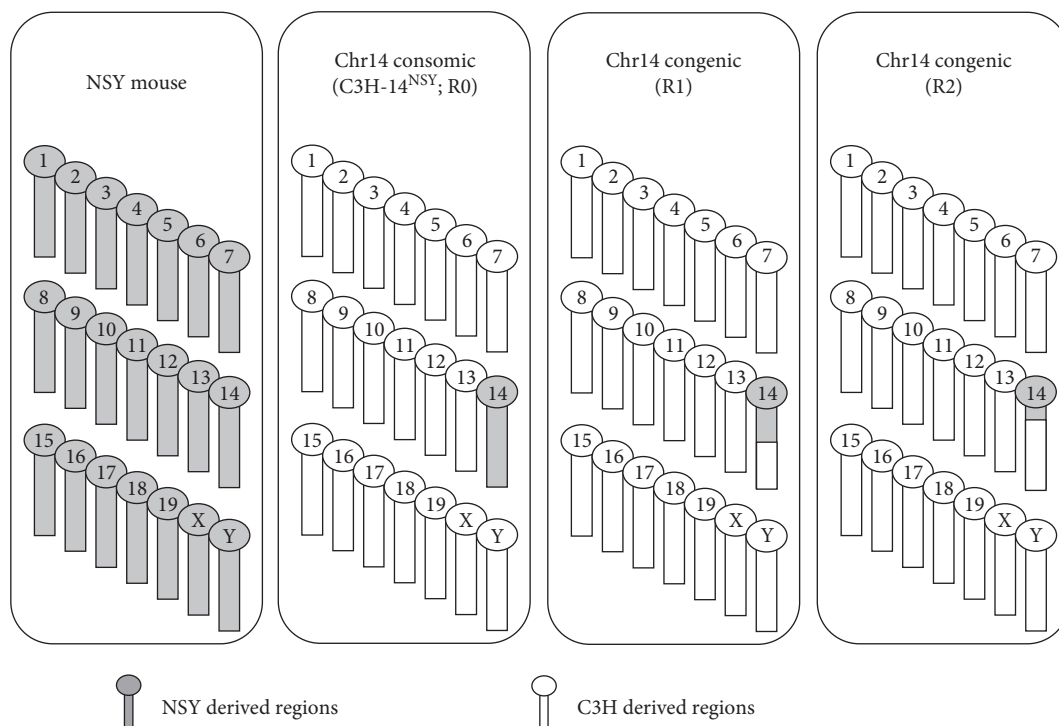


FIGURE 1: Schematic illustration of NSY, Chr14 of consomic mice (C3H-14^{NSY}; R0) and congenic mice (R1 and R2), which carry NSY-derived susceptible regions onto a C3H-derived resistance background. Regions from NSY mice are shown in gray, and regions from C3H mice are shown in white.

STZ-sensitive strains [5, 7, 11], which suggests a shared genetic basis in the vulnerability of β -cells between these strains. β -cell fragility may be shared between type 1 and type 2 diabetes [6, 12, 13]. These lines of evidence indicate that three types of diabetes (STZ-induced, type 1, and type 2 diabetes) share common genetic factors and mechanisms. Therefore, the identification of STZ-susceptible genes is important to clarify the mechanism of β -cell vulnerability in type 1 and type 2 diabetes.

We previously identified three major quantitative trait loci (QTLs) for diabetes-related phenotypes (*Nidd1n*, *Nidd2n*, and *Nidd3n*) on chromosome (Chr) 11, 14, and 6, respectively [14]. A QTL for fatty liver (*Flnn*) and a QTL for body weight (*Bw1n*) on Chr6 [15] were found using NSY and C3H (nondiabetic) mice. Subsequent studies using consomic C3H-11^{NSY} and C3H-14^{NSY} mice in which the entire NSY-Chr11 and NSY-Chr14 were introgressed onto the genetic background of control C3H mice clearly demonstrated that NSY-Chr11 and NSY-Chr14 harbor loci for diabetes [16]. Subsequent studies using consomic C3H-11^{NSY} mice indicated that NSY-derived Chr11 harbors susceptibility to STZ-induced diabetes [7, 11]. However, the STZ sensitivity of the C3H-11^{NSY} strain is not as strong as that of the NSY parental strain, which suggests that STZ-induced diabetes is under polygenic control and that genes on chromosomes other than Chr11 also contribute to STZ susceptibility [7, 11].

In this study, to detect novel loci related to STZ susceptibility, we focused on another diabetogenic chromosome, i.e., NSY-Chr14. C3H-14^{NSY} mice and their congenic strains were administered a single high dose of STZ, and the STZ

sensitivities of these strains were compared with those of the parental strains.

2. Materials and Methods

2.1. Animals. We used five strains, namely, NSY [9, 10, 14, 17, 18], C3H/HeNcrj (C3H), consomic C3H-14^{NSY} (R0) [16], congenic R1, and R2 mice [19]. NSY mice were originally obtained from the Branch Hospital of Nagoya University School of Medicine. C3H mice were purchased from Charles River Laboratories (Kanagawa, Japan).

R0 mice, which were homozygous for the NSY-derived whole Chr14 on the control C3H background, were previously constructed [16] using the speed congenic method [20, 21]. Briefly, F1 male mice were obtained by mating (NSY \times C3H). These males were mated with C3H females, and their progeny heterozygous for Chr14 were used for next generation. This backcross was repeated until all the markers for background typing became homozygous for C3H genotype, at which point the heterozygous consomic strains were obtained. The mice heterozygous for Chr14 were intercrossed to obtain mice homozygous for Chr14.

Recently, we also constructed two novel congenic lines, R1 and R2, obtained from R0 (Figure 1) [19]. Briefly, heterozygous R1 and R2 male mice were produced by mating (R0 \times C3H) F1 with C3H and selecting males that possessed the genomic region of interest on Chr14, and then, the heterozygous R1 and R2 male mice were mated with C3H females. Their progeny with the genomic region of interest were intercrossed to obtain homozygous mice. R1 mice possess the proximal and middle segments of NSY-

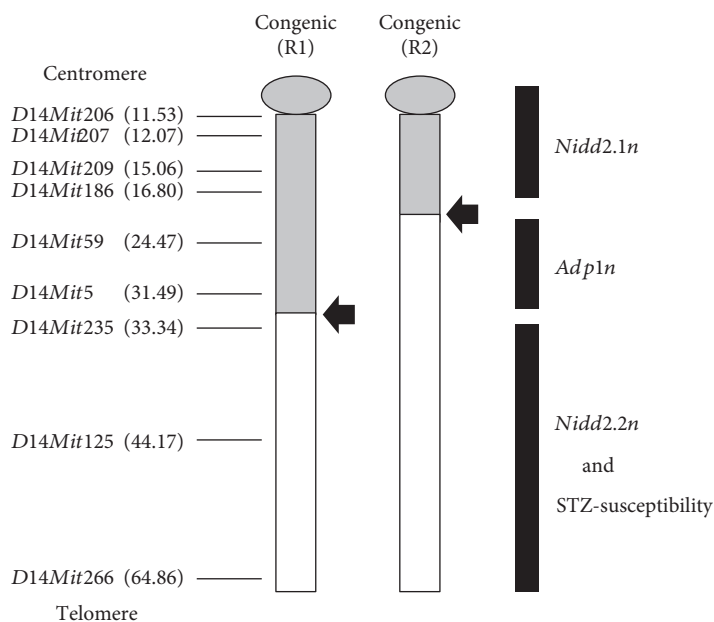


FIGURE 2: Schematic illustration of congenic mice. R1 possesses proximal and middle segments of NSY-Chr14 from the centromere to the recombinant position between *D14Mit5* and *D14Mit235*. R2 mice possess the proximal segment of NSY-Chr14 from the centromere to the recombinant position between *D14Mit186* and *D14Mit59*. Regions from NSY mice are shown in gray, and regions from C3H mice are shown in white. Arrows show each recombinant position. In parentheses, marker map positions from the centromere obtained from the Mouse Genome Database (<http://www.informatics.jax.org>). The diabetogenic loci (*Nidd2.1n* and *Nidd2.2n*) and the adiposity locus (*Adp1n*), which were reported in our previous study [19], and STZ-susceptibility locus, which was demonstrated in this study, are shown in black bars.

Chr14 from the centromere to the recombinant position between *D14Mit5* and *D14Mit235* (Figure 2). R2 mice possess the proximal segment of NSY-Chr14 from the centromere to the recombinant position between *D14Mit186* and *D14Mit59* (Figure 2). The positions of the diabetogenic loci (*Nidd2.1n* and *Nidd2.2n*) and the adiposity locus (*Adp1n*), which were reported in our previous study [19], are shown in Figure 2.

These mice were maintained by brother-sister mating and under specific pathogen-free conditions in the animal facilities of Osaka University Graduate School of Medicine. All mice had free access to tap water and a standard diet (CRF-1: Oriental Yeast, Tokyo, Japan) in a temperature-controlled room (22–25°C) on a 12 h light-dark cycle (6:00–18:00 h). The animal protocols used for this study were approved by the Osaka University Graduate School of Medicine Committee on Animal Welfare. Male mice were used for all experiments.

2.2. Protocols. NSY, C3H, R0, R1, and R2 mice received a single injection of STZ at a dose of 175 mg/kg body weight at 12 weeks of age. STZ was dissolved in sodium citrate buffer (Wako Pure Chemical Industries, Ltd., Osaka, JAPAN) and immediately injected intraperitoneally. Blood glucose levels and body weights were measured ad lib at days 0, 1, 2, 4, 5, 7, 8, and 14 after STZ injection. Blood glucose levels were determined by the glucose oxidase method using Glutest Ace (Sanwa Kagaku Kenkyusho Co., Ltd., Nagoya, Japan) in which the detection limit was 33.34 mmol/l. In this study, glucose values greater than 33.34 mmol/l were reported as

33.34 mmol/l. Mice with glycemia greater than 16.7 mmol/l were considered hyperglycemic because the NSY strain is a model of type 2 diabetes; therefore, the ad lib blood glucose level can exceed 11.1 mmol/l. Some of the data from NSY and C3H mice have been previously reported [7, 11] and were reanalyzed in this study.

2.3. Histological Examination. STZ-treated mice were killed under sevoflurane anesthesia at day 14 after injection, and pancreata were dissected and fixed in neutralized 10% formalin. Paraffin sections of those tissues were stained with hematoxylin-eosin by the standard method. The cellular infiltration in and around islets in NSY, C3H, R0, R1, and R2 mice was graded (0: normal islet; 1: peri-insulinitis or <25% of β -cell area infiltrated; and 2: more than 25% of β -cell area infiltrated). All islets were evaluated by an observer, blinded with respect to the origin of the sections.

2.4. Statistical Analysis. All values are expressed as the mean \pm SEM. Statistical analysis was performed by the Mann-Whitney *U* test or one-way analysis of variance (ANOVA) with post hoc tests (Dunnett's multiple comparison tests). Survival curves were analyzed with the log-rank test. Statistical tests were performed using the Prism software (GraphPad Prism®). $P < 0.05$ was considered statistically significant.

3. Results

3.1. STZ Sensitivity in Consomic C3H-14^{NSY}; R0 (Figure 3, Supplemental Figure 1). Three R0 mice were dead at days

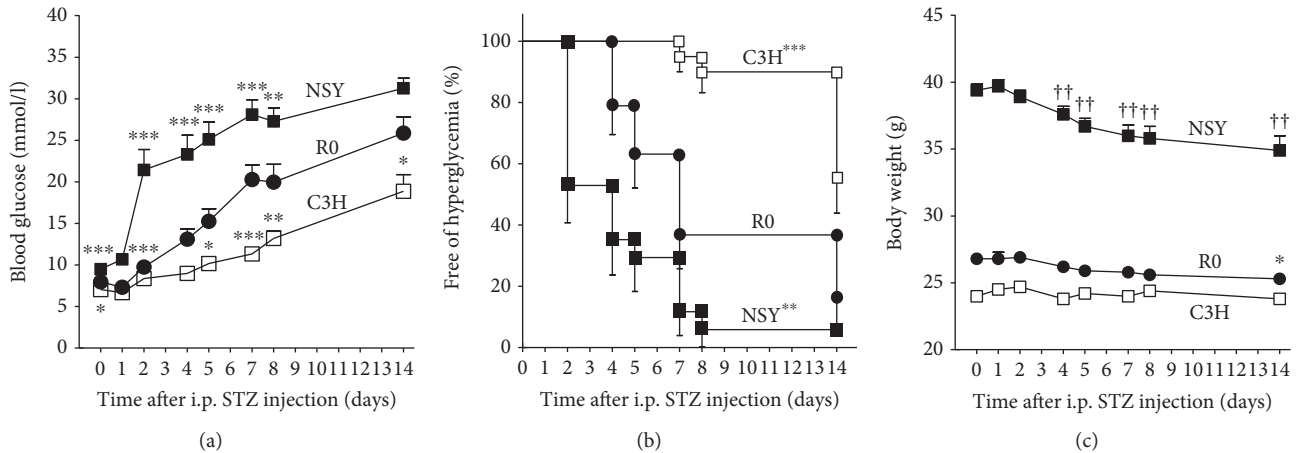


FIGURE 3: STZ sensitivity at 12 weeks of age in NSY ($n = 17$; black squares), R0 ($n = 19$; black circles), and C3H mice ($n = 20$; white squares). Glucose concentrations and body weight are measured ad lib at days 0, 1, 2, 4, 5, 7, 8, and 14 days after STZ injection. Data are expressed as the mean \pm SEM. (a) Blood glucose concentrations. Four NSY mice were dead (one at day 3 and three at days 9–13). Because these dead mice showed hyperglycemia before death, the glucose levels after death were reported as 33.34 mmol/l, which is the detection limit of the glucose sensor. * $p < 0.05$, ** $p < 0.01$, *** $p < 0.001$ compared with R0 (one-way ANOVA with post hoc test (Dunnett's multiple comparison tests)). (b) The percentage of animals free of hyperglycemia. Mice with glycemia higher than 16.7 mmol/l were considered hyperglycemic. ** $p < 0.01$, *** $p < 0.001$ compared with R0 (log-rank test). (c) Body weight changes. Four NSY and three R0 mice were dead (described previously). This figure does not contain the body weight data after death. * $p < 0.05$ compared with the basal body weight of R0 and †† $p < 0.01$ compared with the basal body weight of NSY (Mann-Whitney U test).

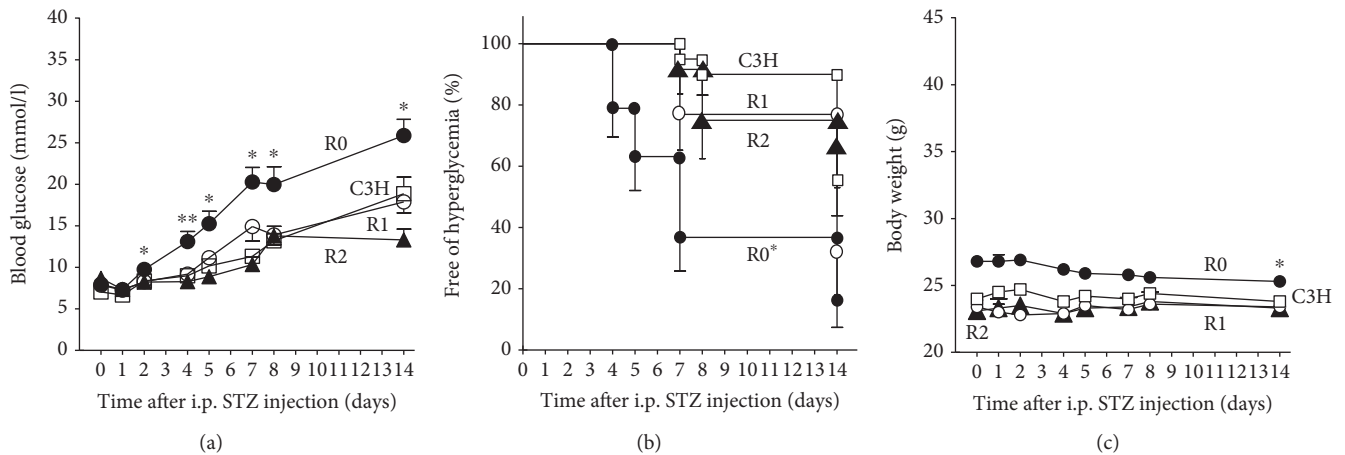


FIGURE 4: STZ sensitivity at 12 weeks of age in R0 ($n = 19$; black circles), C3H ($n = 20$; white squares), R1 ($n = 13$; white circles), and R2 mice ($n = 12$; black triangles). Glucose concentrations and body weight are measured ad lib at days 0, 1, 2, 4, 5, 7, 8, and 14 days after STZ injection. Data are expressed as the mean \pm SEM. (a) Blood glucose concentrations. The values of glucose in the R0 were reported as shown in Figure 3 legend. * $p < 0.05$, ** $p < 0.01$ compared with R1 (one-way ANOVA with post hoc test (Dunnett's multiple comparison tests)). (b) The percentage of animals free of hyperglycemia. Mice with glycemia higher than 16.7 mmol/l were considered hyperglycemic. * $p < 0.05$ compared with R1 (log-rank test). (c) Body weight changes. The values of body weight in R0 were reported as shown in Figure 3 legend. * $p < 0.05$ compared with the basal body weight of R0 (Mann-Whitney U test).

9–13 due to hyperglycemia. R0 mice exhibited significantly higher blood glucose levels after STZ injection than did C3H mice (Figure 3(a)). Life table analysis demonstrated a significant difference in the survival curves of mice free from hyperglycemia between R0 and C3H mice (Figure 3(b), $p < 0.001$). At 14 days post-STZ injection, body weights (Figure 3(c)) were significantly reduced in R0 mice (-5.6% from the basal, $p < 0.05$). In contrast, no body weight reduction was observed in C3H mice ($+0.8\%$ from the basal,

$p = 0.35$). These results indicate that introgression of a single Chr14 from STZ-sensitive NSY mice converted STZ-resistant C3H mice to STZ-sensitive mice.

However, blood glucose levels in R0 mice were not as severe as those in NSY mice (Figure 3(a)). Four NSY mice were dead (one at day 3 and three at days 9–13) because of hyperglycemia. Compared with R0 mice, NSY mice exhibited significantly higher blood glucose levels after STZ injection, and life table analysis demonstrated a significant difference

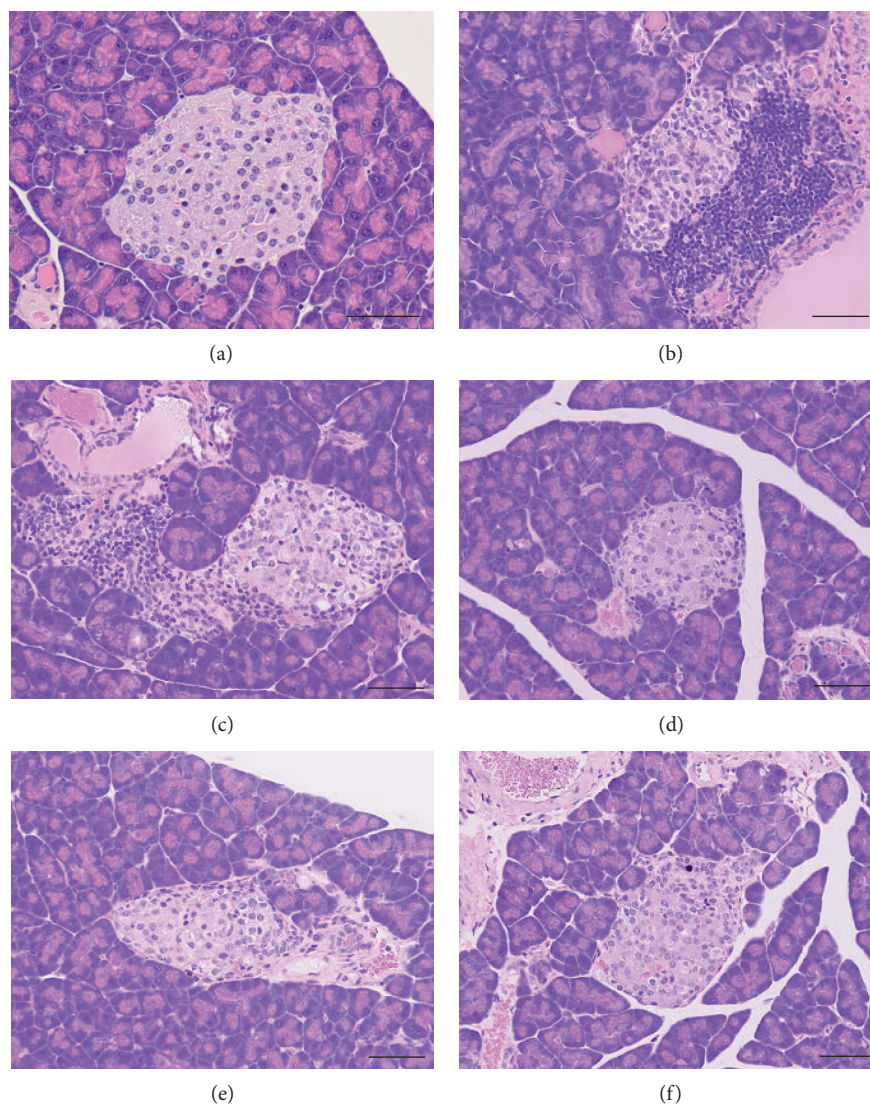


FIGURE 5: Pancreatic islets stained with hematoxylin-eosin. Scale bars, 50 μm . (a) An intact islet from non-STZ-injected NSY mice at 24 weeks of age. Inflammatory changes were not observed. (b–f) Typical islets from STZ-injected NSY (b), R0 (c), R1 (d), R2 (e), and C3H (f) mice at day 14 after STZ injection.

between the survival curves (Figure 3(b), $p < 0.01$). At 14 days after STZ injection, the reduction in the body weights of NSY mice (-11.4% from the basal, $p < 0.01$) was more severe than that of R0 mice (Figure 3(c)). These results indicate that the sensitivity of R0 mice to STZ is not as strong as that of NSY mice, which suggests the contribution of other chromosomes in addition to Chr14 to STZ susceptibility.

3.2. STZ Sensitivity in Congenic Mice; R1 and R2 (Figure 4, Supplemental Figure 1). Glucose levels after STZ injection in R1 mice were similar to those in C3H mice and were significantly lower than those in R0 mice (Figure 4(a)). The cumulative incidence of STZ-induced hyperglycemia in R1 mice was similar to that in C3H mice and was significantly lower than that in R0 mice (Figure 4(b), $p < 0.05$). In R1 mice, no reduction in body weight was observed ($+0.0\%$ from the basal, $p = 0.94$).

Glucose levels after STZ injection in R2 mice were similar to those in R1 and C3H mice (Figure 4(a)). Life table analysis demonstrated no difference in the survival curves of mice free from hyperglycemia among congenic (R1 and R2) and C3H mice (Figure 4(b)). In R2 mice, no reduction in body weight was observed ($+0.9\%$ from the basal, $p = 0.82$).

Since R0 mice but not R1 and R2 mice showed STZ sensitivity, the data in the present study indicate that the distal region of Chr14 retained in R0 mice but not in R1 and R2 mice plays an important role in STZ susceptibility (Figure 2).

3.3. Histological Phenotype in NSY, C3H, R0, R1, and R2 Mice (Figure 5, Supplemental Figure 2). In all strains, the histological sections of islet tissues at day 14 showed degeneration. Architectural disarray of pancreatic islets and cellular infiltration were observed. Histological changes in NSY and R0 mice were more severe than those in R1, R2, and C3H mice. Apparent signs of cellular infiltration in or around

the pancreatic islets were also observed in all strains. Cellular infiltration in NSY and R0 mice was more severe than that in R1, R2, and C3H mice (Supplemental Figure 2).

4. Discussion

We previously reported that Chr11 harbors susceptibility to STZ-induced diabetes in NSY mice [7, 11]. However, Chr11 was insufficient to explain all STZ sensitivity in NSY mice. In this study, we identified an additional STZ-susceptible chromosome, Chr14, and mapped STZ susceptibility to the distal region of Chr14 (from *D14Mit5* to the telomere).

In our previous study, we established two congenic strains in which limited segments of NSY-Chr14 were introgressed onto control C3H background genes [19]. One congenic strain, termed R1, possessed a proximal half segment of NSY-Chr14 (<33.34 cM from the centromere to *D14Mit235*), and the other congenic, termed R2, possessed a more limited segment of NSY-Chr14 (<24.47 cM from the centromere to *D4Mit59*). Analysis of these congenic strains demonstrated that a locus termed *Nidd2.2n* in the distal segment of NSY-Chr14 affects fasting glucose, postchallenge hyperglycemia, and insulin resistance [19]. A locus for STZ susceptibility localized to the distal region of NSY-Chr14 in the present study overlaps with the region for *Nidd2.2n*. Further studies with congenic strains with the distal region of NSY-Chr14 are necessary for fine mapping and identification of the responsible gene.

The distal region of Chr14 where STZ susceptibility was mapped in the present study was not previously linked to STZ-induced diabetes. Gonzalez et al. reported that two genetic loci for STZ susceptibility were identified on Chr 9 and Chr 11 in NOD mice and suggested that the two loci were insufficient to predict resistance or sensitivity to STZ-induced diabetes [5]. In our previous and present studies, the STZ sensitivity of consomic C3H-11^{NSY} and C3H-14^{NSY} mice was less than that of NSY mice, suggesting that STZ-induced diabetes is under polygenic control. We do not know whether NSY-Chr11 and NSY-Chr14 are sufficient for the full expression of the STZ sensitivity of NSY mice. Analysis of C3H-11^{NSY}14^{NSY} mice [16] containing both NSY-Chr11 and NSY-Chr14 on the C3H background will lead to the answer.

A single high dose of STZ is used for experiments attempting to cause type 1 diabetes by direct toxicity, and glucose homeostasis deterioration rapidly arises within a few days [22]. Although only 10% of STZ-treated mice that received a single high dose exhibited mononuclear cell infiltration in pancreatic islets, more than 60% of STZ-treated mice that were treated with a single low dose exhibited this phenomenon [23]. In this study, we used a single high dose of STZ in NSY mice. Hyperglycemia began to appear within 48 h after STZ injection. Mononuclear cell infiltration was detected in all examined pancreata. However, we do not know why NSY mice had severe mononuclear cell infiltration despite the single high-dose STZ injection. One possible reason is that pancreata were dissected at 14 days after STZ injection in our study, whereas dissection occurred within 1 week after the development of

hyperglycemia in a previous study [23]. Another possible reason is simply strain differences.

5. Conclusion

The present study demonstrated that NSY-Chr14 was a STZ-susceptible chromosome and that the STZ-susceptible region was located in the distal segment of NSY-Chr14. Construction of new congenic strains will lead to fine mapping and identification of causal variants of the genes responsible for STZ susceptibility in the NSY mouse.

Data Availability

The data used to support the findings of this study are included within the article.

Conflicts of Interest

The authors declare no conflicts of interest regarding the publication of this paper.

Acknowledgments

This study was supported by the Japan Society for the Promotion of Science, Grants-in-Aid for Scientific Research (JSPS KAKENHI) Grant number JP15K09403. The authors thank M. Moritani for her skillful technical assistance and M. Shibata for his contribution to establishing the NSY colony and discussion.

Supplementary Materials

Supplemental Figure 1: blood glucose concentrations in NSY, C3H, R0, R1, and R2 mice ad lib at days 0, 1, 2, 4, 5, 7, 8, and 14 after STZ injection. Four NSY mice and three R0 mice died during follow-up. The values of glucose in the dead NSY and R0 mice were reported as shown in Figure 3 legend. ** $p < 0.01$, *** $p < 0.001$ (higher) and † $p < 0.05$, †† $p < 0.01$, ††† $p < 0.001$ (lower) compared with R0 (one-way ANOVA with post hoc test (Dunnett's multiple comparison tests)). Supplemental Figure 2: degree of cellular infiltration in and around islets in NSY, C3H, R0, R1, and R2 mice. The cellular infiltration was graded (normal islet: white; peri-insulinitis or <25% 3/4 of β -cell area infiltrated: gray; more than 25% of β -cell area infiltrated: black). Statistical analysis was performed by the Mann-Whitney U test. n.s.: not significant. (Supplementary Materials)

References

- [1] S. Gheibi, K. Kashfi, and A. Ghasemi, "A practical guide for induction of type-2 diabetes in rat: incorporating a high-fat diet and streptozotocin," *Biomedicine and Pharmacotherapy*, vol. 95, no. 11, pp. 605–613, 2017.
- [2] T. Maegawa, Y. Miyasaka, M. Kobayashi et al., "Congenic mapping and candidate gene analysis for streptozotocin-induced diabetes susceptibility locus on mouse chromosome 11," *Mammalian Genome*, vol. 29, no. 3-4, pp. 273–280, 2018.

- [3] M. Radenkovic, M. Stojanovic, and M. Prostran, "Experimental diabetes induced by alloxan and streptozotocin: the current state of the art," *Journal of Pharmacological and Toxicological Methods*, vol. 78, no. 3-4, pp. 13–31, 2016.
- [4] S. Makino, K. Kunimoto, Y. Muraoka, Y. Mizushima, K. Katagiri, and Y. Tochino, "Breeding of a non-obese, diabetic strain of mice," *Experimental Animals*, vol. 29, no. 1, pp. 1–13, 1980.
- [5] C. Gonzalez, S. Cuvellier, C. Hue-Beauvais, and M. Lévi-Strauss, "Genetic control of non obese diabetic mice susceptibility to high-dose streptozotocin-induced diabetes," *Diabetologia*, vol. 46, no. 9, pp. 1291–1295, 2003.
- [6] J. D. Acharya and S. S. Ghaskadbi, "Islets and their antioxidant defense," *Islets*, vol. 2, no. 4, pp. 225–235, 2010.
- [7] N. Babaya, H. Ikegami, T. Fujisawa et al., "Susceptibility to streptozotocin-induced diabetes is mapped to mouse chromosome 11," *Biochemical and Biophysical Research Communications*, vol. 328, no. 1, pp. 158–164, 2005.
- [8] C. E. Mathews, R. T. Graser, A. Savinov, D. V. Serreze, and E. H. Leiter, "Unusual resistance of ALR/Lt mouse beta cells to autoimmune destruction: role for beta cell-expressed resistance determinants," *Proceedings of the National Academy of Sciences of the United States of America*, vol. 98, no. 1, pp. 235–240, 2001.
- [9] H. Ueda, H. Ikegami, E. Yamato et al., "The NSY mouse: a new animal model of spontaneous NIDDM with moderate obesity," *Diabetologia*, vol. 38, no. 5, pp. 503–508, 1995.
- [10] H. Ikegami, T. Fujisawa, and T. Ogihara, "Mouse models of type 1 and type 2 diabetes derived from the same closed colony: genetic susceptibility shared between two types of diabetes," *ILAR Journal*, vol. 45, no. 3, pp. 268–277, 2004.
- [11] N. Babaya, H. Ueda, S. Noso et al., "Dose effect and mode of inheritance of diabetogenic gene on mouse chromosome 11," *Journal of Diabetes Research*, vol. 2013, Article ID 608923, 6 pages, 2013.
- [12] J. Dooley, L. Tian, S. Schonefeldt et al., "Genetic predisposition for beta cell fragility underlies type 1 and type 2 diabetes," *Nature Genetics*, vol. 48, no. 5, pp. 519–527, 2016.
- [13] A. Liston, J. A. Todd, and V. Lagou, "Beta-cell fragility as a common underlying risk factor in type 1 and type 2 diabetes," *Trends in Molecular Medicine*, vol. 23, no. 2, pp. 181–194, 2017.
- [14] H. Ueda, H. Ikegami, Y. Kawaguchi et al., "Genetic analysis of late-onset type 2 diabetes in a mouse model of human complex trait," *Diabetes*, vol. 48, no. 5, pp. 1168–1174, 1999.
- [15] M. Itoi-Babaya, H. Ikegami, T. Fujisawa et al., "Fatty liver and obesity: phenotypically correlated but genetically distinct traits in a mouse model of type 2 diabetes," *Diabetologia*, vol. 50, no. 8, pp. 1641–1648, 2007.
- [16] N. Babaya, T. Fujisawa, K. Nojima et al., "Direct evidence for susceptibility genes for type 2 diabetes on mouse chromosomes 11 and 14," *Diabetologia*, vol. 53, no. 7, pp. 1362–1371, 2010.
- [17] H. Ueda, H. Ikegami, Y. Kawaguchi et al., "Paternal-maternal effects on phenotypic characteristics in spontaneously diabetic Nagoya-Shibata-Yasuda mice," *Metabolism*, vol. 49, no. 5, pp. 651–656, 2000.
- [18] H. Ueda, H. Ikegami, Y. Kawaguchi et al., "Age-dependent changes in phenotypes and candidate gene analysis in a polygenic animal model of type II diabetes mellitus; NSY mouse," *Diabetologia*, vol. 43, no. 7, pp. 932–938, 2000.
- [19] N. Babaya, H. Ueda, S. Noso et al., "Genetic dissection of susceptibility genes for diabetes and related phenotypes on mouse chromosome 14 by means of congenic strains," *BMC Genetics*, vol. 15, no. 1, p. 93, 2014.
- [20] P. Markel, P. Shu, C. Ebeling et al., "Theoretical and empirical issues for marker-assisted breeding of congenic mouse strains," *Nature Genetics*, vol. 17, no. 3, pp. 280–284, 1997.
- [21] J. B. Singer, A. E. Hill, L. C. Burrage et al., "Genetic dissection of complex traits with chromosome substitution strains of mice," *Science*, vol. 304, no. 5669, pp. 445–448, 2004.
- [22] M. C. Deeds, J. M. Anderson, A. S. Armstrong et al., "Single dose streptozotocin-induced diabetes: considerations for study design in islet transplantation models," *Laboratory Animals*, vol. 45, no. 3, pp. 131–140, 2011.
- [23] S. W. Huang and G. E. Taylor, "Immune insulinitis and antibodies to nucleic acids induced with streptozotocin in mice," *Clinical and Experimental Immunology*, vol. 43, no. 2, pp. 425–429, 1981.

Research Article

Spontaneously Diabetic Torii (SDT) Fatty Rat, a Novel Animal Model of Type 2 Diabetes Mellitus, Shows Blunted Circadian Rhythms and Melatonin Secretion

Katsuya Sakimura ¹, Tatsuya Maekawa ¹, Shin-ichi Kume,² and Takeshi Ohta¹

¹Biological/Pharmacological Research Laboratories, Central Pharmaceutical Research Institute, Japan Tobacco Inc., 1-1 Murasaki-cho, Takatsuki, Osaka, Japan

²Laboratory of Animal Physiology and Functional Anatomy, Graduate School of Agriculture, Kyoto University, Kitashirakawa Oiwake-cho, Sakyo-ku, Kyoto, Japan

Correspondence should be addressed to Katsuya Sakimura; katsuya.sakimura@jt.com

Received 7 June 2018; Accepted 14 August 2018; Published 23 September 2018

Academic Editor: Masayo Koide

Copyright © 2018 Katsuya Sakimura et al. This is an open access article distributed under the Creative Commons Attribution License, which permits unrestricted use, distribution, and reproduction in any medium, provided the original work is properly cited.

In patients with diabetes mellitus (DM), impairments of circadian rhythms, including the sleep–wake cycle, blood pressure, and plasma melatonin concentrations, are frequently observed. Animal models of DM are also reported to show aberrant circadian rhythms. However, the changes in the circadian rhythms of plasma soluble substances, including melatonin, in diabetic animals are controversial. In the present study, we investigated the circadian rhythms of spontaneous locomotor activity, metabolic parameters (plasma glucose, triglyceride, and total cholesterol), and plasma melatonin concentrations in Spontaneously Diabetic Torii (SDT) fatty rats, a novel animal model of type 2 DM. Although SDT fatty rats exhibited low locomotor activity in the dark phase, no phase shifts were observed. The circadian variations of plasma metabolic parameters were more apparent in the SDT fatty rats compared with control Sprague–Dawley (SD) rats. The circadian rhythms of plasma melatonin concentrations were significantly impaired in SDT fatty rats. To get an insight into the mechanism underlying the impaired melatonin secretion in SDT fatty rats, the expression of arylalkylamine N-acetyltransferase (*Aanat*) and acetylserotonin O-methyltransferase (*Asmt*) mRNA, which encode the rate-limiting enzymes for melatonin synthesis, was investigated in the pineal gland. There were no significant differences in *Aanat* and *Asmt* expression between the control SD and SDT fatty rats. These results suggest that SDT fatty rats show impaired circadian rhythms and dysregulated melatonin secretion.

1. Introduction

It is well known that mammals have circadian rhythms not only for many kinds of behaviors, such as the sleep–wake cycle and feeding behavior, but also for several fundamental physiological functions, including hormone secretion. The circadian rhythm is organized by the so-called clock genes (e.g., period (*PER*), circadian locomotor output cycles kaput (*CLOCK*), and brain and muscle Arnt-like protein (*BMAL*)) in the suprachiasmatic nucleus (SCN) of the brain as “master regulators,” with the amplitude and/or phase of the rhythm modulated in response to extracellular stimuli such as light [1], feeding [2], and melatonin [3].

Circadian rhythms and metabolic function are known to be reciprocally linked [4]. For example, it has been reported that impairment of circadian rhythms leads to the development of diabetes via the induction of abnormal insulin secretion, decreased sensitivity to insulin, and exacerbated inflammation [5, 6]. In contrast, patients with diabetes reportedly exhibit circadian rhythms of blood pressure and plasma cortisol concentrations [7, 8], suggesting that metabolic functions substantially affect circadian rhythms. However, the mechanisms underlying the disrupted circadian rhythms in diabetes remain to be fully elucidated, because the metabolic disorders are very complex, with many factors, including hyperglycemia, obesity, and hypertension, involved. Several

animal models of diabetes mellitus (DM) have been reported to exhibit deficits in circadian rhythms. For example, streptozotocin- (STZ-) induced diabetic rats exhibit a blunted circadian rhythm of locomotor activity with a normal phase entrainment [9], whereas Zucker obese rats, an animal model of type 2 DM (T2DM), exhibit a phase advance and blunted amplitude of locomotor activity [10].

Melatonin, a hormone secreted from the pineal gland in the brain, is known as a regulator of many physiological circadian rhythms including the sleep–wake cycle [11]. Growing evidence suggests an important role for melatonin in DM. For example, melatonin is known to decrease plasma insulin concentrations in humans [12] and rodents [13–15]. Moreover, the physiological increase in nocturnal plasma melatonin concentrations is not observed in diabetic patients, especially those with neuropathy [16]. Similarly, Peschke et al. [17] reported reduced diurnal circulating melatonin levels in patients with T2DM, suggesting that melatonin secretion is impaired in DM patients. Similarly, several animal models of DM have been reported to exhibit aberrant plasma melatonin concentrations. For example, plasma melatonin concentrations at midnight are attenuated in Goto-Kakizaki (GK) rats, and melatonin synthesis efficiency is decreased [18]. Conversely, Peschke et al. [19] reported that melatonin synthesis was increased in the pineal glands of STZ-induced diabetic rats. Moreover, another study demonstrated that diabetic rats transgenic for human islet amyloid polypeptide (HIP rats), an established nonobese model of T2DM, showed normal circadian rhythms and melatonin secretion [20]. Thus, the relationship between metabolic disorders, including hyperglycemia, and aberrant circadian rhythms of melatonin is still controversial.

The Spontaneously Diabetic Torii (SDT) fatty rat is a novel animal model of T2DM, developing not only hyperglycemia but also hyperlipidemia and insulin resistance from a young age [21]. In the present study, we investigated whether SDT fatty rats show impaired circadian rhythms of spontaneous locomotor activity (SLA), plasma metabolic parameters, and plasma melatonin concentrations, as well as changes in the expression of arylalkylamine-N-acetyltransferase (*Aanat*) and acetylserotonin O-methyltransferase (*Asmt*) mRNA, which encode the rate-limiting enzymes for melatonin synthesis [22–24] in the pineal glands of SDT fatty rats.

2. Materials and Methods

2.1. Animals. The present study was performed in compliance with the Guidelines for Animal Experimentation of Japan Tobacco Biological/Pharmacological Research Laboratories. The animal protocol was designed to minimize pain or discomfort to the animals. SDT fatty rats and age-matched Sprague–Dawley (SD) rats (as controls) were used in the study. The age of animals used in each experiment were as follows: 8 weeks of age for measurement of SLA, plasma glucose, triglyceride (TG), total cholesterol (TC), and melatonin concentrations and 12 weeks of age for measurement of mRNA expressions. All rats were obtained from CLEA Japan (Tokyo, Japan). Rats were housed in groups of two to three per bracket cage in a climate-controlled room (temperature

$23^{\circ}\text{C} \pm 3^{\circ}\text{C}$, humidity $55\% \pm 15\%$) under a 12 h light–dark cycle (lights on at 0800 hours), with free access to a commercial diet (CRF-1; Charles River Japan, Yokohama, Japan) and water.

2.2. Locomotor Activity. The SLA of rats was assessed using a Supermex apparatus (Muromachi Kikai, Tokyo, Japan). An infrared beam sensor was set on top of a Plexiglas cage, and the number of movements was counted. Activity was integrated every 1 h. SLA was measured during the 12 h light–dark cycle for 5 days. Rats had free access to food and water during the measurements.

2.3. Blood Sampling and Measurement of Metabolic Parameters and Melatonin. Blood samples were collected from the tail vein at 1000, 1600, 2100, and 0400 hours by cutting the edge of the tail with a razor. Plasma was separated by centrifugation ($15,000 \times g$ for 5 min at 4°C) and stored at -80°C until analysis. Metabolic parameters, namely, plasma glucose, TG, and TC concentrations, were measured using an automatic analyzer (Hitachi Clinical Analyzer 7180; Hitachi, Tokyo, Japan). Plasma melatonin concentrations were determined using a commercially available ELISA kit (RE54021; IBL International, Hamburg, Germany) according to the manufacturer's instructions.

2.4. Sample Preparation for mRNA Measurement. Rats were killed by decapitation, and the pineal gland was dissected at 0400 hours under dim red light. RNA from the pineal gland was extracted using the RNeasy mini kit (Qiagen, Valencia, CA, USA). RNA was quantified using the Nanodrop D8000 (Thermo Scientific, Wilmington, DE, USA). The purity of RNA samples was assessed using the ratio of absorbance at 260/280 nm, and samples with an absorbance ratio of 1.8–2.0 were used to prepare cDNA. The RNA was transcribed into cDNA using high-capacity cDNA reverse transcription kits with RNA inhibitors (Applied Biosystems). The reaction mixture was incubated for 10 min at 25°C , for 2 h at 37°C and then for 5 s at 85°C . The cDNA was stored at -20°C until use.

2.5. Quantitative Reverse Transcription Polymerase Chain Reaction. Quantitative reverse transcription polymerase chain reaction (qRT-PCR) was performed in a $20 \mu\text{L}$ reaction mixture with an automated sequence detector combined with StepOne plus (Applied Biosystems). The reaction mixture was created using TaqMan Gene Expression Master Mix (Applied Biosystems) and contained approximately 50 ng synthesized cDNA, $0.9 \mu\text{mol/L}$ primers, $0.25 \mu\text{mol/L}$ probes or TaqMan gene expression assays on demand, and Universal Master Mix (primer/probe set). The reaction mixture was incubated for 2 min at 50°C and then 10 min at 95°C , followed by 40 cycles of 15 s at 95°C and 60 s at 60°C . The expression of beta-actin (*Actb*; purchased from Applied Biosystems), *Aanat* (Rn00664873_g1), and *Asmt* (Rn00595341_m1) was investigated using TaqMan gene expression assays and the Universal Master Mix (primer/probe set), with the expression of *Aanat* and *Asmt* in each sample normalized against that of *Actb*.

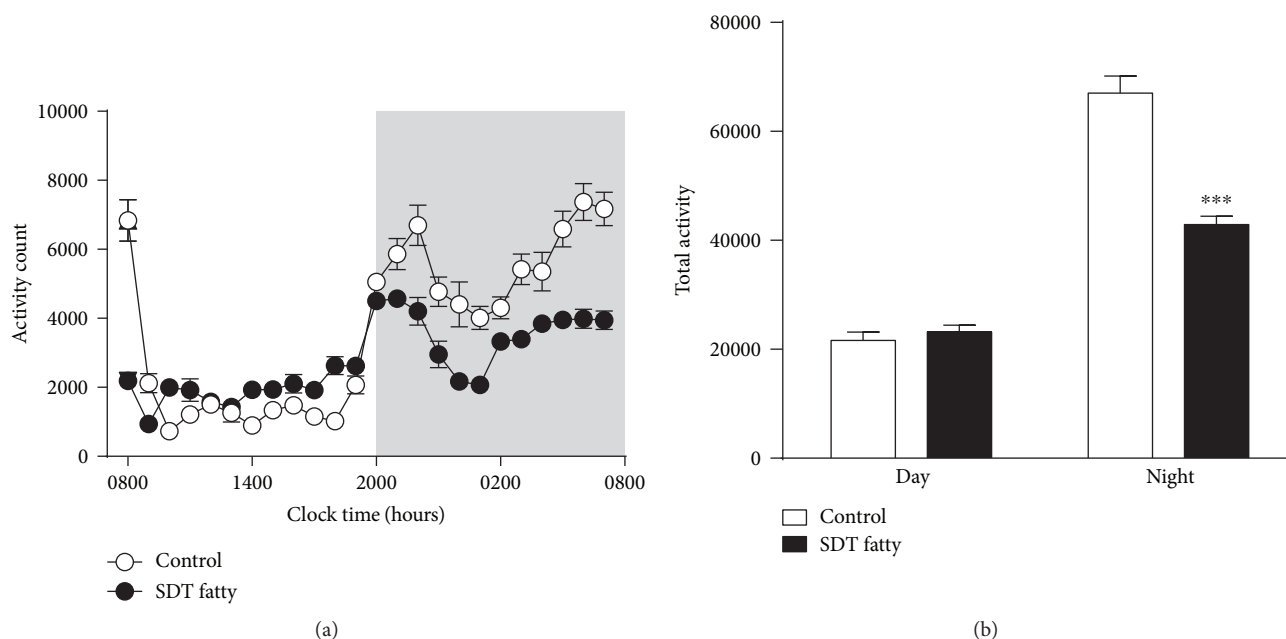


FIGURE 1: Circadian rhythm of spontaneous locomotor activity (SLA) in control Sprague-Dawley (SD) and Spontaneously Diabetic Torii (SDT) fatty rats. (a) Hourly averages of SLA over a 24 h period for 5 consecutive days under a standard light-dark cycle (the shaded area indicates the dark phase). (b) Total activity during the light and dark phases in control SD and SDT fatty rats. Data are mean \pm SEM ($n = 8$ in each group). *** $P < 0.001$ compared with control SD rats (Aspin-Welch test).

2.6. Statistical Analysis. Results are expressed as mean \pm SEM (standard error of the mean). Comparisons between control SD and SDT fatty rats were performed using two-way analysis of variance (ANOVA) with post hoc tests where appropriate for SLA and plasma parameters over time, whereas qRT-PCR data were compared using unpaired t -tests. All data were analyzed using Excel (Microsoft Corp., Bellevue, WA, USA) or EXSUS software (CAC Croit, Tokyo, Japan). A two-sided P value of <0.05 was considered significant. A P value of <0.05 was considered statistically significant.

3. Results

3.1. Circadian Rhythms of SLA in SDT Fatty Rats. In order to investigate whether there were any disruptions to circadian rhythms of SDT fatty rats, the SLA of control SD and SDT fatty rats was monitored over a period of 5 consecutive days. As shown in Figure 1, SLA during the dark phase was significantly lower in SDT fatty than in control SD rats ($P < 0.001$). In addition, SLA during the first 1 h during the light phase (0800–0900 hours) was markedly decreased in SDT fatty compared with control SD rats. However, the SLA of SDT fatty rats in the light phase was slightly high compared with that of control SD rats, though total activity did not differ significantly between the two groups.

3.2. Circadian Rhythms of Metabolic Parameters in SDT Fatty Rats. It is well known that several metabolic parameters, including glucose and TG, show circadian rhythms regulated by diet and/or hormones. This led us to investigate whether glucose, TG, and TC exhibit aberrant circadian rhythms in SDT fatty rats. Comparisons of plasma glucose, TG, and

TC concentrations in control SD and SDT fatty rats are shown in Figure 2. Two-way ANOVA of the circadian pattern of plasma glucose revealed significant effects of group ($F_{1,8} = 16.0$, $P < 0.01$), time ($F_{3,24} = 29.3$, $P < 0.001$), and their interaction ($F_{3,24} = 14.4$, $P < 0.001$). Post hoc analysis using the Aspin-Welch test revealed that plasma glucose concentrations were significantly higher in SDT fatty than in control SD rats at 1600 ($P < 0.05$), 2100 ($P < 0.01$), and 0400 hours ($P < 0.05$). Two-way ANOVA of the circadian pattern of plasma TG showed significant effects of group ($F_{1,8} = 17.0$, $P < 0.05$) and time ($F_{3,24} = 4.6$, $P < 0.05$). Post hoc analysis using the Aspin-Welch test revealed that plasma TG concentrations were significantly higher in SDT fatty than in control SD rats at all time points measured (i.e., 1000, 1600, and 0400 hours ($P < 0.05$ for all), as well as at 2100 hours ($P < 0.01$)). Unlike glucose and TG concentrations, there were no obvious changes in TC in either strain, with TC concentrations in the range 80–100 mg/dL in control SD rats and 100–120 mg/dL in SDT fatty rats. Plasma TC levels peaked at 0400 hours in control SD rats, compared with 1000 hours in SDT fatty rats. Two-way ANOVA of the circadian pattern of plasma TC showed significant effects of group ($F_{1,8} = 8.9$, $P < 0.05$), but not time ($F_{3,24} = 2.7$, $P > 0.05$). Post hoc analysis using the Aspin-Welch test revealed that plasma TC concentrations were significantly higher in SDT fatty than in control SD rats at 1000 ($P < 0.01$) and 2100 ($P < 0.05$) hours.

3.3. Circadian Rhythms of Plasma Melatonin. In order to obtain an insight into the mechanism(s) underlying the aberrant circadian rhythms in SDT fatty rats, we measured plasma melatonin concentrations. As shown in Figure 3,

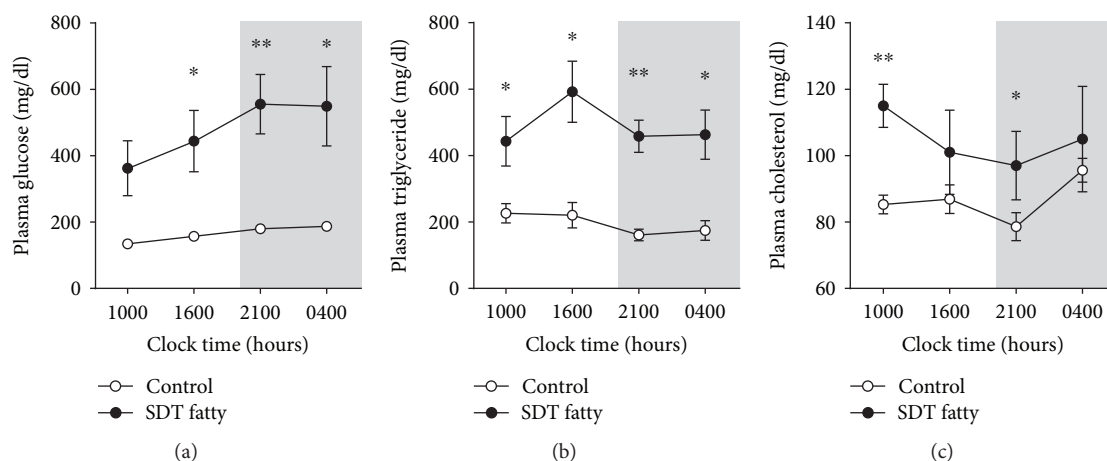


FIGURE 2: Circadian rhythms of plasma metabolic parameters in control Sprague-Dawley (SD) and Spontaneously Diabetic Torii (SDT) fatty rats: (a) glucose, (b) triglyceride, and (c) total cholesterol. Data are mean \pm SEM ($n = 5$ in each group). * $P < 0.05$ and ** $P < 0.01$ compared with the control group at the same time point (two-way ANOVA with post hoc Aspin-Welch tests).

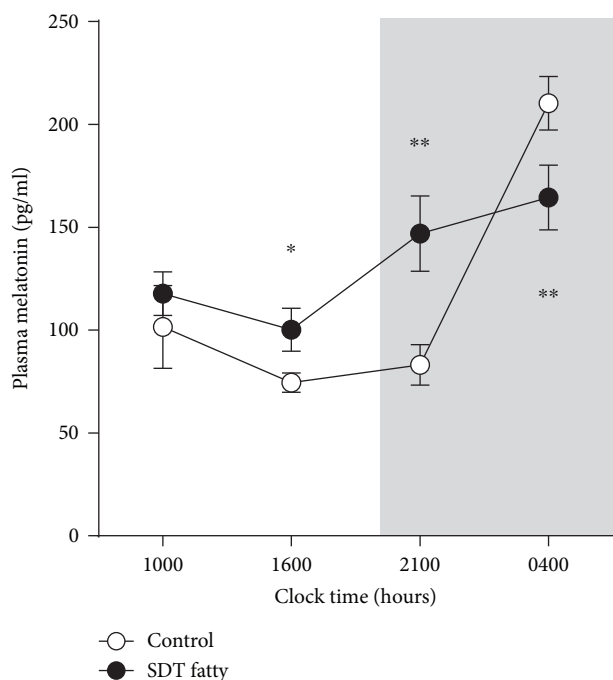


FIGURE 3: Circadian rhythm of plasma melatonin concentrations in control Sprague-Dawley (SD) and Spontaneously Diabetic Torii (SDT) fatty rats. Data are mean \pm SEM ($n = 5$ in each group). * $P < 0.05$ and ** $P < 0.01$ compared with the control group at the same time point (two-way ANOVA with post hoc Aspin-Welch tests).

there was an obvious circadian rhythm for melatonin in control SD rats, with low concentrations during the light phase (1000 and 1600 hours) and early dark phase (2100 hours), with the greatest increase in contrast during the night (0400 hours). Two-way ANOVA and subsequent post hoc analysis revealed significant effects of time ($F_{3,42} = 16.0$, $P < 0.001$), but not group ($F_{1,14} = 1.9$, $P = 0.19$). Their interaction was significant ($F_{3,42} = 7.4$, $P < 0.001$) on changes over time in

plasma melatonin concentrations between the control SD and SDT fatty rats. Plasma melatonin concentrations were significantly higher in SDT fatty than in control SD rats at 1600 ($P < 0.05$) and 2100 ($P < 0.01$) hours but were significantly lower at 0400 hours ($P < 0.01$). In addition, the total melatonin production was also analyzed, and it was found that there was a higher tendency in SDT fatty rats than in control SD rats, with the area under the curve value of 1949.1 ± 163.0 pg-day/mL (SD rats) vs. 2422.7 ± 206.2 pg-day/mL (SDT fatty rats) ($P = 0.093$).

3.4. Expression of Melatonin-Synthesizing Enzymes. The observation that SDT fatty rats showed blunted circadian rhythms of plasma melatonin led us to investigate whether the expression of *Aanat* and *Asmt* mRNA, enzymes important for melatonin synthesis, in the pineal gland of SDT fatty rats was impaired compared with that of control SD rats at night, when melatonin expression was highest. Although there were no significant differences in *Aanat* and *Asmt* mRNA expression in the pineal glands of the two groups, there was a tendency for higher *Aanat* and *Asmt* mRNA expression in SDT fatty than in control SD rats (Figure 4).

4. Discussion

In the present study, we found that (1) SDT fatty rats showed aberrant circadian rhythms of SLA, (2) the circadian fluctuations of plasma glucose, TG, and TC concentrations were found to be more apparent in SDT fatty rats, and (3) these rats exhibited blunted circadian rhythms of plasma melatonin secretion, even though the mRNA expression of melatonin-synthesizing enzymes did not differ significantly from that in the control SD rats.

Because rats are generally nocturnal, their activity increases in the dark phase and decreases markedly during the light phase. However, SLA in SDT fatty rats was decreased during the dark phase, with a tendency for higher SLA compared with control SD rats during the light phase. This observation suggests that SDT fatty rats have blunted

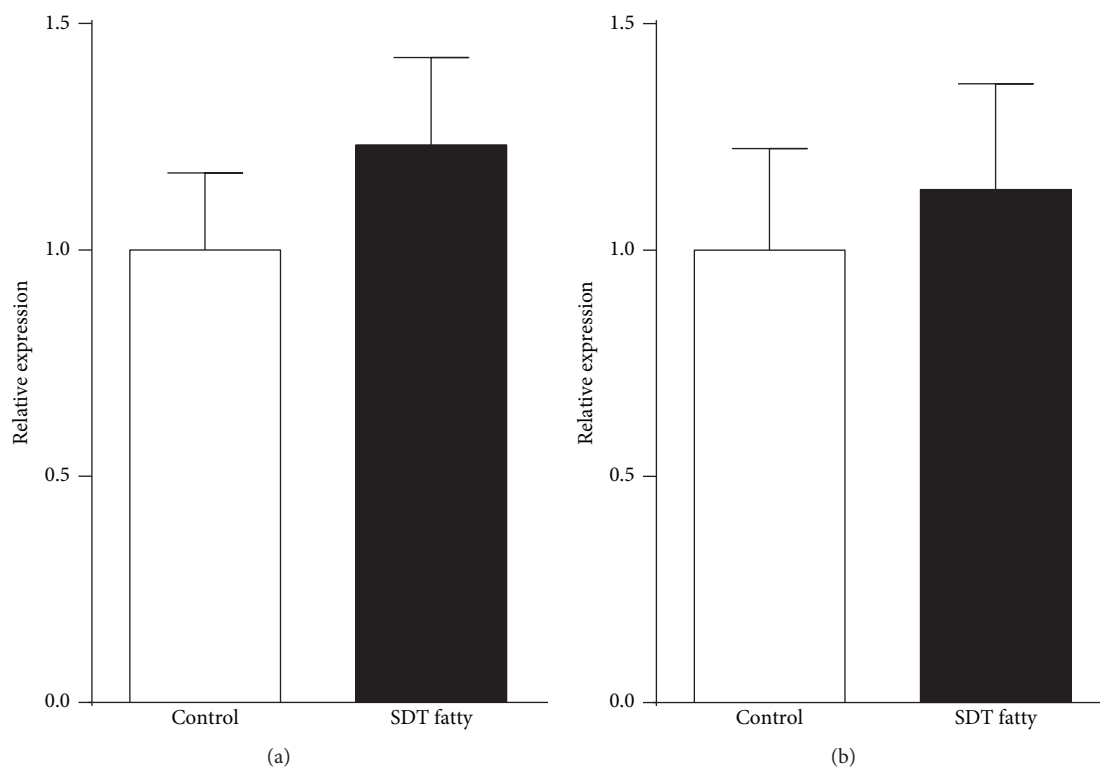


FIGURE 4: Relative expression of (a) arylalkylamine N-acetyltransferase (*Aanat*) and (b) acetylserotonin O-methyltransferase (*Asmt*) mRNA in the pineal gland of control Sprague–Dawley (SD) and Spontaneously Diabetic Torii (SDT) fatty rats at night (0400 hours). Data are mean + SEM ($n=6$ in each group). There were no significant differences in *Aanat* and *Asmt* expression between the two strains ($P > 0.05$, Student's *t*-test).

circadian rhythms of SLA. In addition, the entrainment by light stimuli seemed normal in the SDT fatty rats, as revealed by the observation that the SDT fatty rats exhibited the same SLA pattern over a period of 5 consecutive days of monitoring, although actograms were not measured in the present study. The findings of the present study confirm those of previous reports demonstrating impaired circadian rhythms in animal models of T2DM. For example, Zucker obese rats, an animal model for T2DM with mutations in the leptin receptor, exhibit a phase advance and a decreased amplitude of activity and body temperature [10]. In addition, Otsuka Long-Evans Tokushima Fatty (OLETF) rats have been reported to show decreased nocturnal locomotor activity before developing hyperglycemia [25]. Furthermore, STZ-induced diabetic rats, an animal model of type 1 DM, also show a blunted circadian rhythm for locomotor activity, but no phase shift [9]. Together, these findings suggest that hyperglycemia and/or obesity may induce blunted circadian rhythms while phase entrainment is preserved.

Circadian rhythms are known to be affected by food-taking behavior [26, 27]. As our previous studies have revealed that SDT fatty rats show hyperphagia [28, 29], this feature may underlie the deficits of circadian rhythm in the SDT fatty rats. Although there is no data on the food intake pattern of SDT fatty rats, the relatively higher SLA during the light phase may reflect the food-taking behavior. Consistent with this, plasma glucose, TG, and TC concentrations

are significantly higher than those of control SD rats even in the light phase as well as in the dark phase.

As mentioned in Introduction, diabetes and impaired circadian rhythms are known to be closely linked [4]. In addition, Yoda et al. [30] recently reported that the increased HbA1c associated with poor glycemic control in T2DM induces sleep disorder with exacerbated sleep quality. Furthermore, those authors demonstrated that sleep disorders in T2DM can increase the risk of cardiovascular events via aberrant hypertension in the morning [30]. Future studies investigating the relationship between hyperglycemia and the quality of sleep in SDT fatty rats are needed in order to elucidate the underlying pathophysiology.

In addition to the impaired circadian rhythm of SLA in SDT fatty rats, the rhythm of melatonin secretion was blunted in SDT fatty compared with control SD rats. Melatonin signaling, including its synthesis and secretion, is known to be suppressed by light inputs from eyes and usually reaches peak values at night both in humans and in rodents [31–33]. Consistent with this, in the present study, melatonin concentrations in control SD rats were low during the light and early dark phases and were highest in samples collected at 0400 hours. In contrast, melatonin concentrations during the light phase (1600 hours) and at 2100 hours were higher in SDT fatty than in control SD rats, whereas they were lower at 0400 hours in the SDT fatty rats, suggesting that SDT fatty rats have blunted circadian rhythms of melatonin secretion. To get an insight into the mechanism underlying this

aberrant melatonin secretion, we investigated the mRNA expression of melatonin-synthesizing enzymes in the pineal glands of SDT fatty rats by focusing on the peak time of melatonin secretion (0400 hours). Unexpectedly, there was no significant difference in the expression of *Aanat* and *Asmt* between the SDT fatty and control SD rats, while there was a tendency for higher expression in the SDT fatty rats. In the present study, we did not investigate the levels of *Aanat* and *Asmt* proteins, nor the precursors of melatonin including tryptophan and serotonin in the pineal gland of SDT fatty rats. Thus, further study is required in order to expand the understanding about the alteration of melatonin synthesis of SDT fatty rats. One possibility is that the not obvious changes in the mRNA expression in the SDT fatty rats were due to a time lag between the mRNA expression and the protein production. Thus, in addition to the time course measurement of melatonin protein, the time course of mRNA expression is needed in order to unveil the exact melatonin synthesis regulation in the SDT fatty rats. Similar findings have been reported by Frese et al. [18] who demonstrated that melatonin synthesis was impaired in the pineal glands of GK rats. They also found that the mRNA expression of three of four melatonin-synthesizing enzymes (i.e., tryptophan hydroxylase, aromatic amino acid decarboxylase, and *Asmt*) was significantly increased in the pineal gland of GK rats [18]. Based on these findings, the authors suggested that the upregulated mRNA expression may be a compensatory response to a decrease in the efficiency of melatonin synthesis. Although melatonin content and its synthesis in the pineal gland of SDT fatty rats were not investigated in the present study, it may be that a similar compensatory response occurs in SDT fatty rats. Meanwhile, the mRNA expression of *Aanat* was decreased by approximately 50% in GK rats in contrast to SDT fatty rats [18]. The findings from the present study confirm the findings of Frese et al. [18] in part; however, the opposite direction of changes in *Aanat* mRNA expression between the two studies suggests that the mechanism regulating melatonin synthesis in the pineal gland may differ between these two rat strains.

Altered melatonin secretion in diabetic patients has also been reported. For example, the physiological increase in nocturnal plasma melatonin concentrations was not observed in diabetic patients, especially those with neuropathy [16]. Similarly, Peschke et al. [17] reported reduced diurnal circulating melatonin levels in T2DM patients. The findings of the present study support these clinical findings. Moreover, a relatively large clinical case-control study suggested that the decreased nocturnal melatonin secretion may be the cause of T2DM [34]. It is important to investigate any intervention such as antidiabetics that will improve the circadian rhythm deficits as well as the symptoms of T2DM. Such an investigation should be performed in the future in order to judge the validity of this model as T2DM is comorbid with circadian rhythm deficit.

5. Conclusions

The results of the present study provide important evidence of the deficits in the circadian rhythms, as well as dysregulation

of melatonin secretion, in animal models of T2DM. Unlike other animal models of DM, SDT fatty rats develop not only hyperglycemia but also hyperlipidemia and insulin resistance from a young age as described in Introduction. Thus, given the findings in this study, SDT fatty rats may be a useful animal model for investigating the relationship between deficits in the circadian rhythm and metabolic dysfunction.

Data Availability

The data used to support the findings of this study are available from the corresponding author upon request.

Conflicts of Interest

K. S., T. M. and T. O. are employees of Japan Tobacco Inc. S. K. declares no conflict of interest.

Acknowledgments

The authors thank Inter-Biotech (<http://www.inter-biotech.com>) for the English language editing of this paper. The authors also thank Ms. Kumiko Ayukawa for her support with the mRNA expression analysis. This work was supported by Japan Tobacco Inc.

References

- [1] G. C. Brainard, A. J. Lewy, M. Menaker et al., "Dose-response relationship between light irradiance and the suppression of plasma melatonin in human volunteers," *Brain Research*, vol. 454, no. 1-2, pp. 212–218, 1988.
- [2] G. Asher, H. Reinke, M. Altmeyer, M. Gutierrez-Arcelus, M. O. Hottiger, and U. Schibler, "Poly(ADP-ribose) polymerase 1 participates in the phase entrainment of circadian clocks to feeding," *Cell*, vol. 142, no. 6, pp. 943–953, 2010.
- [3] T. Akerstedt, J. E. Froberg, Y. Friberg, and L. Wetterberg, "Melatonin excretion, body temperature and subjective arousal during 64 hours of sleep deprivation," *Psychoneuroendocrinology*, vol. 4, no. 3, pp. 219–225, 1979.
- [4] J. Bass and J. S. Takahashi, "Circadian integration of metabolism and energetics," *Science*, vol. 330, no. 6009, pp. 1349–1354, 2010.
- [5] G. Boden, X. Chen, and J. L. Urbain, "Evidence for a circadian rhythm of insulin sensitivity in patients with NIDDM caused by cyclic changes in hepatic glucose production," *Diabetes*, vol. 45, no. 8, pp. 1044–1050, 1996.
- [6] E. Van Cauter, J. D. Blackman, D. Roland, J. P. Spire, S. Refetoff, and K. S. Polonsky, "Modulation of glucose regulation and insulin secretion by circadian rhythmicity and sleep," *The Journal of Clinical Investigation*, vol. 88, no. 3, pp. 934–942, 1991.
- [7] F. Pistrosch, E. Reissmann, J. Wildbrett, C. Koehler, and M. Hanefeld, "Relationship between diurnal blood pressure variation and diurnal blood glucose levels in type 2 diabetic patients," *American Journal of Hypertension*, vol. 20, no. 5, pp. 541–545, 2007.
- [8] C. Cuspidi, S. Meani, L. Lonati et al., "Short-term reproducibility of a non-dipping pattern in type 2 diabetic hypertensive patients," *Journal of Hypertension*, vol. 24, no. 4, pp. 647–653, 2006.

- [9] A. Velasco, I. Huerta, and B. Marin, "Plasma corticosterone, motor activity and metabolic circadian patterns in streptozotocin-induced diabetic rats," *Chronobiology International*, vol. 5, no. 2, pp. 127–135, 1988.
- [10] R. E. Mistlberger, H. Lukman, and B. G. Nadeau, "Circadian rhythms in the Zucker obese rat: assessment and intervention," *Appetite*, vol. 30, no. 3, pp. 255–267, 1998.
- [11] C. Cajochen, K. Krauchi, and A. Wirz-Justice, "Role of melatonin in the regulation of human circadian rhythms and sleep," *Journal of Neuroendocrinology*, vol. 15, no. 4, pp. 432–437, 2003.
- [12] G. Boden, J. Ruiz, J. L. Urbain, and X. Chen, "Evidence for a circadian rhythm of insulin secretion," *The American Journal of Physiology*, vol. 271, no. 2, pp. E246–E252, 1996.
- [13] D. D. Rasmussen, B. M. Boldt, C. W. Wilkinson, S. M. Yellon, and A. M. Matsumoto, "Daily melatonin administration at middle age suppresses male rat visceral fat, plasma leptin, and plasma insulin to youthful levels," *Endocrinology*, vol. 140, no. 2, pp. 1009–1012, 1999.
- [14] S. Nishida, R. Sato, I. Murai, and S. Nakagawa, "Effect of pinealectomy on plasma levels of insulin and leptin and on hepatic lipids in type 2 diabetic rats," *Journal of Pineal Research*, vol. 35, no. 4, pp. 251–256, 2003.
- [15] J. A. Tresguerres, S. Cuesta, R. A. Kireev, C. Garcia, D. Acuna-Castroviejo, and E. Vara, "Beneficial effect of melatonin treatment on age-related insulin resistance and on the development of type 2 diabetes," *Hormone Molecular Biology and Clinical Investigation*, vol. 16, no. 2, pp. 47–54, 2013.
- [16] I. A. D. O'Brien, I. G. Lewin, J. P. O'hare, J. Arendt, and R. J. M. Corral, "Abnormal circadian rhythm of melatonin in diabetic autonomic neuropathy," *Clinical Endocrinology*, vol. 24, no. 4, pp. 359–364, 1986.
- [17] E. Peschke, T. Frese, E. Chankiewitz et al., "Diabetic Goto Kakizaki rats as well as type 2 diabetic patients show a decreased diurnal serum melatonin level and an increased pancreatic melatonin-receptor status," *Journal of Pineal Research*, vol. 40, no. 2, pp. 135–143, 2006.
- [18] T. Frese, A. G. Bach, E. Mühlbauer et al., "Pineal melatonin synthesis is decreased in type 2 diabetic Goto-Kakizaki rats," *Life Sciences*, vol. 85, no. 13–14, pp. 526–533, 2009.
- [19] E. Peschke, S. Wolgast, I. Bazwinsky, K. Ponicke, and E. Mühlbauer, "Increased melatonin synthesis in pineal glands of rats in streptozotocin induced type 1 diabetes," *Journal of Pineal Research*, vol. 45, no. 4, pp. 439–448, 2008.
- [20] J. Qian, A. P. Thomas, A. M. Schroeder, K. Rakshit, C. S. Colwell, and A. V. Matveyenko, "Development of diabetes does not alter behavioral and molecular circadian rhythms in a transgenic rat model of type 2 diabetes mellitus," *American Journal of Physiology. Endocrinology and Metabolism*, vol. 313, no. 2, pp. E213–E221, 2017.
- [21] Y. Katsuda, T. Sasase, H. Tadaki et al., "Contribution of hyperglycemia on diabetic complications in obese type 2 diabetic SDT fatty rats: effects of SGLT inhibitor phlorizin," *Experimental Animals*, vol. 64, no. 2, pp. 161–169, 2015.
- [22] S. Ebihara, T. Marks, D. J. Hudson, and M. Menaker, "Genetic control of melatonin synthesis in the pineal gland of the mouse," *Science*, vol. 231, no. 4737, pp. 491–493, 1986.
- [23] P. H. Roseboom, M. A. A. Namboodiri, D. B. Zimonjic et al., "Natural melatonin 'knockdown' in C57BL/6J mice: rare mechanism truncates serotonin N-acetyltransferase," *Brain Research. Molecular Brain Research*, vol. 63, no. 1, pp. 189–197, 1998.
- [24] M. F. Rath, S. L. Coon, F. G. Amaral, J. L. Weller, M. Moller, and D. C. Klein, "Melatonin synthesis: acetylserotonin O-methyltransferase (ASMT) is strongly expressed in a subpopulation of pinealocytes in the male rat pineal gland," *Endocrinology*, vol. 157, no. 5, pp. 2028–2040, 2016.
- [25] M. Sei, H. Sei, and K. Shima, "Spontaneous activity, sleep, and body temperature in rats lacking the CCK-A receptor," *Physiology & Behavior*, vol. 68, no. 1–2, pp. 25–29, 1999.
- [26] H. Abe, M. Kida, K. Tsuji, and T. Mano, "Feeding cycles entrain circadian rhythms of locomotor activity in CS mice but not in C57BL/6J mice," *Physiology & Behavior*, vol. 45, no. 2, pp. 397–401, 1989.
- [27] F. K. Stephan, "The 'other' circadian system: food as a zeitgeber," *Journal of Biological Rhythms*, vol. 17, no. 4, pp. 284–292, 2002.
- [28] T. Ohta, Y. Katsuda, K. Miyajima et al., "Gender differences in metabolic disorders and related diseases in spontaneously diabetic Torii-*Lepr^{fa}* rats," *Journal of Diabetes Research*, vol. 2014, Article ID 841957, 7 pages, 2014.
- [29] Y. Toriniwa, T. Saito, K. Miyajima et al., "Investigation of pharmacological responses to anti-diabetic drugs in female Spontaneously Diabetic Torii (SDT) fatty rats, a new nonalcoholic steatohepatitis (NASH) model," *The Journal of Veterinary Medical Science*, vol. 80, no. 6, pp. 878–885, 2018.
- [30] K. Yoda, M. Inaba, K. Hamamoto et al., "Association between poor glycemic control, impaired sleep quality, and increased arterial thickening in type 2 diabetic patients," *PLoS One*, vol. 10, no. 4, article e0122521, 2015.
- [31] A. J. Lewy, T. A. Wehr, F. K. Goodwin, D. A. Newsome, and S. P. Markey, "Light suppresses melatonin secretion in humans," *Science*, vol. 210, no. 4475, pp. 1267–1269, 1980.
- [32] H. Aoki, N. Yamada, Y. Ozeki, H. Yamane, and N. Kato, "Minimum light intensity required to suppress nocturnal melatonin concentration in human saliva," *Neuroscience Letters*, vol. 252, no. 2, pp. 91–94, 1998.
- [33] T. J. Badness, J. B. Powers, M. H. Hastings, E. L. Bittman, and B. D. Goldman, "The timed infusion paradigm for melatonin delivery: what has it taught us about the melatonin signal, its reception, and the photoperiodic control of seasonal responses?," *Journal of Pineal Research*, vol. 15, no. 4, pp. 161–190, 1993.
- [34] C. J. McMullan, E. S. Schernhammer, E. B. Rimm, F. B. Hu, and J. P. Forman, "Melatonin secretion and the incidence of type 2 diabetes," *Journal of the American Medical Association*, vol. 309, no. 13, pp. 1388–1396, 2013.

Research Article

Long-Term Dietary Nitrate Supplementation Does Not Prevent Development of the Metabolic Syndrome in Mice Fed a High-Fat Diet

V. B. Matthews ¹, R. Hollingshead,² H. Koch,¹ K. D. Croft,¹ and N. C. Ward ^{2,3}

¹School of Biomedical Sciences, The University of Western Australia, Perth, WA, Australia

²School of Biomedical Sciences & Curtin Health Innovation Research Institute, Curtin University, Perth, WA, Australia

³Medical School, The University of Western Australia, Perth, WA, Australia

Correspondence should be addressed to N. C. Ward; natalie.ward@curtin.edu.au

Received 2 May 2018; Accepted 19 July 2018; Published 5 August 2018

Academic Editor: Masayo Koide

Copyright © 2018 V. B. Matthews et al. This is an open access article distributed under the Creative Commons Attribution License, which permits unrestricted use, distribution, and reproduction in any medium, provided the original work is properly cited.

Background. Nitric oxide (NO) is an important vascular signaling molecule that plays a role in vascular homeostasis. A reduction in NO bioavailability is thought to contribute to endothelial dysfunction, an early risk factor for both cardiovascular disease and type 2 diabetes. Dietary nitrate, through the nitrate-nitrite-NO pathway, may provide an alternate source of NO when the endogenous eNOS system is compromised. In addition to a role in the vascular system, NO may also play a role in the metabolic syndrome including obesity and glucose tolerance. **Aim.** To investigate the effect of long-term dietary nitrate supplementation on development of the metabolic syndrome in mice fed a high-fat diet. **Methods.** Following 1 week of acclimatisation, male (6–8 weeks) C57BL6 mice were randomly assigned to the following groups (10/group) for 12 weeks: (i) normal chow + NaCl (1 mmol/kg/day), (ii) normal chow + NaNO₃ (1 mmol/kg/day), (iii) high-fat diet + NaCl (1 mmol/kg/day), and (iv) high-fat diet + NaNO₃ (1 mmol/kg/day). Body weight and food consumption were monitored weekly. A subset of mice (5/group) underwent running wheel assessment. At the end of the treatment period, all mice underwent fasting glucose tolerance testing. Caecum contents, serum, and tissues (liver, skeletal muscle, white and brown adipose, and kidney) were collected, frozen, and stored at –80°C until analysis. **Results.** Consumption of the high-fat diet resulted in significantly greater weight gain that was not affected by dietary nitrate. Mice on the high-fat diet also had impaired glucose tolerance that was not affected by dietary nitrate. There was no difference in adipose tissue expression of thermogenic proteins or energy expenditure as assessed by the running wheel activity. Mice on the high-fat diet and those receiving dietary nitrate had reduced caecum concentrations of both butyrate and propionate. **Conclusions.** Dietary nitrate does not prevent development of the metabolic syndrome in mice fed a high-fat diet. This may be due, in part due, to reductions in the concentration of important short-chain fatty acids.

1. Introduction

Nitric oxide (NO) is an important vascular signaling molecule that plays a major role in the control of vascular function and tone [1]. The majority of the body's NO is synthesised endogenously through conversion of L-arginine to citrulline by endothelial cell-derived nitric oxide synthase (eNOS). Once released, NO diffuses to the underlying smooth muscle cells and stimulates the production of cyclic guanosine monophosphate (cGMP) and subsequent relaxation of the vessel wall. A reduction in the bioactivity and/

or bioavailability of endogenously-derived NO is thought to be the main cause of endothelial dysfunction, an early risk factor for cardiovascular disease (CVD) and type 2 diabetes (T2DM) [2].

There is substantial epidemiological evidence to suggest that diets rich in fruits and vegetables have beneficial effects on CVD and its risk factors [3]. Dietary nitrate (NO₃⁻), found predominantly in green leafy vegetables, may be one of the beneficial components of such a diet as it represents an alternative source of NO. Dietary nitrate is well absorbed, and approximately 25% of ingested nitrate is secreted into the

saliva and 20% of this (~5% of ingested nitrate) is converted to nitrite (NO_2^-) by bacteria in the mouth. The nitrite is then swallowed and absorbed where it can be stored to act as a pool of NO or have direct vasodilatory effects [4]. This nitrate/nitrite-derived NO pool represents a NOS-independent pathway that can be used to supplement endogenous NO supplies or replace them when they are compromised.

The metabolic syndrome is classified as a cluster of risk factors that include hypertension, obesity, impaired glucose/insulin tolerance, and dyslipidaemia, and is a significant contributor to the development of both CVD and type 2 diabetes [5]. Endothelial dysfunction is often present in the metabolic syndrome, and studies have shown that reduced NO production and/or bioavailability has a role in the pathogenesis of many risk factors associated with the condition [6]. We have previously shown that low and moderate dose dietary nitrate can prevent endothelial dysfunction and improve plaque composition and stability in the ApoE^{-/-} mouse [7]. Dietary nitrate has also been shown to reduce triglycerides and improve intravenous glucose tolerance in eNOS-deficient mice [8]. Additionally, nitrate has been shown to induce antiobesity effects, including weight loss and reductions in body fat, via increases in the expression of thermogenic genes in brown adipose tissue [9]. Despite this, there is little evidence examining the effect of long-term dietary nitrate supplementation on the development of features of the metabolic syndrome. Therefore, the aim of the present study was to investigate the effect of long-term dietary nitrate supplementation on weight gain, glucose and insulin tolerance, and indices of thermogenesis in C57BL6 mice fed a high-fat diet.

2. Methods

2.1. Animal Study. Male C57BL6 mice (6–8) weeks were purchased from the Animal Resource Centre (Perth, Australia) and maintained at $23 \pm 2^\circ\text{C}$ under a 12-hour light–dark cycle. Following a week of acclimatisation, the mice were randomly divided into one of four groups ($n = 10$, 5 mice/cage): (i) normal chow + NaCl-supplemented water (1 mmol/kg/day), (ii) normal chow + NaNO_3 -supplemented water, (iii) high-fat diet + NaCl-supplemented water (1 mmol/kg/day), and (iv) high-fat diet + NaNO_3 -supplemented water (1 mmol/kg/day). The normal chow diet was commercial rodent chow consisting of 4.8% wt/wt fat, while the high-fat diet (HFD) contained 23.5% wt/wt fat (clarified butter). The nitrate dose is both physiologically relevant and comparable to the dose previously used where we observed beneficial effects on both vascular function and atherosclerotic plaque composition [7]. Mice were allowed ad libitum access to water and food, with all diets prepared by Specialty Feeds (Glenn Forrest, Australia). The level of nitrate and nitrite in the food pellet was $9.9 \mu\text{g/g}$ and $0.8 \mu\text{g/g}$, respectively [7]. The mice were maintained on their respective diets for 12 weeks. Body weight and food intake were measured weekly. The study was approved by the Royal Perth Hospital Animal Ethics Committee (R534/17-18) with reciprocal approval from Curtin University Animal Ethics Committee. All animal experiments were compliant with the National Health and

Medical Research Council (NHMRC) guidelines for the Care and Use of Laboratory Animals in Australia.

2.2. Glucose Tolerance Tests. Intraperitoneal glucose tolerance tests (IPGTT) were performed on fasting (5 hr) mice at week 11. To measure blood glucose levels, blood samples were taken from the tail of fasting (5 hr) mice before ($t = 0$ min) and at subsequent time intervals of $t = 15, 30, 45, 60, 90,$ and 120 min following intraperitoneal administration of 1 g glucose/kg. Blood glucose levels were measured using Accu-Chek Performa Strips and Glucometer (Roche Diagnostics, Australia). The area under the curves (AUCs) was calculated using the trapezoidal method.

2.3. Tissue Histology and Pathology. Fasted (5 hr) mice were anaesthetised with methoxyflurane at week 12, and liver and white adipose tissues were collected and fixed in 4% formaldehyde overnight before being incubated in 50% ethanol and embedded in paraffin. The tissues were then cut into $4 \mu\text{m}$ sections and stained with hematoxylin and eosin (CellCentral, UWA) before being visualized and photographed using a Nikon Eclipse TS100 microscope. Additional liver, white and brown adipose tissues, gastrointestinal tract, kidney, and skeletal muscle were collected and snap frozen in liquid nitrogen and stored at -80°C until analysis. White and brown adipose tissue protein expression of AMPK (Cell Signaling, USA), phosphorylated AMPK (Cell Signaling, USA), ACC (Cell Signaling, USA), phosphorylated ACC (Cell Signaling, USA), and UCP-1 (Cell Signaling, USA) were determined using western blot and normalised to actin (Sigma, USA), as previously described [7]. In a subset of mice (5/group), kidneys were also collected and stained with antisodium glucose cotransporter 2 (SGLT2, Santa Cruz Biotechnology) as previously described [10].

2.4. Energy Expenditure. Subsets of mice (5/treatment group) were housed individually with wireless running wheels during week 10 of the treatment period. Each mouse was allowed free access to their running wheel, which collected data on behaviour and activity, assessed as wheel revolutions and distance covered by the mouse using the Running Wheel Manager Acquisition Software (Med Associates Inc.). Individual mice were housed with their wheel for a period of 6 days. The first 3 days were an acclimatisation period with all measurements discarded from final analysis. The final 3 days of activity were collected and averaged using the Wheel Analysis Software (Med Associates Inc.) to provide information on daily activity level and mean overall activity level.

2.5. Caecum Short-Chain Fatty Acid (SCFA) Analysis. Caecum samples isolated from the gastrointestinal tract were collected and snap frozen in liquid nitrogen and stored at -80°C until analysis. SCFA concentrations of acetate, butyrate, and propionate were analysed using gas chromatography–mass spectrometry as previously described [11].

2.6. Serum Nitrate/Nitrite Concentrations. Fasted (5 hr) mice were anaesthetised with methoxyflurane at week 12, and blood samples were obtained via cardiac puncture. Serum

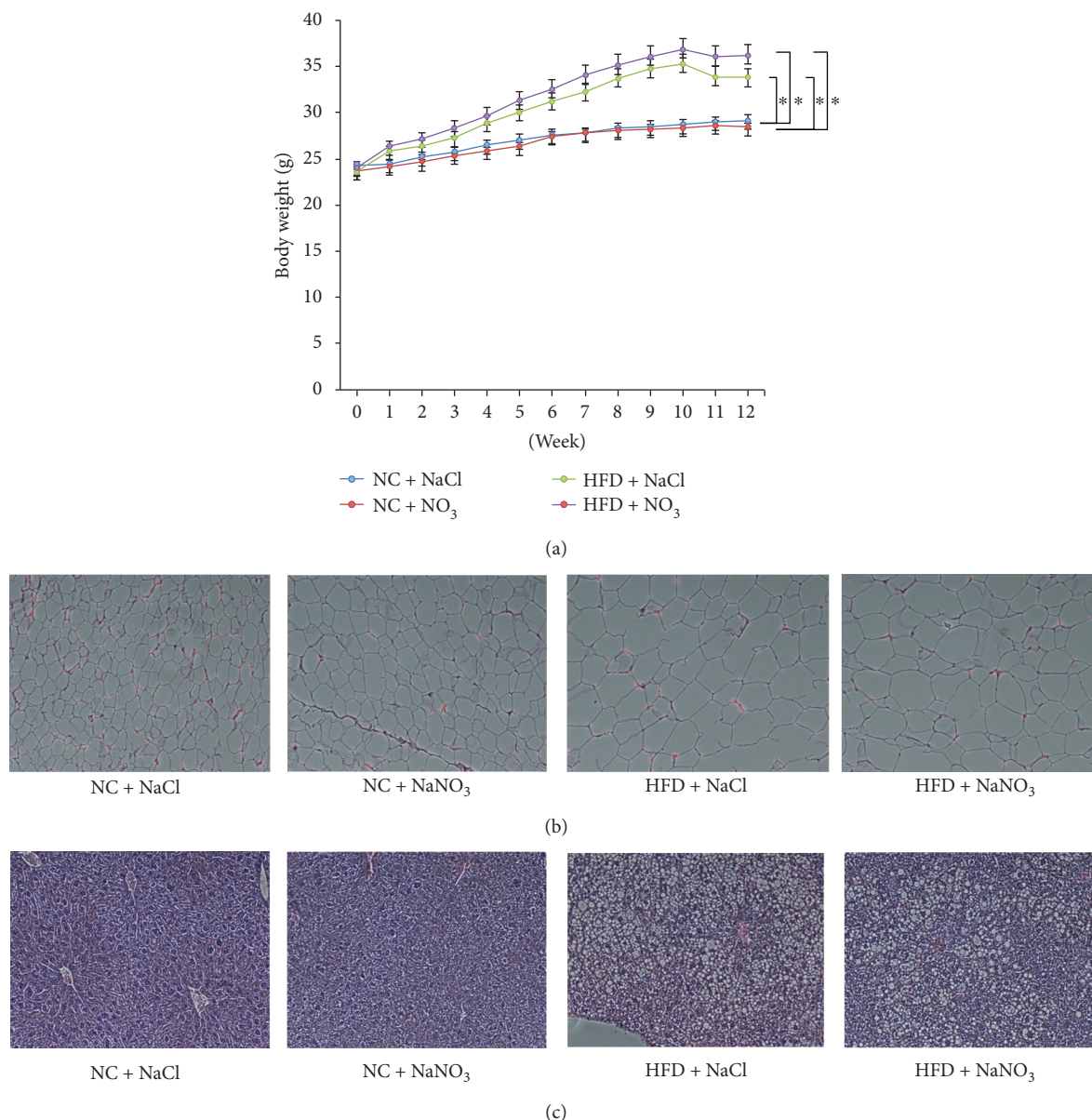


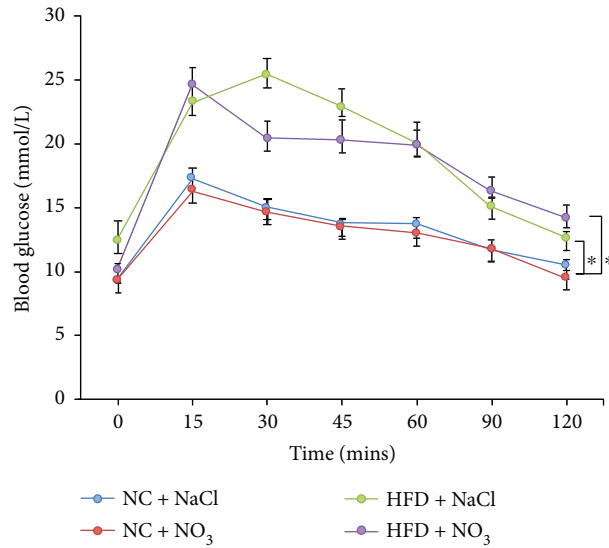
FIGURE 1: (a) Body weight gain, (b) adipocyte hypertrophy, and (c) hepatic lipid droplet accumulation in C57BL6 mice fed a normal chow or HFD with or without dietary nitrate for 12 weeks. $n = 10/\text{group}$, ANOVA ($*p < 0.05$).

was separated via centrifugation (3000 rpm, 4°C, 10 mins) and stored at -80°C until analysis. Nitrate and nitrite concentrations were determined using gas chromatography–mass spectrometry (GC–MS) as previously described [12].

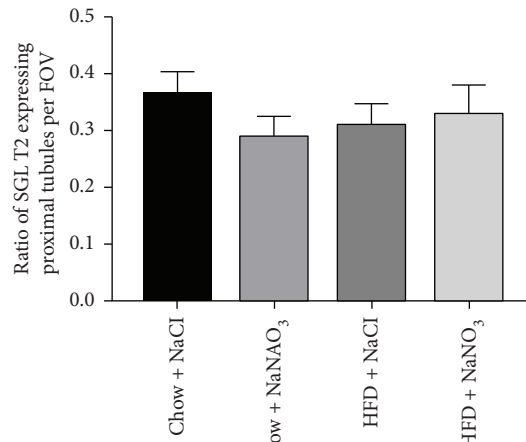
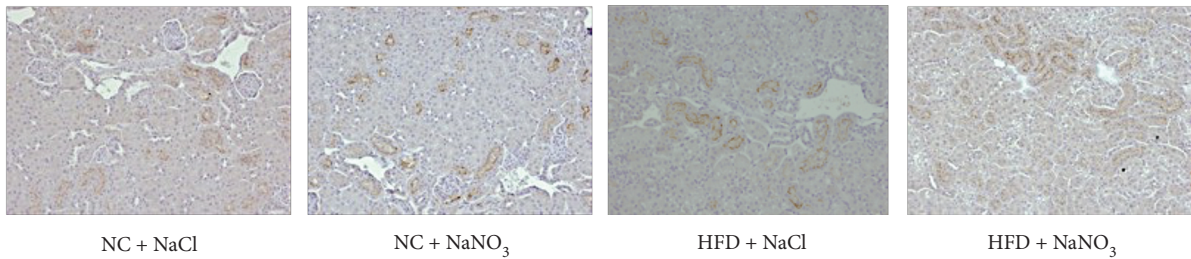
2.7. Statistical Analysis. Statistical analysis was performed using SPSS (version 21.0). All values are expressed as mean \pm standard error (SEM). Data was analysed using repeated measures analysis of variance (ANOVA) and one-way ANOVA with Tukey post hoc analysis to determine differences between groups. A $p < 0.05$ was determined to be of statistical significance. The data used to support the findings of this study are available from the corresponding author upon request.

3. Results

3.1. Nitrate Diet and the Effect of Dietary Nitrate on Obesity, Hepatic Fat, and Food Intake. Previous studies suggest mice consume approximately 5 g of chow and 6 mL of water per day [13]. Our previous nitrate study demonstrated that water supplemented with 1 mmol of nitrate contains $130 \mu\text{g}/\text{mL}$ of nitrate and $3 \mu\text{g}/\text{mL}$ of nitrite [7]. In the present study, mice consuming the HFD gained significantly more weight over 12 weeks compared to mice consuming the normal chow diet. The addition of nitrate had no effect on weight gain when added to either the normal chow or HFD (Figure 1(a)). Average food consumption (g/mouse/day) was lower in mice consuming the HFD compared to normal chow. When



(a)



(b)

FIGURE 2: (a) Fasting glucose tolerance testing in C57BL6 mice fed a normal chow or HFD with or without dietary nitrate for 12 weeks. $n = 10/\text{group}$, ANOVA ($*p < 0.05$). (b) Representative immunohistochemistry images (depicted by brown staining, magnification at 200 \times) and the ratio of renal proximal tubule expression of SGLT2 in C57BL6 mice fed a normal chow or HFD with or without dietary nitrate for 12 weeks ($n = 5/\text{group}$; FOV: field of view).

measured as calories/mouse/day, mice fed the HFD consumed more than those fed the normal chow diet. Neither of these reached statistical significance, and dietary nitrate supplementation had no effect on food consumption with either diet (data not shown).

There was noticeable adipocyte hypertrophy in mice consuming the HFD compared to normal chow; however, addition of dietary nitrate had no effect on this (Figure 1(b)). Hepatic fat accumulation as evidenced by lipid droplets was also higher in mice consuming the HFD compared

to normal chow, and once again, this was not affected by dietary nitrate (Figure 1(c)).

3.2. The Effect of Dietary Nitrate on the Development of Diet-Induced Glucose Intolerance. Mice fed the HFD for 12 weeks had significantly impaired glucose tolerance compared to mice receiving the normal chow diet. Addition of dietary nitrate had no significant effect on glucose tolerance with either diet (Figure 2(a)). As SGLT2 is responsible for glucose reabsorption and may influence blood glucose levels, we assessed SGLT2 expression in the renal proximal tubules in a subset of mice (5/group). We observed no difference in renal proximal tubule SGLT2 expression, regardless of the diet they were receiving (Figure 2(b)).

3.3. The Effect of Dietary Nitrate on Markers of Metabolic Activity and Energy Expenditure. There was no significant difference in white or brown adipose tissue expression of AMPK, p-AMPK, ACC, or p-ACC in mice fed the normal chow or HFD, with or without the addition of nitrate (data not shown). UCP1 expression was not detectable in white adipose tissue in any of the dietary treatment groups (data not shown) and was not significantly different in brown adipose tissue between the normal chow and HFD, with or without nitrate (data not shown).

Energy expenditure as assessed via running wheel use revealed no significant difference between any of the dietary treatment groups in the amount of exercise as assessed via the total distance or the total revolutions over a 3-day period (Table 1).

3.4. The Effect of Dietary Nitrate Supplementation on Circulating Nitrate and Nitrite. Circulating serum nitrate and nitrite levels were increased in mice receiving the nitrate supplemented diet, and this appeared most pronounced and significant in the HFD group (Figures 3(a) and 3(b)).

3.5. The Effect of Dietary Nitrate on Production of Short-Chain Fatty Acids. There was no effect of any dietary treatment on caecum levels of acetate (Figure 4(a)). Caecum concentrations of butyrate and propionate were significantly reduced in the nitrate-supplemented normal chow and both the HFD and nitrate-supplemented HFD compared to normal chow diet alone (Figures 4(b) and 4(c)).

4. Discussion

Inorganic nitrate was originally believed to be an inert by-product of NO metabolism that was readily excreted by the body but could be potentially toxic and carcinogenic when given in supraphysiological doses [14]. However, nitrate is present in the diet, particularly green leafy vegetables [15], and discovery of the nitrate-nitrite-NO conversion pathway in mammals [16] has highlighted the possibility of using this system to enhance or supplement the body's NO supplies. This may be particularly important in disease states where NO levels are compromised, such as CVD and T2DM. Inorganic nitrate has previously been shown to improve risk factors for CVD such as endothelial dysfunction and blood pressure in humans [17], protect against myocardial

TABLE 1: Energy expenditure as assessed by running wheel distance and revolutions over a 3-day period.

	NC + NaCl	NC + NaNO ₃	HFD + NaCl	HFD + NaNO ₃
Distance (meters)				
Day 1	185 ± 44	156 ± 24	104 ± 12	91 ± 39
Day 2	198 ± 51	206 ± 41	157 ± 22	111 ± 50
Day 3	221 ± 32	267 ± 65	238 ± 26	139 ± 60
Average	206 ± 38	213 ± 48	166 ± 20	114 ± 50
Revolutions				
Day 1	502 ± 126	412 ± 63	417 ± 59	296 ± 133
Day 2	528 ± 136	547 ± 108	417 ± 59	296 ± 133
Day 3	591 ± 87	684 ± 135	633 ± 69	369 ± 159
Average	541 ± 106	548 ± 99	442 ± 52	302 ± 131

Mean ± SEM (*n* = 5/group).

ischaemia-reperfusion injury in mice [18], reverse features of the metabolic syndrome in the eNOS knockout mouse [8] and mice having undergone ovariectomy [19], prevent endothelial dysfunction, and improve plaque composition and stability in the ApoE^{-/-} mouse [7].

In the present study, we examined the potential for long-term dietary nitrate supplementation to prevent development of the metabolic syndrome in the C57BL6 mouse fed a high-fat diet for 12 weeks. Despite seeing significant increases in circulating nitrate and nitrite in mice receiving the nitrate-supplemented diets, this did not result in improvements in any features of the metabolic syndrome. Mice on the HFD gained more weight and had significant glucose intolerance compared to their normal chow-fed counterparts, and addition of nitrate to their diet did not ameliorate this. Furthermore, there was no effect of dietary nitrate on white or brown adipose tissue expression of proteins involved in thermogenesis or fatty acid oxidation. Moreover, dietary nitrate significantly reduced caecum concentrations of the short-chain fatty acids, butyrate, and propionate, regardless of whether the mice were consuming a normal chow or high-fat diet.

Obesity, caused by excessive accumulation of white adipose tissue, is a major component of the metabolic syndrome. White adipose tissue is the primary site of energy storage and hormone and cytokine release. In contrast, brown adipose tissue is important for both basal and thermal energy expenditure [20]. A previous *in vitro* study has shown that cGMP promotes a healthy expansion and browning of white adipose tissue to so-called "brown-like" or "brite" cells that have been suggested to have both antiobesity and insulin-sensitising effects [21]. As cGMP is a target of NO, it is possible that dietary nitrate treatment, through conversion via the nitrate-nitrite-NO pathway, could target cGMP in adipose tissue and enhance this browning phenomenon. Through a series of *in vitro* and *in vivo* studies, Roberts et al. found out that this browning effect of nitrate was mediated through both a cGMP and protein kinase-G mediated

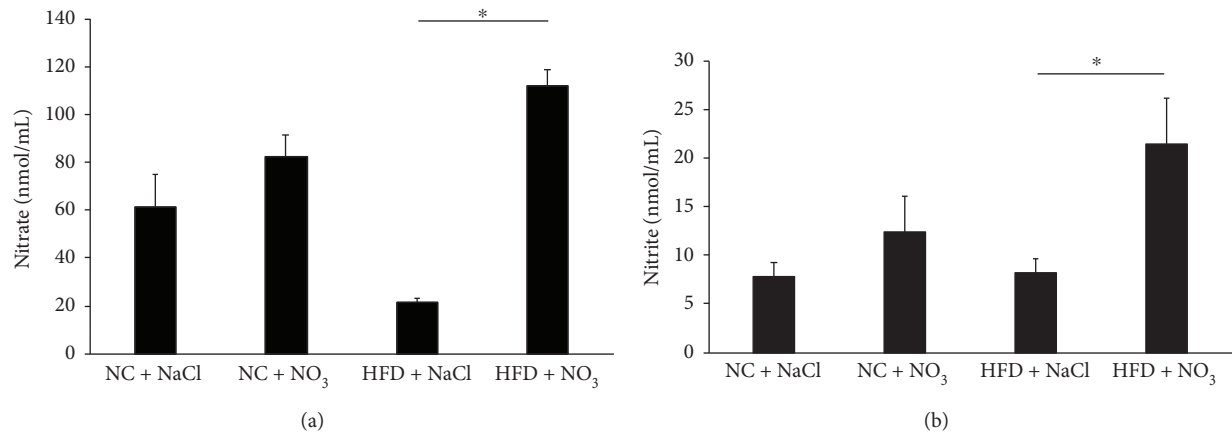


FIGURE 3: Serum (a) nitrate and (b) nitrite concentrations in C57BL6 mice fed a normal chow or HFD with or without dietary nitrate for 12 weeks. $n = 10/\text{group}$, ANOVA ($*p < 0.05$).

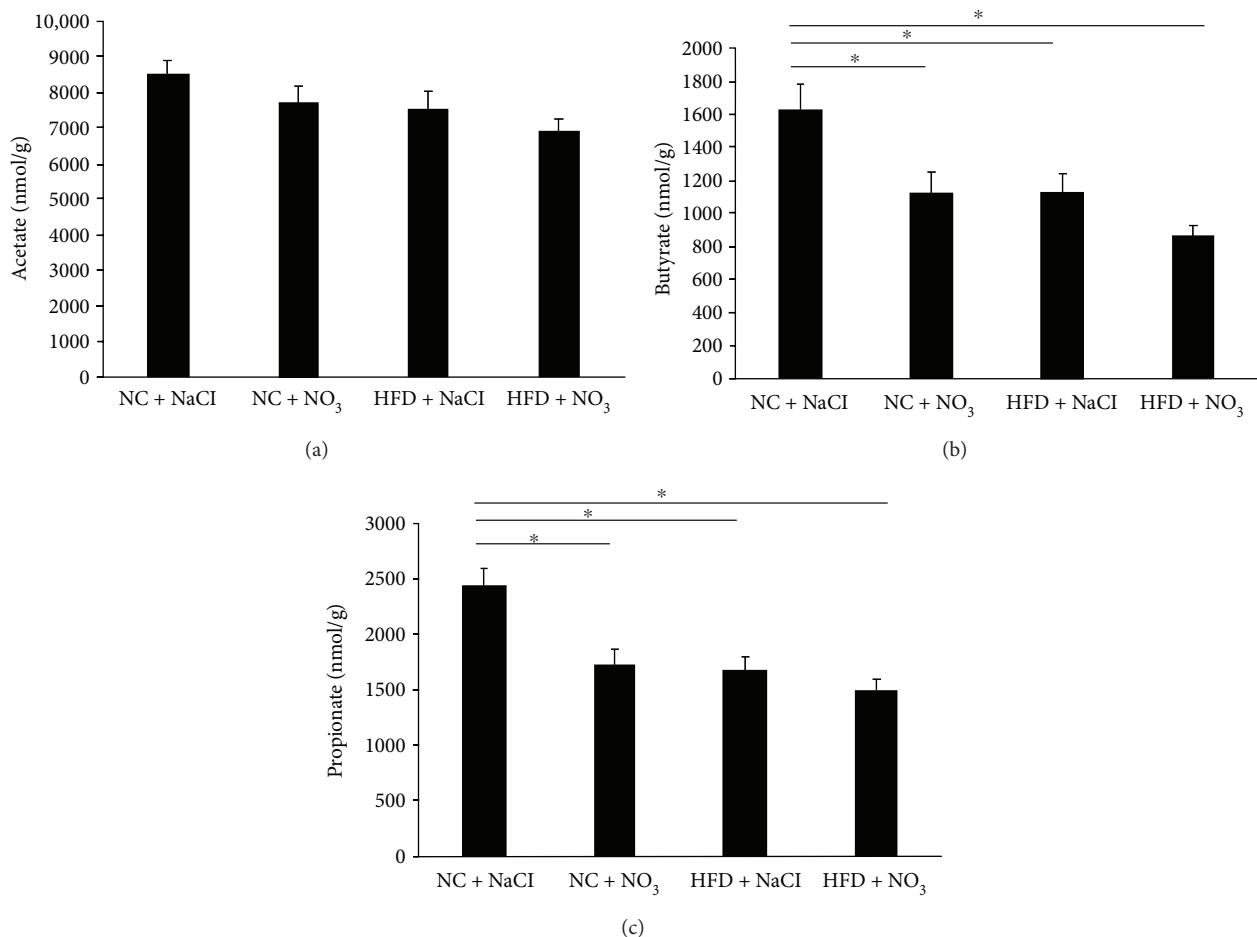


FIGURE 4: Caecum (a) acetate, (b) butyrate, and (c) propionate concentrations in C57BL6 mice fed a normal chow or HFD with or without dietary nitrate for 12 weeks. $n = 10/\text{group}$, ANOVA ($*p < 0.05$).

mechanism that was further enhanced in hypoxia [9, 22]. Despite this, in the present study, we saw no beneficial effects of dietary nitrate on weight gain, adipocyte hypertrophy, or hepatic lipid accumulation, as well as no difference in markers of thermogenesis or fatty acid oxidation in the white

or brown adipose tissue of these mice. While the reason for the lack of beneficial effect in our study is unknown, it is possible that differences in the dose of nitrate, mouse model, and severity of disease (vascular versus metabolic endpoints) or study duration may have all contributed. This is supported

by our previous study where we saw dose-dependent effects of dietary nitrate on endothelial function and atherosclerotic plaque size and composition [7] and the known negative cross talk that exists between the nitrate-nitrite-NO and eNOS pathways [23]. It is also possible that the benefits of dietary nitrate are more apparent in a disease model that specifically targets the endogenous eNOS pathway, resulting in detrimental effects on the vasculature, as seen in the eNOS^{-/-} and ApoE^{-/-} mouse models [7, 8]. In addition, despite seeing significant increases in circulating nitrate and nitrite suggesting conversion of the dietary nitrate to nitrite by the mouse oral bacteria, subsequent tissue uptake of nitrate/nitrite may have been impaired or reduced, limiting any potential beneficial effects. While future studies with higher doses or supplementation with nitrite are warranted, in the present study, we chose to use a moderate dose of dietary nitrate, which is both physiologically relevant and represents what could be achieved through a diet rich in fruits and vegetables, in contrast to nitrite, which is predominately found in processed meats [15].

An alternate possibility for the lack of beneficial effect may be related to the reduction we observed in the caecum concentrations of the SCFAs butyrate and propionate. SCFAs are produced by the gut microbiome and have been associated with several key metabolic processes, including adiposity, food intake, lipid metabolism, glucose homeostasis, and insulin resistance [24, 25]. Gut-derived propionate is used in the hepatic synthesis of odd-chain fatty acids, which are associated with a reduced risk of T2DM [26], and butyrate supplementation has been shown to improve insulin sensitivity and increase energy expenditure in mice fed a HFD [27]. In the present study, we saw significant reductions in both propionate and butyrate in the HFD-fed mice compared to normal chow-fed mice, which support these HFD-fed mice developing features of the metabolic syndrome. Unexpectedly, however, dietary nitrate supplementation was unable to prevent this reduction in the HFD-fed mice and, in fact, significantly reduced the levels of these two important SCFA in mice fed the normal chow diet. This may partly explain the lack of beneficial effect we observed on development of the metabolic syndrome, although we acknowledge that 16S RNA sequencing and analysis to confirm gut remodeling would further support this.

In conclusion, despite previous studies suggesting that dietary nitrate supplementation has beneficial effects on risk factors associated with CVD and T2DM, we observed no beneficial effect on the development of the metabolic syndrome in mice fed a HFD for 12 weeks. Although the mechanisms for this are unknown, it may be partly attributable to reductions in the concentration of the important SCFAs butyrate and propionate. Future studies investigating different doses and duration as well as intervention after disease has been established are warranted.

Data Availability

The data used to support the findings of this study are available from the corresponding author upon request.

Conflicts of Interest

The authors declare that they have no conflicts of interest.

Acknowledgments

The authors acknowledge the laboratory assistance of Helen O'Donoghue and Caroline Rudnicka and Dr. Shelley Gorman for the use of the running wheels as well as Nick Grainger in the RPH Animal House. This study was funded by a Royal Perth Hospital Medical Research Foundation Research Grant (KDC, NCW).

References

- [1] U. Forstermann and T. Munzel, "Endothelial nitric oxide synthase in vascular disease: from marvel to menace," *Circulation*, vol. 113, no. 13, pp. 1708–1714, 2006.
- [2] W. C. Sessa, "eNOS at a glance," *Journal of Cell Science*, vol. 117, no. 12, pp. 2427–2429, 2004.
- [3] L. A. Bazzano, J. He, L. G. Ogden et al., "Fruit and vegetable intake and risk of cardiovascular disease in US adults: the first National Health and Nutrition Examination Survey epidemiologic follow-up study," *The American Journal of Clinical Nutrition*, vol. 76, no. 1, pp. 93–99, 2002.
- [4] J. O. Lundberg and E. Weitzberg, "NO generation from nitrite and its role in vascular control," *Arteriosclerosis, Thrombosis, and Vascular Biology*, vol. 25, no. 5, pp. 915–922, 2005.
- [5] P. L. Huang, "A comprehensive definition for metabolic syndrome," *Disease Models & Mechanisms*, vol. 2, no. 5–6, pp. 231–237, 2009.
- [6] M. Gilchrist, P. G. Winyard, K. Aizawa, C. Anning, A. Shore, and N. Benjamin, "Effect of dietary nitrate on blood pressure, endothelial function, and insulin sensitivity in type 2 diabetes," *Free Radical Biology & Medicine*, vol. 60, pp. 89–97, 2013.
- [7] J. R. Bakker, N. P. Bondonno, T. A. Gaspari et al., "Low dose dietary nitrate improves endothelial dysfunction and plaque stability in the ApoE^{-/-} mouse fed a high fat diet," *Free Radical Biology & Medicine*, vol. 99, pp. 189–198, 2016.
- [8] M. Carlstrom, F. J. Larsen, T. Nystrom et al., "Dietary inorganic nitrate reverses features of metabolic syndrome in endothelial nitric oxide synthase-deficient mice," *Proceedings of the National Academy of Sciences of the United States of America*, vol. 107, no. 41, pp. 17716–17720, 2010.
- [9] L. D. Roberts, T. Ashmore, A. O. Kotwica et al., "Inorganic nitrate promotes the browning of white adipose tissue through the nitrate-nitrite-nitric oxide pathway," *Diabetes*, vol. 64, no. 2, pp. 471–484, 2015.
- [10] V. B. Matthews, R. H. Elliot, C. Rudnicka, J. Hricova, L. Herat, and M. P. Schlaich, "Role of the sympathetic nervous system in regulation of the sodium glucose cotransporter 2," *Journal of Hypertension*, vol. 35, no. 10, pp. 2059–2068, 2017.
- [11] J. A. Caparrós-Martín, R. R. Lareu, J. P. Ramsay et al., "Statin therapy causes gut dysbiosis in mice through a PXR-dependent mechanism," *Microbiome*, vol. 5, no. 1, p. 95, 2017.
- [12] X. Yang, C. P. Bondonno, A. Indrawan, J. M. Hodgson, and K. D. Croft, "An improved mass spectrometry-based measurement of NO metabolites in biological fluids," *Free Radical Biology & Medicine*, vol. 56, pp. 1–8, 2013.

- [13] A. A. Bachmanov, D. R. Reed, G. K. Beauchamp, and M. G. Tordoff, "Food intake, water intake, and drinking spout side preference of 28 mouse strains," *Behavior Genetics*, vol. 32, no. 6, pp. 435–443, 2002.
- [14] B. McNally, J. L. Griffin, and L. D. Roberts, "Dietary inorganic nitrate: from villain to hero in metabolic disease?," *Molecular Nutrition & Food Research*, vol. 60, no. 1, pp. 67–78, 2016.
- [15] L. C. Blekkenhorst, R. L. Prince, N. C. Ward et al., "Development of a reference database for assessing dietary nitrate in vegetables," *Molecular Nutrition & Food Research*, vol. 61, no. 8, 2017.
- [16] J. O. Lundberg and M. Govoni, "Inorganic nitrate is a possible source for systemic generation of nitric oxide," *Free Radical Biology & Medicine*, vol. 37, no. 3, pp. 395–400, 2004.
- [17] V. Kapil, A. B. Milsom, M. Okorie et al., "Inorganic nitrate supplementation lowers blood pressure in humans: role for nitrite-derived NO," *Hypertension*, vol. 56, no. 2, pp. 274–281, 2010.
- [18] N. S. Bryan, J. W. Calvert, J. W. Elrod, S. Gundewar, S. Y. Ji, and D. J. Lefer, "Dietary nitrite supplementation protects against myocardial ischemia-reperfusion injury," *Proceedings of the National Academy of Sciences of the United States of America*, vol. 104, no. 48, pp. 19144–19149, 2007.
- [19] K. Ohtake, N. Ehara, H. Chiba et al., "Dietary nitrite reverses features of postmenopausal metabolic syndrome induced by high-fat diet and ovariectomy in mice," *American Journal of Physiology. Endocrinology and Metabolism*, vol. 312, no. 4, pp. E300–E308, 2017.
- [20] A. M. Cypess, S. Lehman, G. Williams et al., "Identification and importance of brown adipose tissue in adult humans," *The New England Journal of Medicine*, vol. 360, no. 15, pp. 1509–1517, 2009.
- [21] M. M. Mitschke, L. S. Hoffmann, T. Gnad et al., "Increased cGMP promotes healthy expansion and browning of white adipose tissue," *The FASEB Journal*, vol. 27, no. 4, pp. 1621–1630, 2013.
- [22] L. D. Roberts, "Does inorganic nitrate say NO to obesity by browning white adipose tissue?," *Adipocytes*, vol. 4, no. 4, pp. 311–314, 2015.
- [23] M. Carlström, M. Liu, T. Yang et al., "Cross-talk between nitrate-nitrite-NO and NO synthase pathways in control of vascular NO homeostasis," *Antioxidants & Redox Signaling*, vol. 23, no. 4, pp. 295–306, 2015.
- [24] M. Kasubuchi, S. Hasegawa, T. Hiramatsu, A. Ichimura, and I. Kimura, "Dietary gut microbial metabolites, short-chain fatty acids, and host metabolic regulation," *Nutrients*, vol. 7, no. 4, pp. 2839–2849, 2015.
- [25] A. Koh, F. De Vadder, P. Kovatcheva-Datchary, and F. Backhed, "From dietary fiber to host physiology: short-chain fatty acids as key bacterial metabolites," *Cell*, vol. 165, no. 6, pp. 1332–1345, 2016.
- [26] K. Weitkunat, S. Schumann, D. Nickel et al., "Odd-chain fatty acids as a biomarker for dietary fiber intake: a novel pathway for endogenous production from propionate," *The American Journal of Clinical Nutrition*, vol. 105, no. 6, pp. 1544–1551, 2017.
- [27] Z. Gao, J. Yin, J. Zhang et al., "Butyrate improves insulin sensitivity and increases energy expenditure in mice," *Diabetes*, vol. 58, no. 7, pp. 1509–1517, 2009.

Review Article

Focusing on Sodium Glucose Cotransporter-2 and the Sympathetic Nervous System: Potential Impact in Diabetic Retinopathy

Lakshini Y. Herat,¹ Vance B. Matthews ¹, P. Elizabeth Rakoczy,² Revathy Carnagarin,³ and Markus Schlaich^{3,4}

¹Dobney Hypertension Centre, School of Biomedical Science, University of Western Australia, Crawley, WA, Australia

²Lions Eye Institute, Nedlands, WA, Australia

³Dobney Hypertension Centre, School of Medicine, University of Western Australia, Crawley, WA, Australia

⁴Department of Cardiology and Department of Nephrology, Royal Perth Hospital, Perth, WA, Australia

Correspondence should be addressed to Vance B. Matthews; vance.matthews@uwa.edu.au

Received 6 April 2018; Accepted 14 June 2018; Published 5 July 2018

Academic Editor: Tomohiko Sasase

Copyright © 2018 Lakshini Y. Herat et al. This is an open access article distributed under the Creative Commons Attribution License, which permits unrestricted use, distribution, and reproduction in any medium, provided the original work is properly cited.

The prevalence of diabetes is at pandemic levels in today's society. Microvascular complications in organs including the eye are commonly observed in human diabetic subjects. Diabetic retinopathy (DR) is a prominent microvascular complication observed in many diabetics and is particularly debilitating as it may result in impaired or complete vision loss. In addition, DR is extremely costly for the patient and financially impacts the economy as a range of drug-related therapies and laser treatment may be essential. Prevention of microvascular complications is the major treatment goal of current therapeutic approaches; however, these therapies appear insufficient. Presently, sodium glucose cotransporter-2 (SGLT2) inhibitors may offer a novel therapy beyond simple glucose lowering. Excitingly, the EMPA-REG clinical trial, which focuses on the clinically used SGLT2 inhibitor empagliflozin, has been extremely fruitful and has highlighted beneficial cardiovascular and renal outcomes. The effects of SGLT2 inhibitors on DR are currently a topic of much research as outlined in the current review, but future studies are urgently needed to fully gain mechanistic insights. Here, we summarize current evidence and identify gaps that need to be addressed.

1. Diabetes and Its Complications

Diabetes mellitus is a chronic metabolic disorder marked by high blood glucose levels resulting from defects in insulin secretion, insulin action, or both. At present, diabetes is at pandemic levels. As per the International Diabetes Federation, in the year 2015, the global diabetic population was ~415 million. By the year 2040, this number is expected to increase to 642 million. All forms of diabetes can lead to the development of diabetes-specific macrovascular and/or microvascular complications. These macrovascular complications commonly affect the arteries of the heart (coronary artery disease), brain, and lower body whereas

the microvascular complications can affect small blood vessels of the heart, kidney, foot, and the eye [1]. In this review, we will focus our attention on the microvascular complication of the eye which is known as diabetic retinopathy (DR).

2. Diabetic Retinopathy (DR)

Diabetic retinopathy is recognized as one of the most prevalent complications of both type 1 (T1D) and type 2 diabetes (T2D), and it is a leading cause of vision impairment [2]. Globally, the number of people with DR is estimated to grow from 126.6 million in 2011 to 191.0 million by

2030, and vision-threatening DR is projected to increase from 37.3 million in 2010 to 56.3 million by 2030 [3].

Retinal vascular abnormalities observed via ophthalmoscopy form the basis of the clinical diagnosis for DR [4]. However, a growing body of evidence supports that DR is both a vascular and a neurodegenerative disease of the retina [5]. Characteristic features of DR include hemorrhages, microaneurysms, and intraretinal microvascular abnormalities (IRMA) such as dilated preexisting capillaries, cotton wool spots, hard exudates (lipid deposits), retinal edema, and neovascularization [2, 6].

In general, DR is known to progress from a mild nonproliferative DR (NPDR) to a severe proliferative DR (PDR). The early stage of the disease often does not show recognizable retinal changes, leaving patients unaware of the condition. As retinopathy progresses, patients may invariably experience vision loss [6].

The early retinal change in DR is called nonproliferative or background DR. Nonproliferative DR can be subdivided into mild, moderate, severe, and very severe NPDR, according to the modified Airlie House classification of DR severity scale [4, 6]. During the NPDR stage, patients usually have no symptoms and have normal vision. Although the presence of microaneurysms is the hallmark of NPDR, histopathological observations of diabetic retinas show the presence of pericyte ghosts, acellular capillaries, and thickening of the capillary basement membrane [7] marking the mild or early NPDR stage. However, microaneurysms are the earliest ophthalmoscopically detectable, clinical manifestation of DR. Typically, the pericyte to endothelial cell ratio is 1:1. Due to diabetes, pericytes necrotise significantly reducing the number of functional pericytes on capillary walls [7]. This selective loss of pericytes from the retinal capillaries is a characteristic lesion that occurs in the very early stages of DR. It is speculated that the loss of pericytes affects the integrity of the capillaries, leading to the formation of acellular capillaries, microaneurysms, or capillary occlusion [8]. Capillary occlusion is histologically manifested as an increased number of acellular capillaries. These capillaries are mere basement membrane tubes lacking endothelial cells and pericyte nuclei [9]. In addition, the mild NPDR stage can also manifest as hemorrhages and/or hard exudates [4, 6]. The presence of microaneurysms and retinal hemorrhages along with cotton wool spots or IRMA marks the moderate NPDR stage [4]. Moderate NPDR progresses to severe NPDR and shows microaneurysms with venous beading, hemorrhages, or both [6].

Cotton wool spots, also known as soft exudates, are round or oval spots with feathered edges. They appear white, grayish-white, or pale yellow-white under ophthalmoscopic observation. On the other hand, hard exudates are waxy, white, or yellow in colour with sharp edges. IRMA occur in intraretinal blood vessels between the arterioles and venules, closer to areas with capillary nonperfusion. The IRMA can be tortuous blood vessels formed due to intraretinal neovascularization or dilation of preexisting capillaries [10]. When very severe NPDR approaches, features of mild to moderate NPDR increase by severalfold in all four quadrants of the eye [6]. All microvascular changes of NPDR

are limited to the inner retina and do not extend beyond the internal limiting membrane [11].

Proliferative DR occurs once NPDR progresses to its next level, with the growth of new blood vessels from preexisting vessels (neovascularization) on the innermost layer of the retina. These blood vessels develop towards the vitreous body and its cavity. The neovascularization or formation of new blood vessels takes place in addition to the clinical features of NPDR. Extensive lack of oxygen leads to the development of neovascularization which is a random growth pattern of blood vessels. Winding of vessels and other various complicated formations indicates neovascular events. The newly formed preretinal vessels are thin, leaky, and fragile in structure and susceptible to hemorrhages, causing the leakage of blood into the vitreous body. As PDR progresses, fibrovascular scar tissue can form around new vessels. This tissue can be vascular or avascular. This fibrovascular variety can lead to retinal tearing and tractional retinal detachment followed by blindness [11]. The exact chronological sequence of development of the above lesions is still incompletely understood.

3. Molecular Aspects of the Pathogenesis of DR

One aspect of the pathogenesis of DR is linked to changes in retinal haemodynamics. The decreased blood flow through the retinal tissue leads to retinal hypoxia and has a significant impact on metabolic activities of the retina. The development of a hypoxic environment in the diabetic retina is evident prior to occurrence of other symptoms observed in diabetic patients [12] and diabetic animals [13] and is linked to capillary occlusion, a well-defined mechanism occurring in early DR [14]. As more capillaries become occluded with time, hypoxia in the surrounding retinal tissue enhances vascular endothelial growth factor (VEGF) expression [15]. This promotes breakdown of the blood-retinal barrier, increases vascular permeability, and stimulates endothelial cell growth and retinal neovascularization in the ischemic retina in PDR [16].

A number of other growth factors have been associated with the development of DR and these include platelet-derived growth factors (PDGFs), angiopoietin-1 and angiopoietin-2, basic fibroblast growth factor (bFGF), insulin-like growth factor-1 (IGF-1), stromal-derived factor-1, epidermal growth factor (EGF), transforming growth factor-beta 2 (TGF- β 2), and erythropoietin. In addition to these, VEGF has been demonstrated as the main mediator of ocular neovascularization [16].

4. Perturbed Glucose Homeostasis and DR

Prolonged duration of diabetes and poorer glycemic and blood pressure control are strongly associated with DR. The storage of glucose in the retina is minimal compared to its high metabolic activity [17]. Thus, the retina is heavily dependent on the systemic circulation for the delivery of adequate glucose [18]. The endothelial cells of the capillaries of the inner blood-retinal barrier and the choroidal vessels across the retinal pigment epithelium (RPE) of the outer

blood-retinal barrier are responsible for the transport of glucose across the retina. Excessive transport of glucose across the retina leading to high glucose concentrations within cells of the retina is a common factor leading to the pathogenesis of DR. Increased metabolic dysfunction due to high glucose levels and activation of signalling pathways as mentioned below lead to the development and progression of DR. Of the biochemical pathways involved, four major mechanisms have been found to explain the fate of cells and tissues exposed to hyperglycemia (Table 1). These include (1) activation of protein kinase C (PKC), (2) increased glucose flow via the polyol pathway, (3) increased advanced glycation end product (AGE) formation, and (4) increased hexosamine pathway flux [19]. All these pathways ultimately lead to increased oxidative stress, inflammation, and vascular dysfunction and upregulation of a wide range of growth factors and eventually contributes to the pathogenesis of DR.

At present, tight control of blood glucose levels is viewed as the primary means by which to disrupt the abovementioned pathways and slow the progression of retinopathy. However, the precise mechanism by which glucose enters the retina and how hyperglycemia causes retinopathy remains unclear. Therefore, in the past two decades, a major focus has been placed in understanding the role and mechanism of glucose transporters in DR.

5. Glucose Regulatory Mechanisms in DR

The entry of glucose into cells is regulated by facilitative glucose transporters (GLUTs) and sodium-dependent glucose cotransporters (SGLTs). In the sodium-dependent glucose transport process, SGLT1 and SGLT2 have been well characterised. In particular, SGLT1 is considered to be predominantly expressed in the brush border membrane of mature enterocytes in the small intestine and plays a major role in the absorption of glucose from the lumen of the intestine [20]. In contrast, SGLT2 is mainly found in the S1 and S2 segments of the renal convoluted proximal tubules and is required for the reabsorption of glucose [21].

The GLUT protein family is responsible for the glucose movement within the body, which occurs primarily through 14 isoforms [22]. Of these, GLUT1 and GLUT3 isoforms are expressed in a variety of tissue and cell types in the eye [23]. In particular, GLUT1 is expressed extensively throughout the eye and retina [24–26], suggesting GLUT1 as the main glucose transporter of the eye. In the retina, GLUT1 is highly expressed in pigment epithelial cells, Muller cells, and vascular endothelial cells forming the blood-retinal barrier [18, 25, 27, 28]. In contrast, relatively low levels of GLUT3 expression is seen in retinal inner and outer plexiform layers and pigment epithelium. In fact, it is predominantly expressed by the neuronal cells of the retina [26, 29–32]. Due to pathological characteristics of DR being associated with the loss of blood-retinal barrier function which leads to retinal microvascular abnormalities, GLUT1 and GLUT3 have been investigated in DR. Currently, the role of GLUT3 in DR is not well established. A recent study showed downregulation of GLUT3 in the retina of streptozotocin (STZ) diabetic rats with DR features and

suggested this effect was a compensatory response to glucose during hyperglycemia. Furthermore, Knott et al. [32] reported upregulation of GLUT3 mRNA in cultured human retinal endothelial cells exposed to high glucose levels; however, these findings have been controversial due to the expression of GLUT3 being confined to the neurons of the retina [23]. The controversial nature of GLUT3 in DR and the limited number of studies that have investigated its role clearly show the need to further assess the role of GLUT3 in DR.

Given the entry of glucose into the endothelial cells of the inner blood-retinal barrier occurring primarily through GLUT1, its expression and glucose transport could have a major implication on the pathogenic pathways influencing the development and progression of DR. In retinal endothelial cells obtained from postmortem retinas from individuals with long-standing diabetes with minimal or no clinical features of retinopathy, it has been shown that upregulated GLUT1 is localised in the inner blood-retinal barrier. However, this upregulation of GLUT1 can serve to exacerbate the damage to the retinal microvasculature due to ongoing glucose influx [28]. Hypoxia which is a factor associated with the development of more severe retinal lesions in NPDR has been shown to increase GLUT1 expression in retinal endothelial cells [33]. Upregulation of GLUT1 mRNA has been reported in STZ-induced and galactose-fed diabetic rats with DR lesions [34, 35]. Furthermore, knockdown of GLUT1 by intraocular injections of siRNA after 2–4 weeks of STZ-induced diabetes in mice has shown restricted glucose transport by inhibiting GLUT1 expression, which decreased retinal glucose concentrations [36, 37]. In the same mouse model, blockade of GLUT1 reduced early biomarkers of DR such as superoxide radicals, chaperone protein b2 crystallin, and VEGF [36]. Taken together, these studies suggest that upregulation of retinal GLUT1 occurs early in DR and this plays a crucial role in disease progression.

Interestingly and important in the current context, the expression of SGLT1 and SGLT2 (Figure 1) has been reported in the eye and the retina [24, 38, 39]. However, the full spectrum of SGLT expression and its role in the eye is poorly understood. Restricted expression patterns of both SGLT1 and SGLT2 have been reported in the lens [24]. It is suggested that SGLT1 is localised at the basolateral membrane of epithelial cells of the chick RPE [38]. The RPE is responsible for transportation of nutrients, ions, and water from the choroidal circulation to the photoreceptors of the retina. Hence, the RPE is essential for the integrity and survival of the neural retina and consequently visual function [40]. In recent years, alteration of both the structural and secretory functions of RPE has been found in DR [41]. The possible localisation of SGLT1 in the basolateral membrane may cause a transmembrane Na⁺ gradient to drive glucose into the RPE [42], and glucose would diffuse into the neurosensory retina via the apically located GLUT1. Alterations caused to this circuit by high concentrations of glucose may lead to inducible nitric oxide synthase (iNOS) causing nitric oxide-dependent oxidative damage in RPE cells [43]. Although the precise role of SGLT1 in the retina and retinal disease is not well-known,

TABLE 1: Proposed mechanisms involved in the pathogenesis of DR. Prolonged exposure to hyperglycemia leads to the activation of a number of interconnecting biochemical pathways that contribute to the pathogenesis of DR.

Pathway	Mechanism	Reference
Activation of protein kinase C (PKC)	(i) Hyperglycemia increases the synthesis of diacylglycerol (DAG). (ii) Several PKC isoforms (such as PKC- β , α , and δ) are activated. (iii) Phosphorylation of substrate proteins mediated via PKC promotes changes in retinal blood flow, increased vascular permeability, endothelial cell dysfunction, and altered growth factor signaling. (iv) Retinal ischemia and neovascularization result.	[62]
Polyol pathway	(i) Metabolizes excess glucose to sorbitol and then fructose during hyperglycemia. (ii) Intracellular accumulation of sorbitol leads to osmotic stress in retinal cells including ganglion cells, Muller glia, vascular endothelial cells, and pericytes. (iii) Pathophysiological consequences include thickening of capillary basement membrane, pericyte loss, formation of acellular capillaries, microaneurysms, hemorrhages, glial cell activation, and apoptosis.	[63]
Advanced glycation end product (AGE) formation	(i) Hyperglycemia increases the formation of AGEs. (ii) Production of AGEs damages target cells via three mechanisms: (1) Changed extracellular matrix brings about abnormal interactions with matrix receptor proteins and surrounding matrix components. (2) AGE-modified intracellular proteins have altered functions. (3) AGE-modified plasma proteins bind to the receptor for advanced glycation end products (RAGE) on endothelial cells, leading to the production of reactive oxygen species.	[64]
Increased hexosamine pathway flux	(i) During hyperglycemia, ~3% of glucose is processed through the hexosamine pathway. (ii) Fructose-6-phosphate is converted to glucosamine-6-phosphate. (iii) Subsequently, glucosamine-6-phosphate is metabolized to UDP-GluNAc (uridine diphosphate N-acetyl glucosamine). (iv) UDP-GluNAc attaches to serine and threonine residues of transcription factors.	[65]

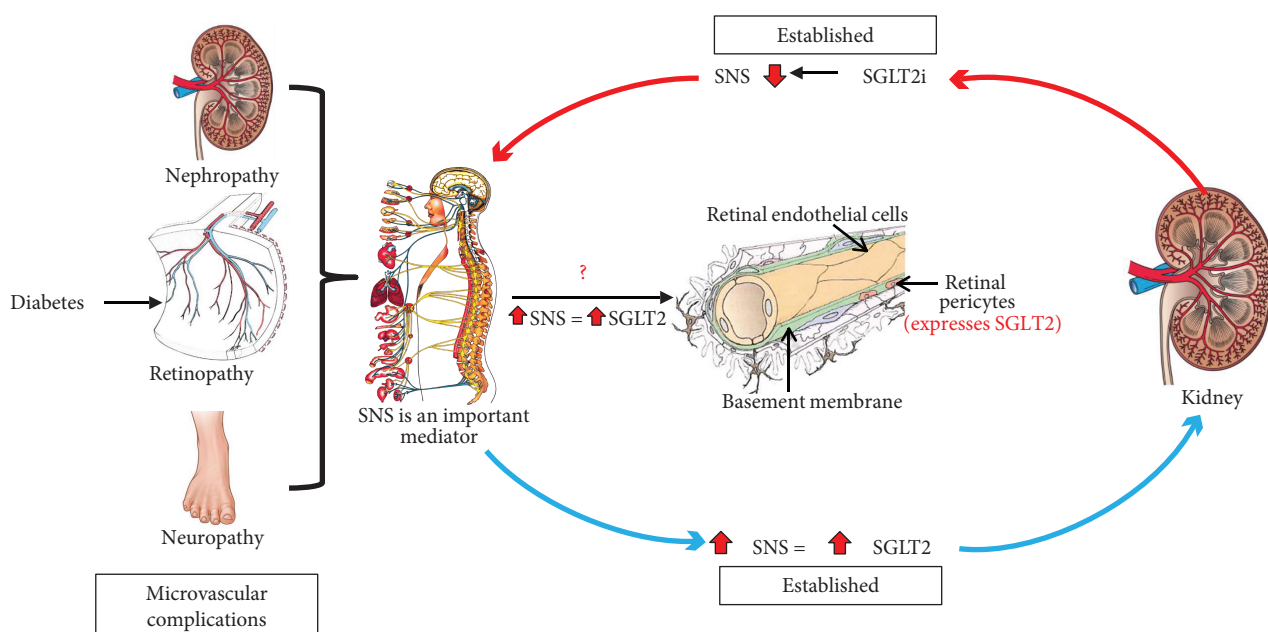


FIGURE 1: The potential molecular role of the SNS and SGLT2 in the pathogenesis of DR. Based on previous studies completed by our team and others, we propose a pivotal role for SGLT2 inhibition (SGLT2i) in the prevention of DR.

the above hypothesis warrants investigations to establish the role of SGLT1 in DR.

Wakisaka and Nagao first reported the expression of SGLT2 in cultured bovine retinal pericytes [39] highlighting

the functional glucose sensor role of SGLT2 in the retinal microvasculature. Excessive Na⁺-dependent glucose entry causes intracellular swelling of pericytes [44] and leads to loss of contractile function, pericyte death, and retinal

hyperperfusion. Overexpression of the extracellular matrix (such as fibronectin, collagen IV, and laminin) is associated with the development of basement membrane thickening followed by microvascular occlusion and retinal hypoperfusion [45]. This shift in retinal haemodynamics can bring about several downstream triggers of DR. SGLT2 inhibitors have shown to reduce pericyte swelling and overexpression of the extracellular matrix [45]. Arresting the haemodynamic shift early in DR is of significant importance for the development of effective therapeutics for DR.

A new class of antidiabetic drugs act by inhibition of SGLT2, which decreases the reabsorption of glucose from the renal proximal tubules. Hence, specific SGLT2 inhibition (SGLTi) leads to the initiation of glucose excretion via the urine (glucosuria) resulting in reduced blood glucose levels [46]. The SGLT2 inhibitors dapagliflozin, empagliflozin, and canagliflozin have shown to reduce glycosylated haemoglobin levels (HbA1c), fasting plasma glucose levels, blood pressure, and body weight [47–50]. Additionally, it has been shown that SGLT2 inhibitors have protective effects, targeting two of the main complications of diabetes which are cardiovascular disease and kidney-related complications [47, 48]. These outcomes have been assessed mainly in T2D; however, many studies are currently underway with T1D [51]. Takakura et al. showed for the first time the effect of ipragliflozin on the diabetic retina in spontaneously diabetic Torii fatty rats. In this study, diabetic rats treated with ipragliflozin demonstrated reduced prolongation of oscillatory potential in the electroretinogram, irregularities of the outer nuclear layers of the neural retina were absent, and ipragliflozin inhibited the progression of cataract formation in the lens [52]. The first patient-based study evaluating the impact of dapagliflozin on the retinal microvasculature showed lowered retinal capillary flow and prevented retinal arteriole changes. In this study, the placebo-treated diabetic group showed increased wall-to-lumen ratio indicative of retinal vascular hypertrophy, while the dapagliflozin-treated group showed no changes in wall-to-lumen ratio, indicating the positive effect of dapagliflozin in the prevention of vascular hypertrophy and remodelling [53]. In addition, evidence exists to highlight that dapagliflozin reduced the incidence of DR by 10% in human T2D cohorts [54]. One possible mechanism of SGLT2i in DR is that it results in blockade of the renin-angiotensin system, improving glycemic control and blood pressure lowering [55, 56]. A recent meta-analysis conducted by Tang et al. showed that the risk of DR with the treatment of SGLT2i was similar to that with placebo suggesting that SGLT2i did not increase the risk of DR [57]. Thus far, clinical evidence has shown a statistically insignificant beneficial effect. However, none of these studies systematically assessed the retinal vascular and neural pathology in detail during the development and progression of DR. This opens up an opportunity to test the effectiveness of SGLT2 inhibitors in mouse models with retinal and neural damage associated with DR (Figure 1), such as the Akita and Akimba mouse models [5]. The Akita and Akimba mouse models develop diabetes ~4–8 weeks of age, and these strains progressively develop characteristics of DR ultimately leading to retinal neovascularization, a hallmark feature of

DR. The ultimate goal of effective DR treatments should ideally arrest the progression of the disease to PDR where neovascularization occurs. Therefore, the availability of well-characterised DR mouse models such as the Akita and Akimba will provide an ideal vehicle to assess the effectiveness of SGLT2 inhibitors in the pathogenesis and progression of DR. These studies are currently being conducted by our team.

6. Possible Interaction with the Sympathetic Nervous System

Recent findings indicate that relevant interactions exist between SGLT2 expression and the sympathetic nervous system. Hyperactivity of the sympathetic nervous system (SNS) is a characteristic feature of obesity and T2D [58, 59]. We have shown for the first time that the major neurotransmitter of the SNS, noradrenaline, upregulates SGLT2 protein expression in human renal proximal tubule cells (Figure 1). In addition, high-fat diet-fed mice treated with dapagliflozin showed a reduction in tissue noradrenaline content and tyrosine hydroxylase expression in both heart and kidney tissue which points to a significant sympathoinhibitory action of SGLT2 inhibitors in our animal model [60]. To date, a limited number of studies have investigated the autonomic nervous system in relation to DR, and these studies suggest DR to be associated with early autonomic dysfunction in T1D and T2D patients [61]. The balance between sympathetic and parasympathetic effects determines the proper function of the autonomic nervous system. We have produced novel data highlighting that in a mouse model of neurogenic hypertension with a substantially activated SNS, neural damage of the outer layer of the retina is evident which is a characteristic feature of DR (Figure 2). We are now conducting mechanistic studies that aim to understand these preliminary findings. As we have already documented [60] that SGLT2 inhibition may downregulate the SNS in the heart and kidney, it is plausible that SGLT2 inhibition may also alleviate detrimental retinal changes that may be underpinned by hyperactivation of the SNS (Figure 1). Our recent results highlight an opportunity to investigate the role of SGLT2 and the SNS in DR.

7. Alternative Therapies for the Management of Diabetic Retinopathy

Controlling systemic factors such as blood glucose levels and blood pressure have shown to reduce the development and the progression of nonproliferative to proliferative DR.

Medical interventions such as the use of antiplatelet agents, PKC inhibitors, aldose reductase inhibitors, growth hormone/insulin-like growth factor, and intravitreal administration of corticosteroids and antiangiogenesis agents have proven to be effective at varying levels in limiting visual loss in DR. Among these, antivascular endothelial growth factor (VEGF) therapy administered into the vitreous cavity represents one of the most beneficial treatment strategies implemented to treat PDR and diabetic macular edema (DME) [16].

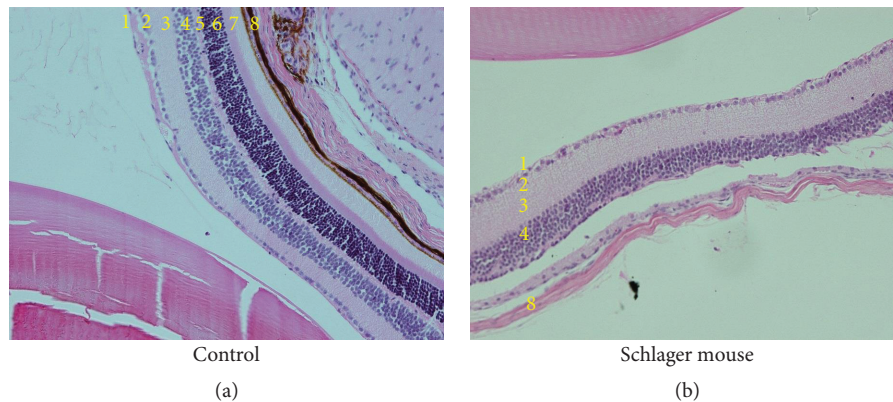


FIGURE 2: Sympathetic nervous system hyperactivation in the Schlager mouse is associated with neural damage of the outer layers of the retina. Haematoxylin and eosin staining of the eye of the Schlager mouse highlights that the outer plexiform, outer nuclear, and photoreceptor layers are all absent. 1: nerve fibre layer; 2: ganglion cell layer; 3: inner plexiform layer; 4: inner nuclear layer; 5: outer plexiform layer; 6: outer nuclear layer; 7: photoreceptor layer, and 8: choroid. Magnification: 200x.

Laser and surgical interventions such as panretinal laser photocoagulation and vitrectomy have proven to be effective in treating severe NPDR and PDR. In fact, until recently, panretinal laser photocoagulation was the first and only choice for treating PDR. Furthermore, vitrectomy has been used for the treatment of PDR with vitreous hemorrhages or fibrosis. Vitrectomy is currently used in treating ongoing DME. In the eyes with DME, focal laser treatment has been able to maintain visual acuity without future deterioration. Despite the availability of several treatments, DR remains a major clinical challenge with prevalence expected to rise further over the next decades. Alternative and preventative measures are therefore urgently needed. Based on the limited data available at this stage, therapeutic targeting of the SGLTs, particularly SGLT2, may provide a novel therapeutic opportunity to curb the global burden of DR. Similarly, targeting sympathetic hyperactivity per se and thereby its haemodynamic and inflammatory consequences may provide a useful novel target for DR. Relevant studies are currently being conducted and may well provide further support for such an approach in due course.

Disclosure

Lakshini Y. Herat and Vance B. Matthews are equal first author.

Conflicts of Interest

Markus Schlaich has received research support from Boehringer Ingelheim.

Acknowledgments

The authors acknowledge the generous funding from the Royal Perth Hospital Medical Research Foundation.

References

- [1] M. J. Fowler, "Microvascular and macrovascular complications of diabetes," *Clinical Diabetes*, vol. 26, no. 2, pp. 77–82, 2008.
- [2] D. S. Fong, L. Aiello, T. W. Gardner et al., "Diabetic retinopathy," *Diabetes Care*, vol. 26, no. 1, pp. 226–229, 2003.
- [3] Y. Zheng, M. He, and N. Congdon, "The worldwide epidemic of diabetic retinopathy," *Indian Journal of Ophthalmology*, vol. 60, no. 5, pp. 428–431, 2012.
- [4] Early treatment diabetic retinopathy study research group, "Grading diabetic retinopathy from stereoscopic color fundus photographs—an extension of the modified Airlie House classification: ETDRS report number 10," *Ophthalmology*, vol. 98, no. 5, pp. 786–806, 1991.
- [5] E. P. Rakoczy, I. S. A. Rahman, N. Binz et al., "Characterization of a mouse model of hyperglycemia and retinal neovascularization," *The American Journal of Pathology*, vol. 177, no. 5, pp. 2659–2670, 2010.
- [6] C. P. Wilkinson, Ferris FL 3rd, R. E. Klein et al., "Proposed international clinical diabetic retinopathy and diabetic macular edema disease severity scales," *Ophthalmology*, vol. 110, no. 9, pp. 1677–1682, 2003.
- [7] M. Mizutani, T. S. Kern, and M. Lorenzi, "Accelerated death of retinal microvascular cells in human and experimental diabetic retinopathy," *Journal of Clinical Investigation*, vol. 97, no. 12, pp. 2883–2890, 1996.
- [8] A. W. Stitt, T. A. Gardiner, and D. B. Archer, "Histological and ultrastructural investigation of retinal microaneurysm development in diabetic patients," *British Journal of Ophthalmology*, vol. 79, no. 4, pp. 362–367, 1995.
- [9] A. J. Barber, D. A. Antonetti, T. S. Kern et al., "The *Ins2^{Akita}* mouse as a model of early retinal complications in diabetes," *Investigative Ophthalmology & Visual Science*, vol. 46, no. 6, pp. 2210–2218, 2005.
- [10] C. Hudson, "A clinical perspective of diabetic retinopathy," *Geriatrics & Aging*, vol. 11, no. 6, pp. 333–341, 2008.
- [11] N. C. Steinle and J. Ambati, "Retinal vasculopathies: diabetic retinopathy," in *Encyclopedia of the Eye*, D. A. Dartt, J. Besharse, and R. Dana, Eds., pp. 109–117, Academic Press, Oxford, 2010.

- [12] A. Harris, O. Arend, R. P. Danis, D. Evans, S. Wolf, and B. J. Martin, "Hyperoxia improves contrast sensitivity in early diabetic retinopathy," *British Journal of Ophthalmology*, vol. 80, no. 3, pp. 209–213, 1996.
- [13] R. A. Linsenmeier, R. D. Braun, M. McRipley et al., "Retinal hypoxia in long-term diabetic cats," *Investigative Ophthalmology and Visual Science*, vol. 39, no. 9, pp. 1647–1657, 1998.
- [14] A. M. Joussen, T. Murata, A. Tsujikawa, B. Kirchhof, S. E. Bursell, and A. P. Adamis, "Leukocyte-mediated endothelial cell injury and death in the diabetic retina," *American Journal of Pathology*, vol. 158, no. 1, pp. 147–152, 2001.
- [15] L. P. Aiello, J. M. Northrup, B. A. Keyt, H. Takagi, and M. A. Iwamoto, "Hypoxic regulation of vascular endothelial growth factor in retinal cells," *Archives of Ophthalmology*, vol. 113, no. 12, pp. 1538–1544, 1995.
- [16] N. Gupta, S. Mansoor, A. Sharma et al., "Diabetic retinopathy and VEGF," *The Open Ophthalmology Journal*, vol. 7, no. 1, pp. 4–10, 2013.
- [17] C. N. Graymore, "Biochemistry of the retina," in *Biochemistry of the eye*, C. N. Graymore, Ed., pp. 645–675, Academic Press, 1970.
- [18] K. Takata, H. Hirano, and M. Kasahara, "Transport of glucose across the blood-tissue barriers," *International Review of Cytology*, vol. 172, pp. 1–53, 1997.
- [19] M. Brownlee, "The pathobiology of diabetic complications: a unifying mechanism," *Diabetes*, vol. 54, no. 6, pp. 1615–1625, 2005.
- [20] E. M. Wright, "The intestinal Na⁺/glucose cotransporter," *Annual Review of Physiology*, vol. 55, no. 1, pp. 575–589, 1993.
- [21] Y. Kanai, W. S. Lee, G. You, D. Brown, and M. A. Hediger, "The human kidney low affinity Na⁺/glucose cotransporter SGLT2. Delineation of the major renal reabsorptive mechanism for D-glucose," *The Journal of Clinical Investigation*, vol. 93, no. 1, pp. 397–404, 1994.
- [22] B. Thorens and M. Mueckler, "Glucose transporters in the 21st century," *American Journal of Physiology. Endocrinology and Metabolism*, vol. 298, no. 2, pp. E141–E145, 2010.
- [23] A. K. Kumagai, "Glucose transport in brain and retina: implications in the management and complications of diabetes," *Diabetes/Metabolism Research and Reviews*, vol. 15, no. 4, pp. 261–273, 1999.
- [24] J. C. Lim, R. D. Perwick, B. Li, and P. J. Donaldson, "Comparison of the expression and spatial localization of glucose transporters in the rat, bovine and human lens," *Experimental Eye Research*, vol. 161, pp. 193–204, 2017.
- [25] A. K. Kumagai, B. J. Glasgow, and W. M. Pardridge, "GLUT1 glucose transporter expression in the diabetic and nondiabetic human eye," *Investigative Ophthalmology & Visual Science*, vol. 35, no. 6, pp. 2887–2894, 1994.
- [26] G. J. Mantych, G. S. Hageman, and S. U. Devaskar, "Characterization of glucose transporter isoforms in the adult and developing human eye," *Endocrinology*, vol. 133, no. 2, pp. 600–607, 1993.
- [27] K. Takata, T. Kasahara, M. Kasahara, O. Ezaki, and H. Hirano, "Ultracytochemical localization of the erythrocyte/HepG2-type glucose transporter (GLUT1) in cells of the blood-retinal barrier in the rat," *Investigative Ophthalmology & Visual Science*, vol. 33, no. 2, pp. 377–383, 1992.
- [28] A. K. Kumagai, S. A. Viores, and W. M. Pardridge, "Pathological upregulation of inner blood-retinal barrier Glut1 glucose transporter expression in diabetes mellitus," *Brain Research*, vol. 706, no. 2, pp. 313–317, 1996.
- [29] R. M. Knott and J. V. Forrester, "Role of glucose regulatory mechanisms in diabetic retinopathy," *The British Journal of Ophthalmology*, vol. 79, no. 11, pp. 1046–1049, 1995.
- [30] H. Takagi, H. Tanihara, Y. Seino, and N. Yoshimura, "Characterization of glucose transporter in cultured human retinal pigment epithelial cells: gene expression and effect of growth factors," *Investigative Ophthalmology & Visual Science*, vol. 35, no. 1, pp. 170–177, 1994.
- [31] T. Watanabe, S. Matsushima, M. Okazaki et al., "Localization and ontogeny of GLUT3 expression in the rat retina," *Brain Research. Developmental Brain Research*, vol. 94, no. 1, pp. 60–66, 1996.
- [32] R. M. Knott, M. Robertson, E. Muckersie, and J. V. Forrester, "Regulation of glucose transporters (GLUT-1 and GLUT-3) in human retinal endothelial cells," *The Biochemical Journal*, vol. 318, no. 1, pp. 313–317, 1996.
- [33] H. Takagi, G. L. King, and L. P. Aiello, "Hypoxia upregulates glucose transport activity through an adenosine-mediated increase of GLUT1 expression in retinal capillary endothelial cells," *Diabetes*, vol. 47, no. 9, pp. 1480–1488, 1998.
- [34] S. Roy, A. Kaminski, and J. Zieske, "Distribution and expression of GLUT1 in the retina of galactose-fed rat," *Investigative Ophthalmology & Visual Science*, vol. 37, no. 3, pp. S1–S1154, 1996.
- [35] R. Poulosom, D. J. Prockop, and R. P. Boot-Handford, "Effects of long-term diabetes and galactosaemia upon lens and retinal mRNA levels in the rat," *Experimental Eye Research*, vol. 51, no. 1, pp. 27–32, 1990.
- [36] L. Lu, C. P. Seidel, T. Iwase et al., "Suppression of GLUT1; a new strategy to prevent diabetic complications," *Journal of Cellular Physiology*, vol. 228, no. 2, pp. 251–257, 2013.
- [37] Z. P. You, Y. L. Zhang, K. Shi et al., "Suppression of diabetic retinopathy with GLUT1 siRNA," *Scientific Reports*, vol. 7, no. 1, p. 7437, 2017.
- [38] L. J. Rizzolo, "Glucose transporters in retinal pigment epithelium development," in *Ocular Transporters in Ophthalmic Diseases and Drug Delivery: Ophthalmology Research*, J. Tombran-Tink and C. J. Barnstable, Eds., pp. 185–199, Humana Press, Totowa, NJ, USA, 2008.
- [39] M. Wakisaka and T. Nagao, "Sodium glucose cotransporter 2 in mesangial cells and retinal pericytes and its implications for diabetic nephropathy and retinopathy," *Glycobiology*, vol. 27, no. 8, pp. 691–695, 2017.
- [40] R. Simó, M. Villarroel, L. Corraliza, C. Hernández, and M. Garcia-Ramírez, "The retinal pigment epithelium: something more than a constituent of the blood-retinal barrier—implications for the pathogenesis of diabetic retinopathy," *Journal of Biomedicine & Biotechnology*, vol. 2010, Article ID 190724, 15 pages, 2010.
- [41] H. Z. Xu, Z. Song, S. Fu, M. Zhu, and Y. Z. le, "RPE barrier breakdown in diabetic retinopathy: seeing is believing," *Journal of Ocular Biology, Diseases, and Informatics*, vol. 4, no. 1-2, pp. 83–92, 2011.
- [42] J. P. Gnana-Prakasam, R. Veeranan-Karmegam, V. Coothankandaswamy et al., "Loss of Hfe leads to progression of tumor phenotype in primary retinal pigment epithelial cells," *Investigative Ophthalmology & Visual Science*, vol. 54, no. 1, pp. 63–71, 2013.

- [43] Z. Yuan, W. Feng, J. Hong, Q. Zheng, J. Shuai, and Y. Gep38MAPK and ERK promote nitric oxide production in cultured human retinal pigmented epithelial cells induced by high concentration glucose," *Nitric Oxide*, vol. 20, no. 1, pp. 9–15, 2009.
- [44] M. Wakisaka, M. Yoshinari, S. Nakamura et al., "Suppression of sodium-dependent glucose uptake by captopril improves high-glucose-induced morphological and functional changes of cultured bovine retinal pericytes," *Microvascular Research*, vol. 58, no. 3, pp. 215–223, 1999.
- [45] S. Roy, E. Bae, S. Amin, and D. Kim, "Extracellular matrix, gap junctions, and retinal vascular homeostasis in diabetic retinopathy," *Experimental Eye Research*, vol. 133, pp. 58–68, 2015.
- [46] A. T. Hattersley and B. Thorens, "Type 2 diabetes, SGLT2 inhibitors, and glucose secretion," *The New England Journal of Medicine*, vol. 373, no. 10, pp. 974–976, 2015.
- [47] B. Zinman, C. Wanner, J. M. Lachin et al., "Empagliflozin, cardiovascular outcomes, and mortality in type 2 diabetes," *New England Journal of Medicine*, vol. 373, no. 22, pp. 2117–2128, 2015.
- [48] C. Wanner, S. E. Inzucchi, J. M. Lachin et al., "Empagliflozin and progression of kidney disease in type 2 diabetes," *New England Journal of Medicine*, vol. 375, no. 4, pp. 323–334, 2016.
- [49] J. Wilding, C. Bailey, U. Rigney, B. Blak, M. Kok, and C. Emmas, "Dapagliflozin therapy for type 2 diabetes in primary care: changes in HbA1c, weight and blood pressure over 2 years follow-up," *Primary Care Diabetes*, vol. 11, no. 5, pp. 437–444, 2017.
- [50] B. Neal, V. Perkovic, K. W. Mahaffey et al., "Canagliflozin and cardiovascular and renal events in type 2 diabetes," *The New England Journal of Medicine*, vol. 377, no. 7, pp. 644–657, 2017.
- [51] A. E. de Leeuw and R. A. de Boer, "Sodium-glucose cotransporter 2 inhibition: cardioprotection by treating diabetes—a translational viewpoint explaining its potential salutary effects," *European Heart Journal - Cardiovascular Pharmacotherapy*, vol. 2, no. 4, pp. 244–255, 2016.
- [52] S. Takakura, T. Toyoshi, Y. Hayashizaki, and T. Takasu, "Effect of ipragliflozin, an SGLT2 inhibitor, on progression of diabetic microvascular complications in spontaneously diabetic Torii fatty rats," *Life Sciences*, vol. 147, pp. 125–131, 2016.
- [53] C. Ott, A. Jumar, K. Striepe et al., "A randomised study of the impact of the SGLT2 inhibitor dapagliflozin on microvascular and macrovascular circulation," *Cardiovascular Diabetology*, vol. 16, no. 1, p. 26, 2017.
- [54] J. Dziuba, P. Alperin, J. Racketa et al., "Modeling effects of SGLT-2 inhibitor dapagliflozin treatment versus standard diabetes therapy on cardiovascular and microvascular outcomes," *Diabetes, Obesity and Metabolism*, vol. 16, no. 7, pp. 628–635, 2014.
- [55] S. J. Shin, S. Chung, S. J. Kim et al., "Effect of sodium-glucose co-transporter 2 inhibitor, dapagliflozin, on renal renin-angiotensin system in an animal model of type 2 diabetes," *PLoS One*, vol. 11, no. 11, article e0165703, 2016.
- [56] B. Wang, F. Wang, Y. Zhang et al., "Effects of RAS inhibitors on diabetic retinopathy: a systematic review and meta-analysis," *The Lancet Diabetes & Endocrinology*, vol. 3, no. 4, pp. 263–274, 2015.
- [57] H. Tang, G. Li, Y. Zhao et al., "Comparisons of diabetic retinopathy events associated with glucose-lowering drugs in patients with type 2 diabetes mellitus: a network meta-analysis," *Diabetes, Obesity & Metabolism*, vol. 20, no. 5, pp. 1262–1279, 2018.
- [58] N. E. Straznicky, M. T. Grima, N. Eikelis et al., "The effects of weight loss versus weight loss maintenance on sympathetic nervous system activity and metabolic syndrome components," *The Journal of Clinical Endocrinology and Metabolism*, vol. 96, no. 3, pp. E503–E508, 2011.
- [59] A. A. Thorp and M. P. Schlaich, "Relevance of sympathetic nervous system activation in obesity and metabolic syndrome," *Journal of Diabetes Research*, vol. 2015, Article ID 341583, 11 pages, 2015.
- [60] V. B. Matthews, R. H. Elliot, C. Rudnicka, J. Hricova, L. Herat, and M. P. Schlaich, "Role of the sympathetic nervous system in regulation of the sodium glucose cotransporter 2," *Journal of Hypertension*, vol. 35, no. 10, pp. 2059–2068, 2017.
- [61] C. K. Kramer, C. B. Leitão, M. J. Azevedo et al., "Diabetic retinopathy is associated with early autonomic dysfunction assessed by exercise-related heart rate changes," *Brazilian Journal of Medical and Biological Research*, vol. 41, no. 12, pp. 1110–1115, 2008.
- [62] P. Geraldès and G. L. King, "Activation of protein kinase C isoforms and Its impact on diabetic complications," *Circulation Research*, vol. 106, no. 8, pp. 1319–1331, 2010.
- [63] M. Lorenzi, "The polyol pathway as a mechanism for diabetic retinopathy: attractive, elusive, and resilient," *Experimental Diabetes Research*, vol. 2007, Article ID 61038, 10 pages, 2007.
- [64] A. W. Stitt, "AGEs and diabetic retinopathy," *Investigative Ophthalmology & Visual Science*, vol. 51, no. 10, pp. 4867–4874, 2010.
- [65] R. A. Kowluru and P. S. Chan, "Oxidative stress and diabetic retinopathy," *Experimental Diabetes Research*, vol. 2007, Article ID 43603, 12 pages, 2007.